UNIVERSITÀ
DEGLI STUDI
DI PADOVA

Sede Amministrativa: Università degli Studi di Padova

Dipartimento di Scienze del Farmaco

SCUOLA DI DOTTORATO DI RICERCA IN SCIENZE MOLECOLARI

INDIRIZZO SCIENZE FARMACEUTICHE

CICLO XXV

NEW QUINOLIZINIUM DERIVATIVES: DESIGN, SYNTHESIS AND STUDY ON BIOLOGICAL AND PHOTOBIOLOGICAL ACTIVITY

Direttore della Scuola: Ch.mo Prof. Antonino Polimeno

Coordinatore d'indirizzo: Ch.mo Prof. Alessandro Dolmella

Supervisore: Ch.ma Prof.ssa Daniela Vedaldi

Dottorando: Manlio Sutera Sardo

A Mamma, Papà

e a Roberta

INDEX

ABSTRACT

Neoplastic diseases have become one of the most important causes of death in the world. In USA, cancer is the second cause of death after the cardiovascular diseases. Therefore, the research, the discovery and the development of new compounds with antitumoral activity have become one of the most important goals in medicinal chemistry, also trying to make a selective toxicity towards the diseased or cancer cells, thus not involving the healthy cells. Many therapeutic approaches are available for the treatment of cancer in clinical use: surgery, radiotherapy are used for localized cancer; chemotherapy, hormone-therapy and immunotherapy are considered useful, as systemic treatments, for leukemia and metastatic tumours. In the chemotherapy a high number of molecules interacts with nucleic acids like groove binders, alkylating and intercalator compounds. The molecules that belong to the latter class, interact with DNA by intercalation in the base pairs through van der Waals interactions, hydrogen bonds, hydrophobic and/or charge transfer forces. Therefore, these molecules have attracted, during their development, particular attention as chemotherapeutic agents in medicinal chemistry because the consequences of DNA intercalation by exogenous molecules lead to a significant modification of the DNA structure and may result in a hindered or suppressed function of the nucleic acid in physiological processes. But the clinic application of these compounds has shown some problems such as multidrug resistance (MDR), and secondary and/or collateral effects. These shortcomings have motivated the search of new compounds to be used either in place of, or in conjunction with, the existing molecules.

Condensed poly(hetero)aromatic compounds are usually regarded as representative DNA intercalators, especially if they contain electron-deficient or charged aromatic cores in the structure. Measurement of the binding constant and biological activity of DNA-intercalator complexes and QSAR studies lead to the conclusion that there should exist a relationship between cytotoxic activity and binding force. Otherwise, cytotoxicity is not only dependent on the ability to interact with DNA, since there are many DNA intercalators that are incapable of working as cytotoxic agents: to be effective, a drug must first overcome many barriers, including metabolic pathways, cytoplasmatic and nuclear membranes. Cytotoxicity could be also a consequence of the

poisoning of topoisomerases, enzymes that are directly involved in DNA recognition and that regulate DNA topology. They induce cytotoxicity when they act as poisons towards the enzymes by stabilizing the ternary DNA-intercalator-topoisomerase complex in such a way that the enzymatic process cannot continue forward or backward. This complex is detected by the cell as a damaged portion, which triggers a series of events such as cell apoptosis.

Some compounds, called photonucleases, which induce DNA damage after UV-VIS-irradiation, have become interesting; while the association of cationic dyes to DNA is a reversible process, the DNA damage, which frequently occurs on irradiation of ligand-DNA complexes, is often irreversible. The latter DNA damage may lead to cell death or mutation, and must be avoided in healthy systems. However, this photoinduced DNA-damage may be applied in photochemotherapy to remove unwanted cells.

Among the compounds investigated along these lines, the quinolizinium derivatives, such as coralyne and the related molecules, have attracted particular attention. They are arenes containing quaternary bridgehead nitrogen atom and have been shown to bind to DNA and may be employed as a central unit in DNA-targeting drugs. During the studies of the influence of the substituition pattern of quinolizinum derivatives on their intercalation with DNA, it has been shown that the chemical structure of the tetracyclic naphtho[1,2-*b*]quinolizinium bromide **2** has interesting properties with respect to the binding to nucleic acids. In particular, these intercalators may exhibit a stronger interaction with nucleic acids as compared with the tricyclic benzo[*b*]quinolizinium **1:** the additional benzene moiety extends the surface of the planar chromophore and increases the π stacking between the dye and the DNA bases, resulting in higher binding constants. Other important aspects are represented by the photobiological properties: it was shown that an efficient DNA-strand cleavage is photoinduced by the naphtho[1,2-*b*]quinolizinium bromide **2**.

The compounds synthesized and analyzed in this project were 3-aryl-substituted-naphtho[1,2-*b*]quinolizinium derivatives; then studies about the DNA-binding properties and cytotoxic activity were carried out. The investigation of these compound allows to evaluate the effects of the extension of π system, by the introduction of fourth aromatic ring, and the effects of the substituent in position 3. This position was chosen for structural analogy with some tricyclic benzo[*b*]quinolizinium **1**, with better biological activity with respect to the not-substituted compound. After these, experiments in comparison to the naphtho[1,2-*b*]quinolizinum bromide **2**, without

substituents in position 3, to investigate preliminary molecular target (topoisomerase I and II), to attempt a structure-relactionship-activity and finally photobiological tests will be carried out.

RIASSUNTO

Le neoplasie risultano essere una delle più importanti cause di morte nel mondo: negli Stati Uniti il cancro rappresenta la seconda causa di morte dopo le malattie cardiovascolari. Quindi la ricerca, la scoperta e lo sviluppo di nuovi composti a potenziale attività antitumorale è considerato uno dei più importanti obiettivi in campo della chimica farmaceutica, cercando anche di distinguere in termini di citotossicità le cellule sane da quelle cancerose e malate. Ad oggi, molti approcci terapeutici sono disponibili per il trattamento del cancro in ambito clinico: chirurgia, radioterapia sono usate nel trattamento di tumori localizzati; chemioterapia, terapie ormonali, immunoterapia si sono invece rivelate utili nella cura di leucemia e tumori metastatici. Nell'approccio chemioterapico un alto numero di molecole interagisce con gli acidi nucleici come groove binders, agenti alchilanti e intercalanti. Le molecole che appartengono a quest'ultima classe interagiscono con il DNA intercalandosi appunto fra le coppie di basi attraverso interazioni di Van der Waals, legami idrogeno, legami idrofobici e/o interazioni di carica. Molte di queste molecole hanno suscitato particolare interesse durante il loro sviluppo come potenziali agenti chemioterapici perché è noto che una conseguenza dell'intercalazione da parte di molecole esogene nella doppia elica è proprio una modifica strutturale e chimico-fisica della struttura che vede come risultato un'alterata o arrestata funzione del DNA nei processi fisiologici. Ma l'applicazione clinica di questi composti ha mostrato problemi in termini di insorgenza di resistenze (MDR), effetti secondari o collaterali. Questi inconvenienti hanno spinto alla ricerca di nuovi composti che potessero sostituire o migliorare i composti già esistenti.

I poli(etero)cicli aromatici condensati sono solitamente considerati buoni agenti intercalanti, specialmente se nel core aromatico presentano cariche positive.

Gli studi sulla valutazione quantitativa della costante di binding e sull'attività biologica dei complessi DNA-agenti intercalanti e di QSAR hanno portano alla conclusione che potrebbe esistere una relazione tra attività citotossica e forza di binding. Comunque la citotossicità non è soltanto dipendente dall'abilità a interagire con il DNA, dal momento che alcuni intercalanti si sono rivelati anche non citotossici: infatti per poter esercitare il suo effetto, un farmaco deve prima passare barriere, vie metaboliche, membrane

citoplasmatiche e nucleari. La citotossicità può anche essere conseguenza dell'azione di veleno contro le topoisomerasi, enzimi direttamente coinvolti in processi che coinvolgono gli acidi nucleici in fondamentali steps della crescita cellulare e regolano la topologia del DNA. Gli intercalanti del DNA possono esplicare un'azione citotossica attraverso stabilizzazione del complesso DNA-intercalatore-topoisomerasi in modo che il ciclo biochimico venga bloccato. Questo complesso con il DNA danneggiato poi può essere riconosciuto dalla cellula che attiva una serie di vie biochimiche che portano all'apoptosi.

Si sono rivelati anche interessanti quei composti, chiamati fotonucleasi, che inducono danno al DNA dopo irradiazione con luce UV-VIS; mentre l'associazione di cationi organici al DNA è un processo reversibile, il danno al DNA generato dopo irradiazione del complesso ligando-DNA è spesso irreversibile e questo può portare a morte cellulare, mutazioni che dovrebbero essere evitati in sistemi sani. Comunque, un fotodanno al DNA potrebbe essere applicato in fotochemioterapia al fine di rimuovere cellule malate.

Tra i composti studiati in tutto questo contesto, i derivati del chinolizinio, come la coralina e molecole correlate, hanno suscitato particolare interesse. Essi constano di anelli aromatici condensati con una carica positiva sull'azoto quaternario e hanno mostrato di legare il DNA. Durante gli studi sulle modifiche chimiche del chinolizinio in termini di legame al DNA, è stato mostrato che la struttura chimica tetraciclica del nafto[1,2-*b*]chinolizinio bromuro **2** presenta interessanti proprietà di binding agli acidi nucleici: in particolare viene osservata una forte interazione se comparata al derivato triciclico benzo[*b*]chinolizinio **1,** dovuta all'addizione del quarto anello aromatico che estende la superficie planare del cromoforo ed aumenta le interazioni π tra il composto e le basi del DNA. Altro aspetto importante è rappresentato dalle attività fotobiologiche: è stato mostrato che esiste un efficiente taglio del DNA fotoindotto appunto dal nafto[1,2-*b*]chinolizinio bromuro **2**.

In questo progetto di ricerca sono stati analizzati e sintetizzati derivati 3-aril del nafto[1,2-*b*]chinolizinio; e successivamente sono stati effettuati studi per determinare la tipologia di binding al DNA e l'attività citotossica. Particolare attenzione è stata riposta sulla valutazione dell'effetto dell'introduzione del quarto anello aromatico e della sostituzione in posizione 3. Quest'ultima posizione è stata scelta in analogia a alcuni derivati del triciclico benzo[*b*]chinolizinio **1** con migliore attività biologica rispetto alla molecola di partenza. Successivamente prendendo come riferimento il nafto[1,2-

b]chinolizinio bromuro **2**, senza quindi sostituenti in posizione 3, si sono condotti studi preliminari sull'identificazione, oltre agli acidi nucleici, di un probabile target molecolare (topoisomerasi I e II); si è cercato di ipotizzare una relazione struttura-attività e infine di valutare l'attività fotobiologica.

1. INTRODUCTION

1.1 CANCER AND CHEMOTHERAPY

Cancer derives from modifications of the genes responsible for cell growth and repair. Normally, healthy cells are under strict control for growth and differentiation. Cells divide and proliferate under influence of various growth stimulators and are subject to arrested growth (senescence) and programmed cell death (apoptosis). In cancer, these regulatory processes have gone awry, and cells grow and divide uncontrollably, losing the structure due to the inability to adequately differentiate. Furthermore, the uncontrolled cell division is accompanied by deactivation of the processes of cell death even leading to genetic alterations.[1] The factors that can cause and generate the cancer are numerous: genetic factors, ultraviolet (UV) and ionizing radiations, chemical carcinogens, biological carcinogens, such as infections by virus (Hepatitis B Virus, Human Papilloma Virus), bacteria (Helicobacter pylori).[2] Anyway all these causes lead to an alteration of the expression of proto-oncogenes whose products control the normal life of the cell; when these genes mutate to become oncogenes, through various steps, leading to the formation of a tumor cell. At the same time, tumor suppressor genes can also be inhibited (*p53, p-21*). In USA every year, 1,3 million cases of cancer are diagnosed, provoking almost 570.000 deaths.[3]

Therefore, the research, the discovery and the development of new compounds with antitumoral activity have become one of the most important goals in medicinal chemistry.

Currently, there many therapeutic approaches are for the treatment of cancer: surgery and radiotherapy, useful techniques to remove localized cancer; systemic treatments, as chemotherapy, hormone-therapy and immunotherapy, useful for leukemia or metastatic tumour. Chemotherapy is based on the use of chemical compounds, which, by a cytotoxic action, can produce antiproliferative effects. In order to have an anticancer drug without side effect, many researchers try to find and to identify specific target, because there are little differences between cancer and somatic cells. Another increasing problem is the chemoresistance due to molecular changes of specific pump or particular membrane protein, such as the class of MDR (*Multi Drug Resistence Proteins*), which decrease the therapeutic action of drugs; the classic form of MDR is due to an increased activity of P-glycoprotein (Pgp), encoded by the human *MDR1* gene. This glycoprotein is located in the plasma membrane and can extrude a range of hydrophobic natural

product drugs from the cell against a concentration gradient. An increase in Pgp activity can result in lowered intracellular drug concentration and, hence, in drug resistance.[4,5] So, at the moment, polychemotherapy is the main strategy against.[6]

The anticancer agents can be classified on the basis of their different mechanism of action.[1]

Alkylating agents

They form a covalent binding to DNA involving base modifications through alkylation by a nucleophilic attack of N7 of a guanine of DNA to the electrophilic part of the drug forming a monoalkylated adduct. Some agents (nitrogen mustards) can also bind two bases of DNA involving two guanine (N7) residues determining the formation of DNA-crosslink between two complementary strands (interstrand) or within a strand of DNA (intrastand), as the case of cisplatin. All these reactions induce a irreversible damage in the double helix and to DNA replication.[1]

Antineoplastic antibiotics

They belong to a high number of natural or semi-synthetic compounds which block DNA-transcription inducing breaks to the DNA structure or inhibiting important enzymes for the DNA-replication process. They can interact directly with DNA, intercalating into double helix in the base pairs, by a strong non-covalent interaction.

Some of these compounds inhibit the topoisomerase II, enzyme responsible for maintaining the correct structure of DNA.[1]

In this class, some compounds, called “code reading agents”, can be considered: they are able to recognize and bind specific sequence of the double helix of DNA by non-covalent interaction. As mentioned before, intercalators and groove binders belong to this class of compounds. Intercalation occurs when ligands of an appropriate size and chemical nature fit themselves in between base pairs of DNA. These ligands are mostly polycyclic, aromatic, and planar[7] and they induce local structural changes to the DNA strand (such as lengthening of the DNA strand or twisting of the base pairs), leading to functional changes such as the inhibition of transcription and replication and DNA repair processes. Formed complexes deform and unwind the DNA, thus they can be applied in the chemotherapeutic treatment to inhibit DNA replication in rapidly growing cancer cells. Examples include doxorubicin and daunorubicin (used in treatment of Hodgkin's lymphoma), and dactinomycin (used in the treatment of Ewing's

Sarcoma). Groove binders are usually cationic molecules that bind in the minor or major groove of DNA.[8]

Antimetabolic agents

They act as false substrates: the chemical structural analogy with one of the metabolites normally present in the cells is used to induce a block of the enzymatic system (polymerases) or the synthesis of inactive substances or with another function, provoking a stop or the destruction of the cancer proliferative apparatus. These compounds are not selective, although the malignant cells have an intensive proliferation. Some examples of these agents are the antagonist of the folic acid (metotrexate) and the analogous of the purinic (6-mercaptopurine) and pyrimidinic bases (5-fluorouracil).

Antimitotic agents

They are natural alkaloid or semi-synthetic compounds which interfere with the normal process of polymerization-depolymerization of heterodimer α-β of the tubulin inducing a damage to structure of microtubules and causing cell death. Some molecules of this class are taxol and the alkaloids of Vinca (vinblastine, vincristine).[1]

Quadruplex-interactive agents

There are special sequences in DNA that can form secondary DNA structure; there are some of these that are rich in guanine and are capable of forming a four-stranded structure (G-quadruplex structure), further stabilized by the presence of a cation, especially potassium, which sits in a central channel between each pair of tetrads.[9] Telomeres and promoters with polypurine-rich strand can induce G-quadruplex and the helicases control the equilibrium between double-strand and G-quadruplex. The drugs can inhibit helicases or facilitate the formation of new quadruplex. They can also sequester newly formed G-quadruplex (telomestatin).[10]

Topoisomerase inhibitors

DNA is also considered a scaffold on which DNA-binding proteins assemble. These proteins are involved in replication, transcription, recombination and repair, crucial processes for normal cellular growth. So a good strategy is blocking the binding protein-DNA. Some agents can act inactivating enzymes, as topoisomerase I (i.e., CPT)

or topoisomerase II: some of these (i.e., doxorubicin) can also binding DNA, while others can bind only on topoisomerase (i.e., etoposide), not interfering directly with other DNA processes.[1,11,12]

Hormone therapy

Glucocorticoid compounds are used as antitumoral agents in leukemia and lymphoma. Antiestrogens (tamoxifene) or antiandrogens (cyproterone), can be used for hormone-dependent cancer (breast and prostate carcinoma).[1]

1.2 DNA

Deoxyribonucleic acid (DNA) is a nucleic acid that contains the genetic instructions used in the development and functioning of all known living organisms and some viruses. The main role of DNA molecules is the long-term storage of information. It contains the instructions needed to construct other components of cells, such as proteins and RNA molecules. The DNA segments that carry this genetic information are called genes, but other DNA sequences have structural purposes, or are involved in regulating the use of this genetic information. Within cells, DNA is organized into long structures called chromosomes. During cell division, these chromosomes are duplicated in the process of DNA replication, providing each cell its own complete set of chromosomes. Eukaryotic organisms store most of their DNA inside the cell nucleus and some of their DNA in organelles, such as mitochondria or chloroplasts.[13]

All the functions of DNA depend on interactions with a large number of enzymes: the polymerases that copy the DNA base sequence in transcription and DNA replication;[14] the topoisomerases to maintain the correct topological structure;[12] the nucleases and ligases,[15,16] used in DNA repair and genetic recombination; helicases for most processes where enzymes need to access the DNA bases.[17]

1.2.1 CHEMICAL STRUCTURE AND FORMS OF DNA

The double helical of DNA is composed by a chemical structure of nucleic acids that draw a linear polymer of nucleotide whose sugars are bonded through phosphodiester groups-bridges at 3' and 5' position. At physiologic pH, the phosphodiesters are acidic, so they show negative charges that determine the polyanionic structure. DNA is composed by the same percentage of nucleotides adenine (A), thymine (T), guanine (G), cytosine (C) (Figure 1.1).

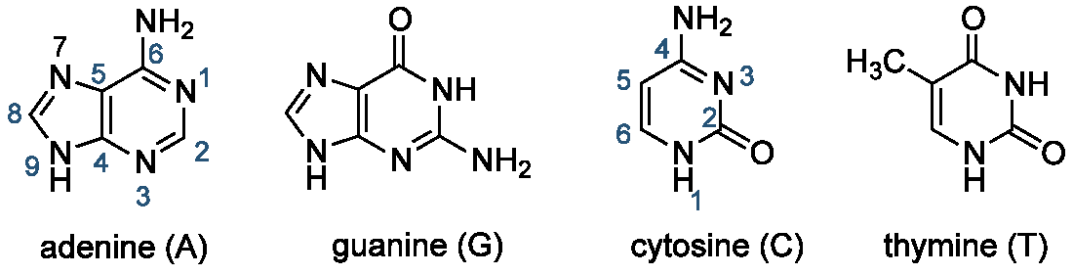

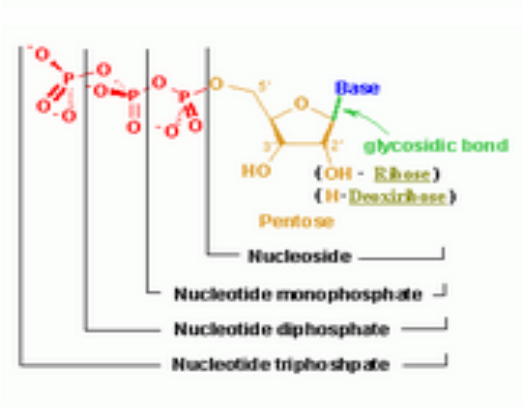

Figure 1.1 Schematic representation of nucleotides and sugar bonded to phosphodiester groups.

DNA is a structurally flexible polymorphic molecule that can adopt a variety of conformations. The main family of DNA forms identified are the right-handed A- and B-forms and the left-handed Z-form (Figure 1.2 and Figure 1.3).[18-20] But there are also many other structures like loops, hairpins or cruciforms, and higher order structures like triplexes,[21] quadruplexes[9] are known to exist.

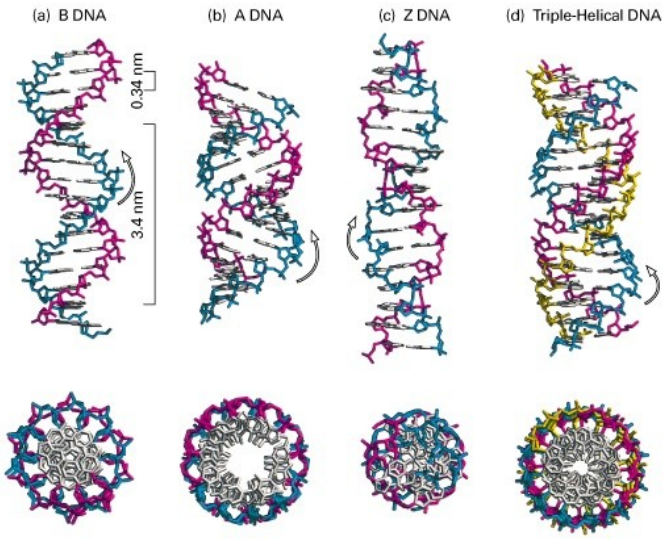

Figure 1.2 Schematic representation of B-, A-, Z- and triplexes structures of DNA

	A-DNA	B-DNA	Z-DNA
Helical sense	Right-handed	Right-handed	Left-handed
Diameter	~26 Å	~20 Å	~18 Å
Base pairs per helical turn	11.6	10	12 (6 dimers)
Helical twist per base pair	31°	36°	9° for pyrimidine–purine steps; 51° for purine–pyrimidine steps
Helix pitch (rise per turn)	34 Å	34 Å	44 Å
Helix rise per base pair	2.9 Å	3.4 Å	7.4 Å per dimer
Base tilt normal to the helix axis	20°	6°	7°
Major groove	Narrow and deep	Wide and deep	Flat
Minor groove	Wide and shallow	Narrow and deep	Narrow and deep
Sugar pucker	C3′-*endo*	C2′-*endo*	C2′-*endo* for pyrimidines; C3 -*endo* for purines
Glycosidic bond	Anti	Anti	Anti for pyrimidines; syn for purines

Source: Mainly Arnott, S., *in* Neidle, S. (Ed.), *Oxford Handbook of Nucleic Acid Structure, p.* 35, Oxford University Press (1999).

Figure 1.3 Parameters of A-, B- and Z-DNA double helices.

The A-form of DNA is a right-handed double helix, with a short and compact helical structure. It can occur only in DNA-RNA hybrid helices and by regions of double-stranded RNA. A-DNA is characterized by base pairs that are highly inclined and displaced away from the helix axis and a helical repeat of 11 bp per turn[22] and the base pairs tilt to 19 degrees with respect to helix axis. This from has a shallow minor groove and a very deep major groove. In addition the sugar has the C3'-endo conformation.[20]
The Z-form is a left-handed double helical structure and occurs in part of DNA rich in guanine and cytosine. The Z-DNA is long and thin and the bases are relatively farther

from the helix axis, creating a deep narrow minor groove, while the major one is not properly a groove. Formation of this structure is generally unfavourable, although certain conditions can promote it, such as alternating purine-pyrimidine sequence (especially poly(dGC)$_2$), negative DNA supercoiling and some cations (all at physiological temperature, 37°C, and pH 7.3-7.4).[23] Z-DNA is a transient structure that is occasionally induced by biological activity and then quickly disappears.[24]

The B-form of DNA is the most common structure, the native conformation of DNA in solution under physiological conditions. It is a right-handed form and the two polynucleotide chains run in opposite directions (antiparallel). The aromatic bases are located internally in the helix, while the phosphate backbone are externally exposed. The sugars are 2'-deoxyribose and are bonded with bases in 1' position and with phosphates in 5' and 3' positions (Figure 1.4). The plane of the bases are perpendicular respect to the double helix axis.

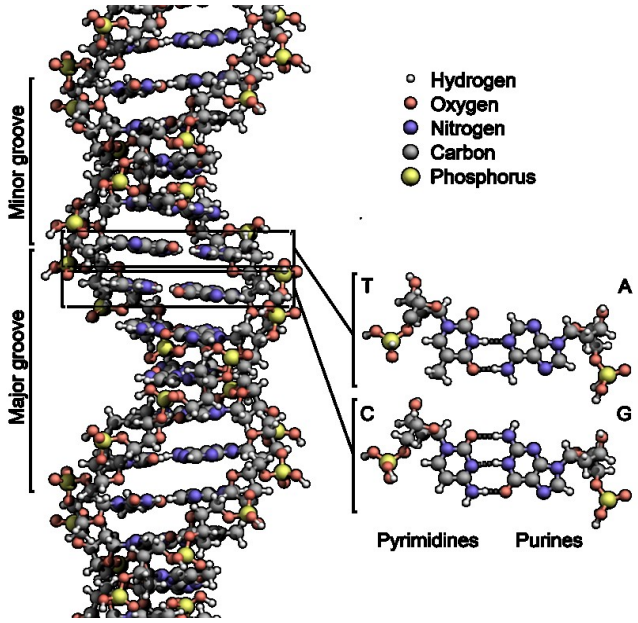

Figure 1.4 Schematic representation of nucleotides and sugar bonded to phosphodiester groups and chemical structure of DNA helix.

The ideal B-DNA has a pitch of 34 Å, because are involved 10 base pairs (bp) per turn and the aromatic rings have a thickness of 3,4 Å. Every base pair axis turn of 36° respect to the axis of the adjacent pairs (Figure 1.4). Bases of opposite strands are coupled through hydrogen bond interactions; the adenine of one strand is coupled to the thymine in the opposite one and any guanine interacts with cytosine (Figure 1.5).

Figure 1.5 Hydrogen bonding in the A·T and C·G Watson-Crick DNA base pairs.

B-DNA presents two external grooves of different size generated by the structure of the two strands of the helix, between the ribose-phosphate backbone and the inner surface of macromolecule (Figure 1.6 and Figure 1.7): the bases in these grooves are exposed to the solvent and this is important because they are available to specific interaction with chemical molecules.

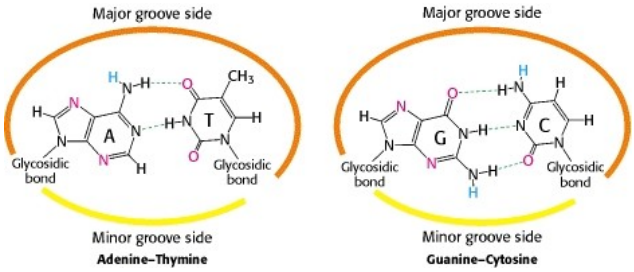

Figure 1.6 Chemical representation of major and minor groove.

The major groove is wide and easily accessible to proteins, while minor groove is narrow; this conformation is favoured at high water concentrations.

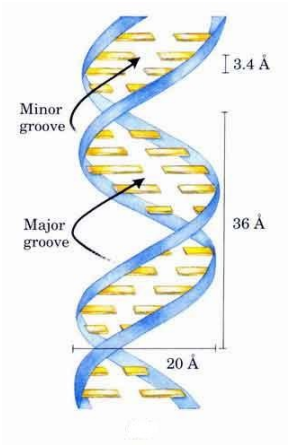

Figure 1.7 B-DNA double helix with the minor and major grooves highlighted.

In order to reduce he tension of sugar ring, four atoms remain almost co-planar and the fifth one stays slightly out of the plane. This determines two conformations: if the out-of-plane atom is on the same side of C5' substituent, it is called *endo*; if it is on the opposite side of C5' it is called *exo*. Generally the out-of-plane atoms are either C2' and C3' (Figure 1.8).

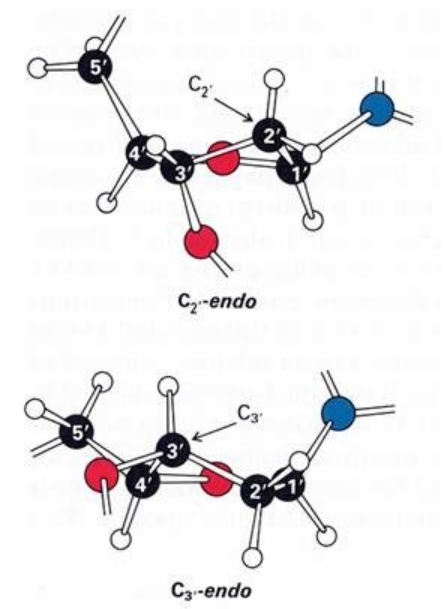

Figure 1.8 Schematic representation of C2'-endo and C3'-endo sugar conformation.

With respect to the glycosidic bond, purine residues may assume two sterically possible conformation, *syn* and *anti* (Figure 1.9), while for pyrimidines only the anti is acceptable (in the syn conformation the C5' atom of sugar would be too close to C2 substituent of base). Generally all bases of B-form DNA are in anti conformation.

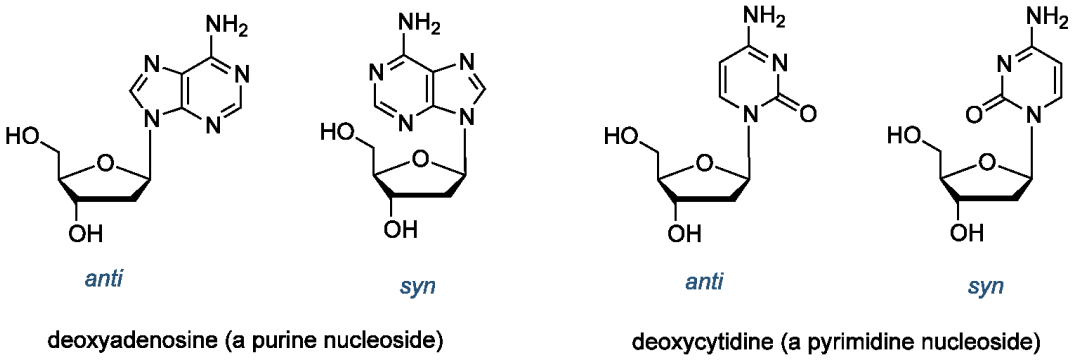

Figure 1.9 Structures of *syn* and *anti* nucleoside conformations.

1.3 INTERACTION AND BINDING MODES OF ORGANIC MOLECULES WITH DNA

The interaction between external molecules and the nucleic acids and the formation of a complex leads to important modifications of the structure of the DNA and may have an important influence on the physiological function of the DNA, such as the suppression of the DNA replication and gene transcription leading to cell death, useful in an antiproliferative approach. So an important goal is the design of DNA-binding molecules which selectively bind to DNA in unwanted cells and lead to cell death without damaging the healthy cells. In these years, many investigations have been performed to clarify different aspects of the association process of large and small molecules with DNA identifying several classes of DNA-binding molecules: some macromolecules as the proteins, after association with DNA, constitute important steps in the gene-transcription process; the oligosaccharides, organometallic complexes and cationic organic dyes.[7,25,26]

There are three binding modes between a molecule and DNA (Figure 1.10): external binding due to attractive electrostatic interactions between a positively charged molecule and the negatively charged phosphate backbone of the DNA and it occurs on the external surface of the double helix,[27] and the most common minor or major groove binding and intercalation.[25]

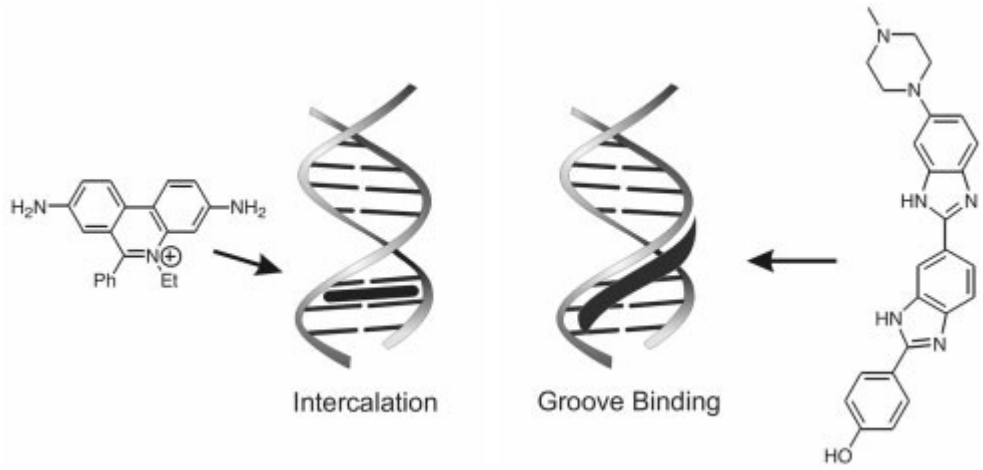

Figure 1.10 Binding modes of small molecules with DNA.

1.3.1 GROOVE BINDING

The DNA helix has two grooves of different size, the minor and the major grooves, which can represent binding sites for guest molecules. Large molecules, like proteins, prefer to bind to the major groove, while small ligands prefer the minor groove. The chemical structure of groove binders presents two aromatic or heteroaromatic rings whose connection allows conformational flexibility and so the molecule can fit into the groove. Additional functional groups can be required to improve the interaction, that usually occurs by hydrogen bonding and hydrophobic.[28] Typical minor-groove binders are Hoechst 33258, netropsin (Figure 1.11). Most groove binders have selectivity and affinity toward AT-rich region because in this area the electrostatic attraction is higher than in GC-rich one and furthermore, the grooves, which consist of GC base pairs, are sterically hindered by the guanine amino functionality at C-2 and its hydrogen bond with the C-2 carbonyl group of cytosine. Anyway, the groove binders with a structure that can form strong attractive interactions with the guanine amino group can also bind GC-rich grooves.[25]

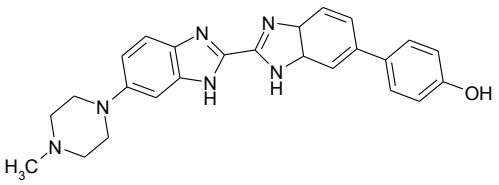

Hoechst 33258

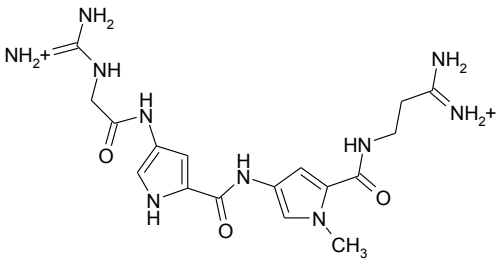

Netropsin

Figure 1.11 Examples of minor-groove binders.

1.3.2 INTERCALATION

In DNA helix, the bases are located in an almost coplanar arrangement. It has been shown the planar polycyclic aromatic molecules to intercalate between two base pairs[25] through a binding mode realized by dipole-dipole interactions and π stacking[29] of the ligand with the aromatic nucleic bases. The intercalation has a significant influence on the DNA structure because it causes DNA unwinding, leading to a lengthening of the helix of more than 3.4 Å, along with a significant change of deoxyribose conformation.
In order to describe theoretically the intercalation, this "neighbour exclusion principle" has to be considered. It can be used as general rule, but not totally explained; a hypothesis could be that the structural changes of DNA on intercalator lead to limited access to the neighbouring binding pocket for steric reasons.[25]
The intercalators have an appropriate size and chemical nature to fit themselves in between base pairs; they are mostly polycyclic (at least two annellated aromatics rings), aromatic, and planar, and therefore often make good nucleic acid stains.[7] In most cases, a positive charge is required for an appropriate binding affinity, in order to enhance the attractive ionic interactions between the cation and the phosphate backbone. So it's easy to think that the pH of the environment has a significant influence on the DNA-binding properties of such ligands. It is interesting the possible introduction of the cationic nitrogen atom as a bridgehead between two annelated rings, as the quinolizinium ion and related derivatives.[30,31] In these cases, the charge is independent of the pH of the environment. The compounds analyzed in this project are derivatives belong to the family of naphthoquinolizinium ion.

The structural modifications after the intercalation can lead to functional changes, often to the inhibition of transcription and replication and DNA repair processes, which makes intercalators potent mutagens. For this reason, DNA intercalators are often carcinogenic, (proflavine[7], ethidium bromide,[26] protoberberine[32]) (Figure 1.12).

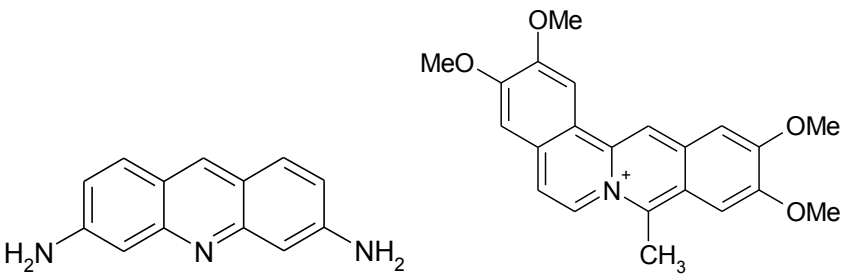

Proflavine **Coralyne**

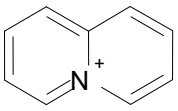

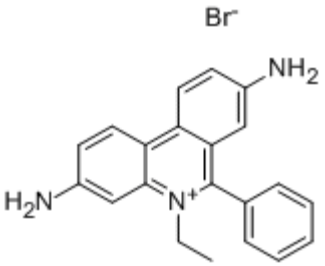

Quinolizinium ion **Ethidium bromide**

Figure 1.12 Examples of intercalators.

DNA binding of an intercalator and its biological activity can be connected. However, cytotoxicity is not only dependent on the ability to interact with DNA because to be effective, a drug must first overcome many barriers, such as cytoplasmatic and nuclear membranes. When it is in the nucleus, it can form a complex with a relatively long half-life. Cytotoxicity could also be a consequence of the binding with some essential proteins, associated with double helix, as topoisomerase I and II, enzymes involved in particular steps of the cellular growth and of cell cycle, in which the topology of the DNA plays a significant role. A damage of DNA usually can lead to a series of events that involve p53 protein, and subsequent apoptosis. Anyway, many efforts are still made to discover new compounds, in order to improve the selectivity and to overcome drug resistance.

1.3.3 EVALUATION AND DETERMINATION OF BINDING MODE

In a host-guest complex, the physical properties of the DNA and the intercalator or groove binder are usually significantly different from those of the uncomplexed host and guest molecules. Complex formation can therefore be assessed by monitoring a change of a particular physical property. The extent of this change usually depends on the binding mode and, thus, enables intercalators and groove binders to be distinguished. If the focus is on the properties of the DNA molecule, hydrodynamic methods such as the viscosity or the sedimentation coefficient are helpful for monitoring the association process. The thermodynamic stability of the DNA helix is also influenced by complex formation, so association with a guest molecule might also be determined by measuring a change of the melting temperature. Hydrodynamic methods are especially reliable and helpful for distinguishing the binding mode, because on intercalation the observed change of the DNA structure and thus the change of the viscosity or the sedimentation coefficient is relatively large whereas groove binding leads to marginal structural changes only. Absorption and emission spectroscopy are also useful tools for monitoring DNA-binding processes. The interaction of dyes, especially, with DNA can be conveniently observed by these methods, because their absorption and emission properties change significantly on complex formation. Along with straight forward determination of absorption or emission intensity and wavelength, several variations and additional experiments are possible. For example, absorption of circularly or linearly polarized light can be used in CD and LD spectroscopy to gain further knowledge of the orientation of the dye molecule relative to the DNA. It should be noted that determination of the binding mode needs to be performed with much care and that the use of only one method can lead to misinterpretation. In critical reviews, it has been pointed out that only a combination of selected methods provides sufficient information to draw conclusions about the mode of binding. Anyway spectrometric methods are considered useful and practical tools for study of the DNA-binding properties of organic dyes.[25]

1.4 CELL CYCLE

The cell cycle is an ordered set of events that lead to biochemical modifications of the cell, culminating in cell growth and division into two daughter cells. It is based upon the rotation of two principal periods: interphase and mitosis (Figure 1.13). The first one can be divided into four steps: G0 (Gap or growth 0), G1 (Gap or growth 1), S (synthesis) and G2 (Gap or growth 2):

- **G0 phase:** is a period of the cell cycle in which cells exist in a quiescent state. G0 phase is viewed as either an extended G1 phase, where the cell is neither dividing nor preparing to divide, or a distinct quiescent stage that occurs outside of cell cycle. On occasion, a distinction in terms is made between a G0 cell and a quiescent cell (heart muscle cells, neurons i.e.,) which will never enter in G1 phase, whereas other G0 cells may. Cells enter the G0 phase from a cell cycle checkpoint in the G1 phase, such as a restriction point. In order to overcome it, growth factors or nutrients are required. In absence of these, the cells remain quiescent without growing and dividing. If these are present and correct, the cells may re-enter in the cycle and subsequently divide.

- **G1 phase**: during this phase the biosynthetic activities of the cell resume at high rate. The cells increase in size, synthesizing RNA and proteins, which will be useful for DNA replication.

- **S phase**: it starts with DNA synthesis; the amount of DNA in the cell has effectively doubled; when it is complete, all of the chromosomes have been replicated. Rates of RNA transcription and protein synthesis are very low during this phase.

- **G2 phase**: during the gap between DNA synthesis and mitosis the cell continues to grow and produces new proteins, involved principally in the production of microtubules, required in the next process of mitosis. Inhibition of protein synthesis during G_2 phase prevents the cell from undergoing mitosis.

- **Mitosis or M-phase**: it can be divided into five stages: prophase, prometaphase, metaphase, anaphases and telophase and it is the process by which a eukaryotic cell separates the chromosomes in its cell nucleus into two identical sets in two nuclei.[33] It is followed by cytokinesis, during which there is the division of the cytoplasm, organelles and cell membrane into two daughter cells containing roughly equal shares of these cellular components. There is also here a checkpoint (Metaphase checkpoint) that ensures the cell is ready to complete cell division.[34]

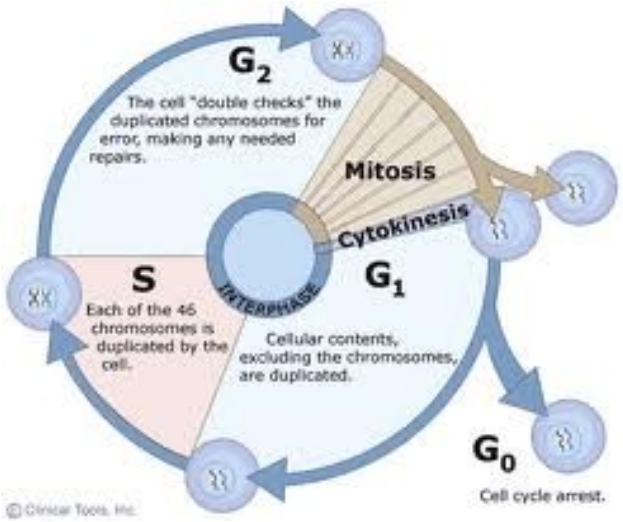

Figure 1.13 Schematic representation of cell cycle.

1.4.1 CELL CYCLE REGULATION

The cell cycle contains numerous checkpoints that allow the cell to check for and repair DNA damage,[35] regulate the progress of cell cycle and they are designed to ensure that damaged or incomplete DNA is not passed on the daughter cells. The cell cannot proceed to the next phase until checkpoint requirements have been met.

The control is of regulated by cyclins and cyclin-dependent kinases (CDKs):[36] cyclins, with their bound and activated CDKs, function during distinct stages of the cell cycle. The level of each cyclin independently increases or decreases within the phases of the

cycle. Cyclin/CDK complexes phosphorylate specific protein substrates to move the cell through the cycle with activation of DNA synthesis (in late G1 and S), and formation of the structural components associated with mitosis (in late G2 and M). So, two important checkpoints[34] are determined: G1/S that ensures that everything is ready for DNA synthesis and G2/M that ensures if the cell can proceed to enter M-phase and consequently division. The periodicity of the cyclins, mediated by their synthesis and subsequent proteolytic degradation, ensures the well-delineated transitions between cell cycle stages.[37]

Furthermore, the p53 protein plays an important role in triggering of the control mechanisms at both checkpoints. A disregulation of the cell cycle components may lead to tumor formation. Some genes like the cell cycle inhibitors (p53), mutating, may cause an uncontrollably cell proliferation, forming a tumor. So, the cell cycle machinery and components of checkpoint pathways have already provided a large number of targets for novel antineoplastics.[38]

1.5 TOPOISOMERASE I AND II

The topological state of DNA in the cell is modulated by enzymes known as DNA topoisomerases, essential enzymes that act (by over- and underwinding, knotting, tangling) in connection with a number of nuclear processes, such as replication, transcription, chromatin remodeling, chromatin condensation/decondensation, recombination and repair. Topoisomerases maintain genomic integrity during this process by forming covalent attachments between active site tyrosyl residues and the terminal DNA phosphates that are generated during the cleavage reaction. As a consequence of their reactions mechanism, these enzymes alter only the spatial orientation of the double helix: the chemical structure of DNA product generated by them is identical to those of their initial substrate molecules.[39-41.]

Cells encode two classes of topoisomerases that are distinguished by their catalytic mechanisms. Type I topoisomerases act by generating a transient single stranded break in the double helix, followed by either a single-stranded DNA passage event or controlled rotation about the break. As a result, these enzymes are able to alleviate torsional stress (i.e., remove superhelical twists) in duplex DNA.

Eukaryotic type I topoisomerases are monomeric enzymes that require no high-energy cofactor and are organized into two subclasses: type IA and type IB. These enzymes alter topology by creating transient single-stranded breaks in the DNA, followed by passage of the opposite intact strand through the break (type IA) or by controlled rotation of the helix around the break (type IB).[12]

Type II topoisomerases act by generating a transient double-stranded DNA break, followed by a double stranded DNA passage event. Consequently, these enzymes are able to remove superhelical twists from DNA and resolve knotted or tangled duplex molecules. Type II topoisomerases function in numerous DNA processes and are required for recombination, the separation of daughter chromosomes, and proper chromosome structure, condensation, and decondensation.[40] Two isoforms of the type II enzyme are known: topoisomerase IIα and IIβ. Topoisomerase I and II have been shown to represent the principal targets of effective antitumor drugs and, hence, have deserved investigation to understand the biochemical and pharmacological basis of drug action.[54] Indeed, topoisomerase poisons, such as antitumor drugs, transform these essential enzymes into lethal DNA-damaging agents increasing the concentration of covalent topoisomerase-cleaved DNA complex. As result of this action, drugs "poison" topoisomerases and convert them to potent cellular toxins that generate breaks in the genetic materials of treated cells.[11,42]

1.5.1 TOPOISOMERASE I

The reaction of topoisomerase I with DNA (Figure 1.14) starts with the binding of the enzyme to the double-stranded superhelical DNA. After binding, the enzyme makes a transient single-stranded break in the double helix, followed by either a single-stranded DNA passage event or controlled rotation about the break; religation and dissociation take place subsequently. In details, the interaction enzyme-DNA is controlled to a large extent by the surface and charge complementarity of the two reacting species. The conformational adaptation of the two partners results in the formation of a tight complex whereby the active site tyrosine of human topoisomerase I (Y723) is brought into a favourable position for attack of the facing DNA strand and subsequent formation of a covalent adduct. After the cut, it happens the release of the superhelical tension by a

mechanism called controlled rotation.[43] Once the DNA is partially relaxed, the covalent intermediate in religated, leaving intact the Y723 residue ready for restarting the catalytic cycle.

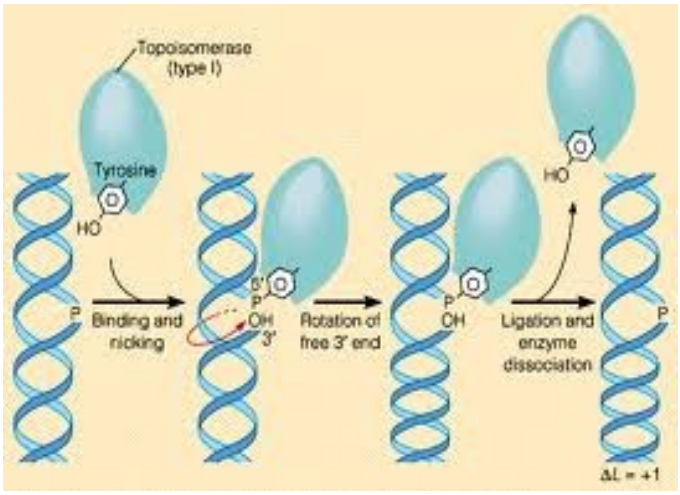

Figure 1.14 The topoisomerization reaction. Schematically, the cyclic process involves binding of topoisomerase I to DNA, followed by DNA cutting and then religation.

Chemically (Figure 1.15), topoisomerase I makes a nucleophilic attack with the tyrosine active site OH group to the ester of phosphate group. The transient covalent binary complex involves the attachment of the enzyme on DNA in the direction of 5'-phosphate, with the release of a free DNA strand containing a 3'-OH group.[42]

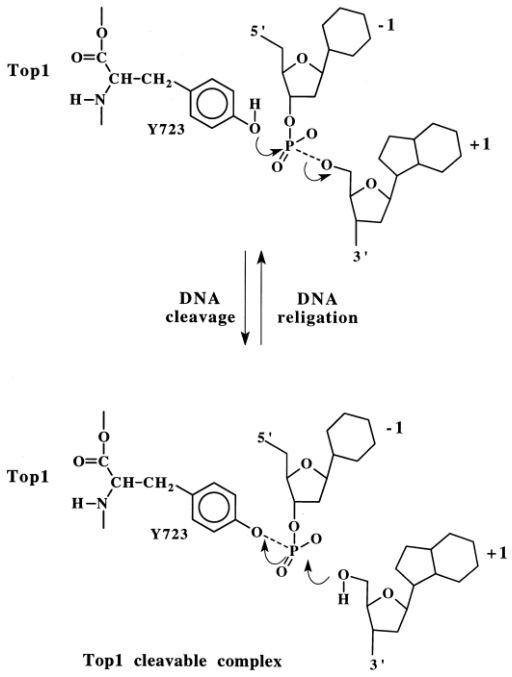

Figure 1.15 Chemical representation of the topoisomerization reaction: cleavage and religation. Y723 refers to the tyrosine involved in the transesterification reaction with the DNA. By convention, the bases flanking the top1 cleavage site are referred to as -1 and +1 for the bases at the 3'P and 5'P DNA termini, respectively.

Depending on the point of the reaction cycle at which the drugs, will act topoisomerase I inhibitor will reduce or increase the extent of DNA cleavage. An important number of topoisomerase I inhibitors have been identified, as coralyne,[44] benzimidoles, CPT (campothecin) and its derivatives, indolocarbazoles;[49] they can be divided into two classes:

- topoisomerase I suppressors correspond to compounds which inhibit the enzyme but do not stabilize the intermediate DNA-topoisomerase I covalent complex. They inhibit the binding of the protein to the DNA cleavage site, blocking the catalytic cycle;

- topoisomerase I poisons (CPT i.e.) act after cleavage of DNA by enzyme and inhibit the religation. The drug may freeze the enzyme-DNA complex by three ways: the enzyme binds to the preformed drug-DNA complex, the drug specifically recognized the enzyme-DNA complex or the drug-enzyme association interacts with DNA.

1.5.2 TOPOISOMERASE II

The reaction of topoisomerase II starts when the enzyme binds two separate segments of DNA. Then it creates a double-stranded break in one of the segments, translocates the second DNA segment through the cleaved nucleic acid "gate," rejoins (i.e., ligates) the cleaved DNA, releases the translocated segment through a gate in the protein, close the protein gate and regains the ability to start a new round of catalysis.[12] The scissile bonds on the two strands of the double helix that are cut by topoisomerase II are staggered and are located across the major groove from one another. Thus, the enzyme generates cleaved DNA molecules that contain four-base single-stranded ends at their 5'-termini. During its cleavage event, topoisomerase II covalently attaches to these newly generated 5'-termini. This covalent enzyme-cleaved DNA complex is known as the "cleavage complex".

Topoisomerase II requires two cofactors in order to carry out its catalytic double-stranded DNA passage reaction. First, it needs a divalent cation for all steps beyond enzyme–DNA binding, Mg^{2+} ; second, topoisomerase II uses the energy of adenosine triphosphate (ATP) to drive the overall DNA strand passage reaction: the protein binds two ATP molecules and undergoes a conformational change that causes the passage of the intact DNA segment through the cleaved double helix.

While ATP is not required for either DNA cleavage or ligation, the binding of this nucleoside triphosphate triggers the translocation of DNA through the double-stranded nucleic acid gate. ATP hydrolysis is necessary for enzyme recycling.

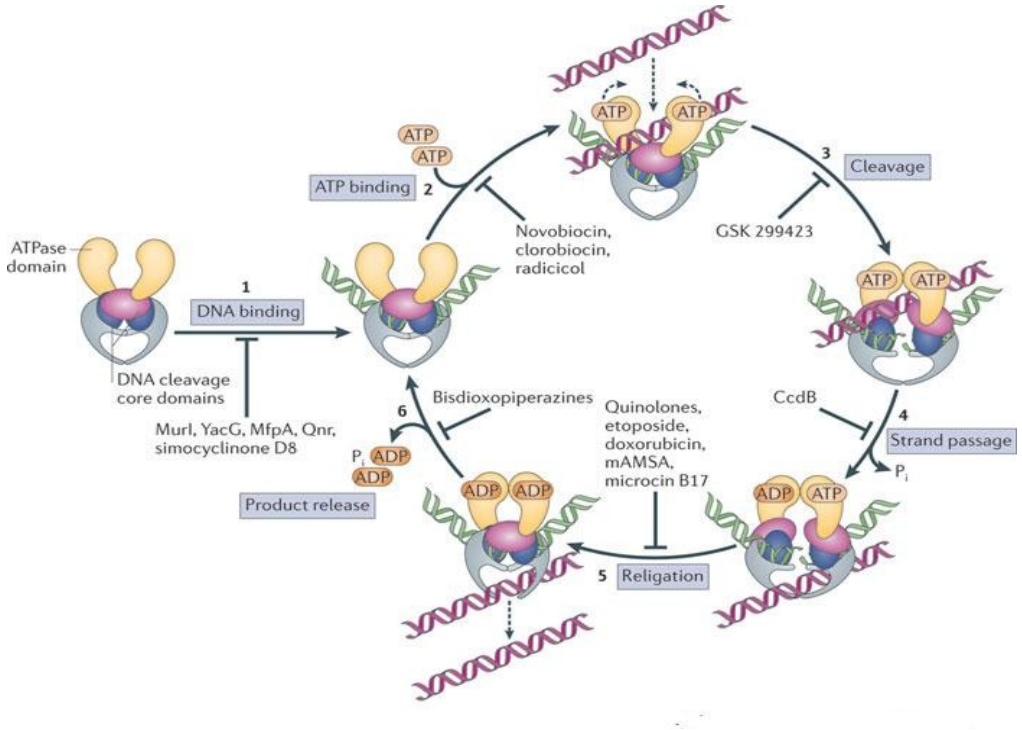

Figure 1.16 Schematic catalytic cycle of topoisomerase II and Effects of inhibitors on the catalytic cycle of topoisomerase II. The catalytic cycle of the tomoisomerase homodimer has been described previously as a series of six individual reaction steps. *Step 1*, topoisomerase II binds its DNA substrate. *Step 2*, a transient enzyme-linked double-stranded break is formed in the "cleavage" . *Step 3*, ATP binding induces a conformational change in the enzyme that converts topoisomerase II into a "protein clamp" on the DNA. Concomitant with this structural reorientation, the "passage" helix is translocated through the break in the cleavage helix. *Step 4*, the enzyme religates the break in the cleavage helix. *Step 5*, upon ATP hydrolysis, the protein clamp opens, allowing *Step 6*, release of the DNA and the initiation of a new round of catalysis. Drugs that inhibit topoisomerase II catalytic function act at different steps of the catalytic cycle.

Normally, topoisomerase II binds two molecules of ATP. Although ATP hydrolysis is not a prerequisite for the strand passage event, it appears that this step proceeds more rapidly if it is preceded by hydrolysis of one of the bound ATP molecules (Figure 1.16).[12,45-47] As a result of these processes, topoisomerase II can relax under- or overwound (negatively or positively supercoiled) DNA molecules and can remove knots and tangles from the genome. These events are essential for cell survival: in absence of enzyme, cells cannot segregate daughter chromosomes and die as a result of a mitotic failure.[48]

Topoisomerase II inhibitors can also be divided in two classes:

- topoisomerase II poisons (mitoxantrone, amsacrine, etoposide and other epipodophyllotoxins) act inducing the permanent formation of the cleavable

complex; their action can happen in three ways: the drug can increase the levels of enzyme-DNA cleavage complexes by interacting with topoisomerase II at the protein-DNA interface in a non-covalent manner; the drugs can act by covalently modifying of enzyme or the structure of DNA;

- topoisomerase II catalytic inhibitors (merbarone, aclarubicin), that inhibit the enzyme, but they are not able to induce the formation of cleavable complex.

Interesting is also a third class of compounds called "dual or mixed poison" because they act toward both type of topoisomerase (Tas 103 or DACA i.e.).[40]

1.6 UV RADIATION IN PHOTOTHERAPY AND PHOTOCHEMOTHERAPY

Ultraviolet light, characterized by its short wavelength, is able to pass through the different layers of the atmosphere and reach earth. Thus, wavelengths of the ultraviolet region of the spectrum, imperceptible to the human eye, are an inherent part of our everyday life.[49] The UV region (190-380 nm) used for photobiological studies, can be divided into four parts:[50] the radiations of UV-A region (320-400 nm) are considered harmless and responsible for pigmentation. They are biologically effective and causes cellular death, mutation, and DNA damage, although the primary chromophores for these effects may be non-DNA sensitizers that are chemically matched to the photon energy and act as intermediates relaying the absorbed energy to DNA. UV-A phototherapy that utilizes long wave UV-A radiation (340-380 nm) has been shown to be very effective in the treatment of several inflammatory skin diseases;[51] the radiations of UV-B region (290-320 nm) as cause of sunburn and photocarcinogenicity (cutaneous tumours). UV-B therapy is still the most frequently used phototherapeutic modality for the treatment of a variety of skin diseases (psoriasis, atopic dermatitis);[52] UV-C (200-290 nm) radiation is photobiologically active because of its mutagenic and antimicrobial activity.[49] In this range some important molecules for cell (DNA) functioning absorb. About Vacuum UV (10-190 nm), photons in this region are absorbed by water and oxygen (transparent indeed in UV regions above 190 nm). Because of this limited penetration, V-UV damage to cells is very weak.

In a biological system, the UV radiation can start a photochemical reaction of a compound such as decomposition, isomerization or rearrangement can occur and unstable photoproducts can react with endogenous molecules resulting in a biological effect.[49] UV radiation is toxic, mutagenic (changes the genotype of cells) and carcinogenic (probably by induction of specific oncogenes): so, DNA can be a chromophore and a target of this radiation. But the DNA can also be chemically modified as a result of the absorption of photon energy by a non-DNA chromophore. In this type of reaction, the compound itself may not be chemically changed by absorption of radiation, but photon energy is passed to another compound (such as DNA) which becomes changed in turn. This process is called photosensitization and the chromophore is the photosensitizer. Often, molecular oxygen becomes activated in the photosensitization process to form reactive species: the interaction of light, photosensitizer and oxygen is also known as photodynamic action. A compound that absorbs UV-A photons in living cell exposed to UV-A radiation has the potential to be a photosensitizer that will absorb photon energy and pass it to DNA, damaging it. Generally, the pathway of energy transfer in a photosensitized reaction is:

$$PS \xrightarrow{h\nu} PS^* \xrightarrow{A} A^* + PS \longrightarrow \text{products}$$

where PS is the photosensitiziers, PS* is the excited-photosensitizer, A and A* are the substrate and an excited substrate, and hν is the photon energy.[53] Although the substrate (A) that receives the photon energy from excited sensitizer may be DNA itself, the most common substrate in the photosensitized reactions of DNA is molecular oxygen.

Direct reactions of excited photosensitizer with substrates by one electron transfer are called Type I reaction, in contrast to the oxygen-mediated Type II reactions.[54]

The last ones can act by the generation of singlet oxygen ($^1O_2$) (major Type II mechanism) or by formation of superoxide anion radical ($O_2^{-\bullet}$) (minor Type II mechanism). $^1O_2$, hydroxyl radical and Type I photosensitization are the main reactive species in the formation of UV-A-induced damage within the cells. Guanine has known to be the base that is modified by this processes (easy oxidation).[55]

Although the photosensitizers provoke this kind of damage, it has been shown that certain drugs (such as psoralens) could be useful for treatment of skin disease (such as

psoriasis) in combination with UV-A irradiation (PUVA therapy), in which the irreversible binding of a photoexcited molecule of psoralen to DNA takes place.[56]
Phototherapy consists in the use of light at different wavelengths depending on the therapeutic effect sought, in the treatment or therapy of some very specific groups of pathologies (especially in the treatment of skin disease). In classic phototherapy, the devices used are in wavelength ranges of UV-B (290-315 nm) and UV-A (315-400 nm). Photochemotherapy combines the effect of a photosensitizer and of light to achieve therapeutic benefits. Without light, the phototerapeutics do not have biological effect and the radiation used (visible light or low UV-A doses) is harmless without the drug. Only as a result of simultaneous exposure to the phototherapeutic and light, a biological effect occurs. So, the properties of light contribute to an high extent to the practical specificity of the phototherapy. Two applications of photochemotherapy are in clinical use:

- **PUVA therapy:** the administration of psoralen (P) and UV-A radiation is commonly referred as PUVA therapy. Mainly two psoralens are in use for PUVA: 5-methoxypsoralen, 8-methoxypsoralen. First applications of PUVA were in the treatment of psoriasis and vitiligo, but now it is used for an important variety of skin disease. A new development of PUVA is an extracorporeal form of photochemotherapy called photopheresis.[57-59]

- **Photodynamic therapy:** it is based on the use of porphyrins and other tetrapyrroles in combination with visible light for treatment of abnormal proliferating tissues and it is selective. This therapeutic modality requires the presence of oxygen: a porphyrin excited by visible light transfer its excess of energy oxygen resulting in the formation of singlet oxygen which is damaging to biological system.[60]

2. AIM OF THE PROJECT

2. AIM OF THE PROJECT

Condensed poly(hetero)aromatic compounds are usually regarded as representative DNA intercalators, especially if they contain electron-deficient or charged aromatic cores in the structure. However, only a few of these compounds interact with nucleic acids exclusively by intercalation. A vast number of ligands, which have an intercalating part endowed with a variety of substituents, binds to the DNA by a mixed mode, since the substituents may also occupy the DNA grooves upon binding and thus determine the selectivity and binding of the ligand. Thus, in the case of the "classical" intercalator ethidium bromide, the phenyl ring occupies the minor groove, resulting in overall heterogeneous DNA binding. At the same time, small changes in the structure of a given ligand may lead to the inversion of the binding mode or complete suppression of DNA binding, which has been shown for the ethidium derivatives, 9-substituited acridizinium salts and diazoniapolycyclic ions.[61]

The consequences of DNA intercalation by exogenous molecules have attracted considerable interest in medicinal chemistry, because such a complex formation leads to a significant modification of the DNA structure and may result in a hindered or supressed function of the nucleic acid in physiological processes (Figure 2.1).

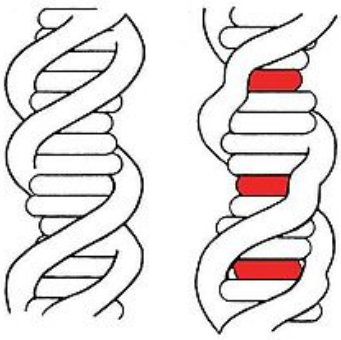

Figure 2.1. Effect of a DNA intercalator agent on DNA structure.

Because such an influence on the biological system is a main requirement for DNA-targeting drugs, the intercalation of small molecules into DNA may be applied in therapeuthic approaches in which the suppression of DNA replication and gene transcription is used to destroy tumor cells or infected tissue. As a result, many studies

have been performed to gain more insight in different aspects of the association process of large and small molecules with DNA in order to obtain highly selective and efficient intercalators.[62] Furthermore, DNA intercalators that inhibit topoisomerase activity or that form stabilized ternary complexes with DNA and topoisomerase have high potential as DNA-targeting anticancer drugs.[63]

While the association of cationic dyes to DNA is a reversible process, the DNA damage, which frequently occurs on irradiation of ligand-DNA complexes, is often irreversible. The latter DNA damage may lead to cell death or mutation, and must be avoided in healthy systems. However, this photoinduced DNA-damage may be applied in photochemotherapy to remove unwanted cells.[31]

Heterocyclic polyaromatic cations with a quaternary nitrogen atom represent attractive and interesting models for the design of water-soluble materials**.** In particular, the quinolizinium derivatives, i.e. arenes containing quaternary bridgehead nitrogen atoms, have been shown to bind to DNA and may be employed as a central unit in DNA-targeting drugs.[64]

During the studies of the influence of the substitution pattern of quinolizinum derivatives on their intercalation with DNA, it has been shown that the tricyclic benzo[*b*]quinolizinium **1** and above all the tetracyclic naphtho[1,2-*b*]quinolizinium bromide **2** (Figure 2.2) have interesting properties with respect to the binding to nucleic acids. In particular, the last intercalators may exhibit a stronger interaction with nucleic acids as compared with the tricyclic benzo[*b*]quinolizinium **1** (Figure 2.2) due to the additional benzene moiety which extends the surface of the planar chromophore and increases the π stacking between the dye and the DNA bases resulting in higher binding constants. Other important aspects are represented by the photobiological properties: it was shown that an efficient DNA-strand cleavage is photoinduced by the naphtho[1,2-*b*]quinolizinium.[31] Furthermore, the studies in progress on evaluation of the introduction of an aryl-substituent in pos. 9 of benzotriciclic structure seems to improve biological activity and DNA binding properties.

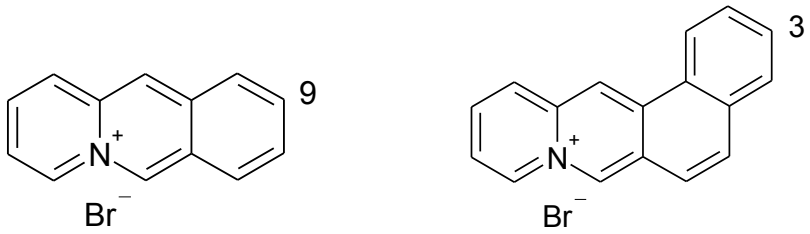

1 **2**

Figure 2.2 Chemical structures of Benzo[b]quinolizinium bromide **1** and Naphtho[1,2-*b*]quinolizinium bromide **2.**

The first aim of the project was the synthesis of 3-substituted-naphtho[1,2-*b*]quinolizinium derivatives **9**; the investigation of these compounds allows to evaluate the effects of the extension of π system by the introduction of fourth aromatic ring and of the substituent in position 3 (similar structurally to one in pos.9 of benzotriciclic **1**) in the interaction with DNA. I performed the synthesis in the laboratory of Prof. Heiko Ihmels at the Department of Organic Chemistry II (University of Siegen, Germany). The strategy was to find a promising general starting material, represented by 3-bromo-naphtho[1,2-*b*]quinolizinium bromide **8**, that allowed the synthesis of a series of corresponding 3-substituted-naphtho[1,2-*b*]quinolizinium derivatives **9** (Scheme 2.1).

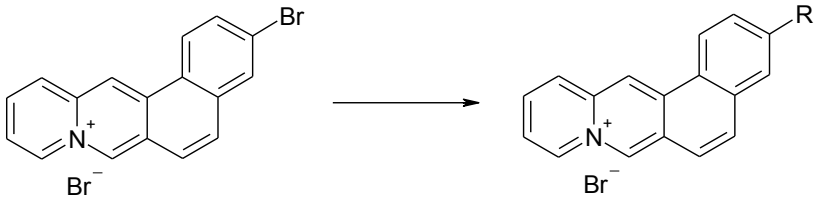

8 **9**

Scheme 2.1 Schematic representation of synthetic strategy.

In many cases, the electrophilic aromatic substitution of cationic heteroarenes is an inefficient and rather unselective reaction and sometimes the substrates are not persistent under the reaction conditions. On the other hand, nucleophilic substitution reactions occasionally give the desired products, but in other cases nucleophilic reagents induce ring-opening reactions that lead to the destruction of the substrate.[64] Thus, an interesting strategy for the synthesis of 3-aryl-substituted-naphtho[1,2-*b*]quinolizinium derivatives **9** was represented by the Suzuki-Miyaura cross-coupling reaction. This

reaction has been shown already to take place between bromo-substituted heterocyclic organic cations (such as 9-bromoacridizinium bromide) and arene boronic acids, with yields around 40%.[65] By this reaction, 3-aryl-substituted-naphtho[1,2-*b*]quinolizinium derivatives were obtained. When the synthesis was completed, the next step was the study about DNA-binding properties; then biological studies (cytotoxicity, experiments to investigate molecular targets in a preliminary way and to attempt a structure-relactionship activity) and finally photobiological tests were carried out.

3. EXPERIMENTAL PROCEDURES

3.1 MATERIALS

3.1.1 COMPOUNDS

All the compounds used in this project were synthesized in the laboratory of Prof. Heiko Ihmels, Department of Organic Chemistry II, University of Siegen, Germany (compounds **9a-9k** were synthesized from starting material in according to scheme 3.1; compound **2** was synthesized for previously studies and so already available for this project):

- **9a = FC01:** 3-Phenylnaphtho[1,2-*b*]quinolizinium chloride
- **9b = FC03:** 3-(*p*-Methoxyphenyl)naphtho[1,2-*b*]quinolizinium bromide
- **9c = FC04:** 3-(*p*-Fluoro)naphtho[1,2-*b*]quinolizinium bromide
- **9d = FC05:** 3-(*p*-Methylthiophenyl)naphtho[1,2-*b*]quinolizinium chloride
- **9e = FC06:** 3-(3-Thienyl)naphtho[1,2-*b*]quinolizinium bromide
- **9f = FC07:** 3-(4-Pyridyl)naphtho[1,2-*b*]quinolizinium chloride
- **9g = FC08:** 3-[4-(*N,N*-dimethylaminophenyl)]naphtho[1,2-*b*]quinolizinium chloride
- **9h = FC09:** 3-(2-naphthalenyl)naphtho[1,2-*b*]quinolizinium bromide
- **9i = FC10:** 3-(3,4,5-trimethoxyphenyl)naphtho[1,2-*b*]quinolizinium bromide
- **9j = FC11:** 3-(6-methoxy-2-naphthalenyl)naphtho[1,2-*b*]quinolizinium bromide
- **9k = FC12:** 3-(5-pyrimidyl)naphtho[1,2-*b*]quinolizinium chloride
- **2 = NQZ:** naphtho[1,2-*b*]quinolizinium bromide

3.1.2 REAGENTS AND SOLVENTS

- Al_2O_3 Neutral, Al_2O_3 sheets were from Macherey-Nagel, Germany
- THF, n-Hexane, EtOAc, CH_2Cl_2, toluene, DMSO, Et_2O, MeOH, DME, Acetone, $CHCl_3$, DIBAL-H 1.0 M in Hexane, Methyl 6-bromo-2-naphthoate, PBr_3, 2-pyridine carboxaldehyde, ethylene glycol, p-toluene sulfonic acid, KF, 3-thiophene boronic acid were from Acros Organics, Belgium

- NaCl, $MgSO_4$, $NaHCO_3$, Na_2SO_4, Na_2CO_3, HBr 48% wt solution in water was from Sigma-Aldrich, Munich, Germany
- Phenyl boronic acid, 4-methoxyphenyl boronic acid, 4-methylthiophenyl boronic acid, Pd(dppf)Cl_2-CH_2Cl_2 ([1,1'-Bis(diphenylphosphino)ferrocene] palladium (II) chloride, complex with dichloromethane (1:1), Pd 13 %), 6-methoxy-2-naphthaleneboronic acid, 3,4,5-trimethoxyphenylboronic acid, 2-naphthaleneboronic acid were from Alfa Aesar, Karlsruhe, Germany
- 4-fluorophenyl boronic acid and 4-pyridine boronic acid were from Fluorochem, UK
- 4-(*N,N*-dimethylamino)phenyl boronic acid was synthesized for previously studies and already available for this project
- 5-pyrimidylboronic acid was from Maybridge, UK
- Isopropanol and HCl were from Carlo Erba, Italy
- FBS (fetal bovine serum) was from Invitrogen S.R.L., Milano, Italy
- Plasmid pBR322 was from Fermentas, Milano, Italy
- Topoisomerase I was from Calbiochem, Italy
- Ethidium bromide, agarose, TRIS (tris(hydroxymethyl)aminomethane), EDTA, DTT (dithiothreitol, bromophenole blue, trypan blue (), xylene cianol FF, SDS (sodium dodecyl solfate), proteinase K, BSA (bovine serum albumin), stDNA (sodium salt from salmon testes DNA), MTT [(3-(4,5-dimethylthiazol2yl)2-5 diphenyl tetrazolium bromide)], HBSS (Hank's Balanced Salt Solution), Trypsin, RPMI-1640 medium, DMEM (Dulbecco's Modified Eagle's Medium), penicillin-streptomycin solutions, Topoisomerase II were purchased from Sigma-Aldrich, Milano, Italy.

3.2 METHODS

3.2.1 SYNTHESIS OF COMPOUNDS

All commercially chemicals were reagent grade and used without further purification. Melting points were determined with a melting point apparatus (Buchi 510K) and are not corrected. NMR spectra were measured on a Bruker Avance 400 (^{1}H: 400 MHz, ^{13}C: 100 MHz) and chemical shift are given in ppm (δ) relative to TMS (δ = 0.00 ppm).

Unambiguous proton NMR assignments were established with the help of {1H, 1H} COSY, HMBC and HSQC experiments. TLC analyses were performed on silica gel sheets (Macherey-Nagel Polygram sil G/UV254; eluent: n-Hexane/EtOAc 1:1) or on Al_2O_3 sheets (Macherey-Nagel Polygram Alox/UV 254; eluent: Chloroform/MeOH 95:5 or 9:1). Elemental analyses were performed on a KEKA-tech EuroEA combustion analyzer by Mr. H. Bodenstedt, Organic Chemistry I, University of Siegen.

3.2.1.1 Synthesis of (6-Bromo-naphthalen-2-yl)-methanol (6a)

A solution of DIBAL-H (1.0 M in Hexane, 39 g, 55 mL, 55 mmol) was slowly added into a solution of methyl 6-bromo-2-naphthoate **5** (5.00 g, 18.9 mmol) in anhydrous THF (90 mL) such that the internal temperature of the reaction mixture did not exceed 25 °C. The reaction mixture was stirred at r.t. until **5** was consumed, as monitored by TLC. Then, the reaction was stopped by slow addition into a cooled 4 N HCl aqueous solution (200 mL) at 25 °C. The resulting mixture was stirred for 2 h and 200 mL of EtOAc were added. The organic layer was separated and the aqueous layer was washed with EtOAc (3 x 100 mL). The combined organic layers were washed with 4 N HCl aqueous solution (100 mL), 5% aqueous $NaHCO_3$ solution (300 mL) and 6% aqueous NaCl solution (300 mL), respectively, and dried with $MgSO_4$. After filtration, the solvent was removed in vacuo to give the essentially pure product **6a** as determined by ^{1}H-NMR as white solid (4.30 g, 96%). M.p.: 153-154 °C (Lit.[66]: 152-153 °C). ^{1}H-NMR (400 MHz, $CDCl_3$): δ = 1.80 (broad s, 1 H, O-H), 4.85 (s, 2 H, CH_2), 7.50 (dd, J = 8.5, 1.7 Hz, 1 H, H-3), 7.55 (dd, J = 8.7, 2.0 Hz, 1 H, H-7), 7.70 (d, J = 8.7 Hz, 1 H, H-8), 7.75 (d, J = 8.5 Hz, 1 H, H-4), 7.79 (s, 1 H, H-1), 8.00 (d, J = 1.9, 1 H, H-5). ^{13}C-NMR (100 MHz, $CDCl_3$): δ = 66.1 (CH_2), 120.6 (C_q), 126.1 (CH_{Ar}), 127.0 (CH_{Ar}), 128.2 (CH_{Ar}), 130.3 (CH_{Ar}), 130.4 (CH_{Ar}), 130.6 (CH_{Ar}), 133.7 (C_q), 134.8 (C_q), 139.6 (C_q).

3.2.1.2 Synthesis of 2-bromo-6-bromomethyl-naphthalene (6b)

To a solution of compound **6a** (1.00 g, 4.20 mmol) in anhydrous CH_2Cl_2 (70 mL), PBr_3 (0.43 mL, d = 2.85 g/mL, 1.22 g, 4.50 mmol) was added at 10 °C and the mixture was stirred at r.t. for 3 h. Then, 60 mL of CH_2Cl_2 were added and the resulting mixture was extracted with water (80 mL). The aqueous layer was extracted with CH_2Cl_2 (3 x 50 mL). The combined organic layers were washed with an aqueous saturated solution of

$NaHCO_3$ (100 mL) and brine (200 mL). The separated organic layer was dried with Na_2SO_4. After filtration, the solvent was removed in vacuo to give the product **6b** as white-light yellow solid (0.80 g, 65 %), pure as determined by ^{1}H-NMR analysis. M.p.: 128-129 °C (Lit.[67]: 124-125 °C). ^{1}H-NMR (400 MHz, $CDCl_3$): δ = 4.64 (s, 2 H, CH_2), 7.53 (dd, J = 8.5, 1.8 Hz, 1 H, H-7), 7.57 (dd, J = 8.7, 1.9 Hz, 1 H, H-3), 7.68 (d, J = 8.7 Hz, 1 H, H-4), 7.74 (d, J = 8.5 Hz, 1 H, H-8), 7.80 (s, 1 H, H-5), 7.99 (d, J = 1.7, 1 H, H-1). ^{13}C-NMR (100 MHz, $CDCl_3$): δ = 33.8 (CH_2), 120.7 (C_q), 127.8 (CH_{Ar}), 127.9 (2 CH_{Ar}), 129.6 (CH_{Ar}), 129.9 (CH_{Ar}), 130.0 (CH_{Ar}), 131.7 (C_q), 134.1 (C_q), 135.7 (C_q).

3.2.1.3 Synthesis of 2-(1,3-dioxolan-2-yl)pyridine (7a)

A solution of 2-pyridine carboxaldehyde (42.8 g, 400 mmol), ethylene glycol (45.0 mL, 800 mmol) and p-toluene sulfonic acid (22.8 g) in toluene (600 mL) was stirred at reflux for 36 h in a flask equipped with a modified Dean-Stark apparatus. The reaction mixture was cooled to r. t. and poured into an aqueous solution of sodium carbonate (2.12 M in water) and the layers were separated. The aqueous layer was extracted with toluene (3 x 200 mL). The combined organic layers were washed with water (300 mL) and brine (200 mL) and dried with $MgSO_4$. After filtration, toluene was removed in vacuo to give the crude product **7a** (35 g, 58 %) as a brown liquid, which was purified by distillation under vacuum (70 °C, 1.2 mbar), to give a light-yellow liquid. ^{1}H-NMR (400 MHz, $CDCl_3$): δ = 4.05-4.22 (m, 4 H, CH_2), 5.87 (s, 1 H, CH), 7.26-7.31 (m, 1 H, CH_{Ar}), 7.54 (d, J = 8.0 Hz, 1 H, CH_{Ar}), 7.74 (td, J = 8.0, 2.0 Hz, 1 H, CH_{Ar}), 8.63 (m, 1 H, CH_{Ar}).

3.2.1.4 Synthesis of 2-(1,3-dioxolan-2-yl)-6-[2-bromo-naphthylmethyl] pyridinium bromide (7b)

A solution of 2-(1,3-dioxolan-2-yl)pyridine **7a** (1.23 g, 8.10 mmol) and compound **6b** (2.43 g 8.10 mmol) in DMSO (60 mL) was stirred under an argon gas atmosphere at r.t. for 7 days. The reaction mixture was poured into EtOAc (1 L) and the white precipitate was collected, washed thoroughly with EtOAc and Et_2O and dried under vacuum to give the product **7b** (2.85 g, 77.9 %), which was used for the following step without further purification. M.p.: 197-198 °C. ^{1}H-NMR (400 MHz, DMSO-d_6): δ = 4.13 (m, 4 H, CH_2), 6.16 (s, 2 H, CH_2), 6.56 (s, 1 H, CH), 7.55 (dd, J = 8.6, 1.8 Hz, 1 H, H-7), 7.70 (dd, J = 8.8, 2.0 Hz, 1 H, H-3), 7.87 (s, 1 H, H-5), 7.91 (d, J = 8.6, 1 H, H-4), 8.00 (d, J

= 8.8 Hz, 1 H, H-8), 8.22 (m, 1 H, H-5'), 8.27 (d, *J* = 1.8 Hz, 1 H, H-1), 8.36 (dd, *J* = 8.0, 1.4 Hz, 1 H, H-3'), 8.75 (m, 1 H, H-4'), 9.1 (dd, *J* = 6.2, 1.0 Hz, 1 H, H-6'). ^{13}C-NMR (100 MHz, DMSO-d_6): δ = 60.0 (CH_2), 65.6 (CH_2), 97.1 (CH), 120.1 (C_q), 126.1 (C_q), 126.6 (CH_{Ar}), 127.5 (CH_{Ar}), 128.1 (CH_{Ar}), 128.7 (CH_{Ar}), 129.6 (CH_{Ar}), 129.8 (C_q), 130.3 (C_q), 131.2 (CH_{Ar}), 132.0 (C_q), 133.9 (C_q), 147.3 (CH_{Ar}), 147.4 (CH_{Ar}), 152.2 (C_q).

3.2.1.5 Synthesis of 3-bromo-naphtho[1,2-*b*]quinolizinium bromide (8)

A solution of the pyridinium derivative **7b** (1.00 g, 2.20 mmol) in aq HBr (48%, 10 mL) was stirred under reflux for 4 h. After cooling to r.t., to the formed precipitate were added 25 mL of THF and the precipitate was collected, washed with THF and Et_2O and dried to give the product **8** as orange solid (0.75 g, 88 %). M.p.: 329-330 °C. ^{1}H-NMR (400 MHz, DMSO-d_6): δ= 8.10 (m, 1 H, H-10), 8.14-8.20 (m, 3 H, H-2, H-5, H-6), 8.30 (m, 1 H, H-11), 8.50 (d, *J* = 2.0, 1 H, H-4), 8.64 (d, *J* = 8.6 Hz, 1 H, H-12), 9.04 (d, *J* = 8.8 Hz, 1 H, H-1), 9.40 (d, *J* = 8.8 Hz, 1 H, H-9), 10.10 (s, 1 H, H-13), 10.30 (s, 1 H, H-7). ^{13}C-NMR (100 MHz, DMSO-d_6): δ = 120.8 (CH_{Ar}), 123.0 (CH_{Ar}), 124.8 (CH_{Ar}), 125.5 (2 C_q), 125.7 (C_q), 127.0 (CH_{Ar}), 127.2 (CH_{Ar}), 131.3 (CH_{Ar}), 131.6 (CH_{Ar}), 131.8 (C_{Ar}), 133.4 (C_{Ar}), 134.7 (C_q), 134.8 (C_q), 135.0 (C_{Ar}), 137.6 (CH_{Ar}), 139.0 (Cq).

3.2.1.6 Synthesis of 3-Phenylnaphtho[1,2-*b*]quinolizinium chloride (9a)

Under inert-gas atmosphere a solution of 3-bromo-naphtho[1,2-*b*]quinolizinium bromide **8** (389 mg, 1.00 mmol), phenyl boronic acid (122 mg, 1.00 mmol), Pd(dppf)Cl_2-CH_2Cl_2 (24.5 mg, 0.03 mmol) and KF (232 mg, 4.00 mmol) in DME/MeOH/H_2O (12 mL; 2:1:1) was stirred under reflux for 18 h. After cooling to room temperature, MeOH (20 mL) was added to the reaction mixture and the yellow precipitate was collected and washed with EtOAc and Et_2O. The solid was dissolved in hot MeOH and the solution was filtered under vacuum. The desired compound was isolated by column chromatography (Al_2O_3, Activity I; $CHCl_3$-MeOH, 95:5). Recrystallization from MeOH gave a pure product **9a** (96 mg; 25 %), as dark yellow needles. ^{1}H-NMR (400 MHz, DMSO-d_6): δ= 7.50 (m, 1 H, H-4'), 7.59 (m, 2 H, H-3', H-5'), 7.96 (m, 2 H, H-2', H-6'), 8.05 (m, 1 H, H-10), 8.14 (d, *J* = 9.2 Hz, 1 H, H-5),

8.23 – 8.29 (m, 2 H, H-6, H-11), 8.31 (dd, *J* = 8.6 Hz, 1.9 Hz, 1 H, H-2), 8.53 (d, *J* = 1.9 Hz, 1 H, H-4), 8.65 (d, *J* = 8.4 Hz, 1 H, H-12), 9.17 (d, *J* = 8.7 Hz, H-1), 9.39 (d, *J* = 6.8 Hz, H-9), 10.10 (s, 1 H, H-13), 10.30 (s, 1 H, H-7) . ^{13}C-NMR (100 MHz, DMSO-d_6): δ = 120.5 (CH_{Ar}), 122.7 (CH_{Ar}), 123.7 (CH_{Ar}), 125.8 (CH_{Ar}), 125.9 (2 C_q), 126.9 (CH_{Ar}), 127.0 (CH_{Ar}), 127.3 (CH_{Ar}), 127.5 (CH_{Ar}), 128.7 (CH_{Ar}), 129.2 (CH_{Ar}), 132.8 (CH_{Ar}), 133.0 (CH_{Ar}), 134.1 (C_q), 134.8 (CH_{Ar}), 135.2 (C_q), 137.5 (CH_{Ar}), 138.5 (C_q), 138.9 (C_q), 143.0 (C_q). M.p.: 345 °C (dec.). Anal. Calcd for C23H16ClN-0.33H2O: C, 79.42; H, 4.83; N, 4.03. Found: C, 79.57; H, 4.97; N, 4.23.

3.2.1.7 Synthesis of 3-(*p*-Methoxyphenyl)naphtho[1,2-*b*]quinolizinium bromide (9b)

Under inert-gas atmosphere a solution of 3-bromo-naphtho[1,2-*b*]quinolizinium bromide **8** (389 mg, 1.00 mmol), 4-methoxyphenyl boronic acid (304 mg, 2.00 mmol), Pd(dppf)Cl_2-CH_2Cl_2 (24.5 mg, 0.03 mmol) and KF (232 mg, 4.00 mmol) in DME/MeOH/H_2O (12 mL; 2:1:1) was stirred under reflux for 18 h. After cooling to room temperature, MeOH (20 mL) was added to the reaction mixture and the yellow precipitate was collected and washed with EtOAc and Et_2O. This precipitate was suspended in acetone (in water-sonic bath for 15 minutes) and the dark yellow solid was collected. Recrystallization from MeOH gave a pure product **9b**, as red-yellow solid (21 mg, 5 %), as ^{1}H-NMR analysis shows. ^{1}H-NMR (400 MHz, DMSO-d_6): δ = 3.86 (s, 3H, -OCH_3), 7.14 (d, *J* = 8.7 Hz, 2 H, H-3', H-5'), 7.94 (d, *J* = 8.7 Hz, 2 H, H-2', H-6'), 8.04 (m, 1 H, H-10), 8.12 (d, *J* = 9.2, 1 H, H-5), 8.22 – 8.27 (m, 2 H, H-6, H-11), 8.31 (dd, *J* = 8.6, 1.8 Hz, 1 H, H-2), 8.49 (d, *J* = 1.8 Hz, 1 H, H-4), 8.62 (d, *J* = 8.7 Hz, 1 H, H-12), 9.13 (d, *J* = 8.6 Hz, 1 H, H-1), 9.35 (d, *J* = 7.0, 1 H, H-9), 10.05 (s, 1 H, H-13), 10.24 (s, 1 H, H-7) . ^{13}C-NMR (100 MHz, DMSO-d_6): δ = 55.3 (-OCH_3), 114.7 (CH_{Ar}), 120.2 (CH_{Ar}), 122.6 (CH_{Ar}), 123.7 (CH_{Ar}), 125.2 (C_q) 125.7 (CH_{Ar}), 125.8 (C_q), 126.1 (CH_{Ar}), 126.9 (CH_{Ar}), 127.0 (CH_{Ar}), 128.5 (C_{Ar}), 130.6 (C_q), 132.9 (2 CH_{Ar}), 134.2 (C_q), 134.7 (CH_{Ar}), 135.3 (C_q), 137.4 (CH_{Ar}), 138.9 (C_q), 142.7 (C_q), 159.9 (C_q). M.p.: 335-336 °C (dec.). Anal. Calcd for $C_{24}H_{18}BrNO$-0.5H_2O: C, 67.74; H, 4.45; N, 3.40. Found: C, 67.77; H, 4.50; N, 3.29.

3.2.1.8 Synthesis of 3-(*p*-Fluorophenyl)naphtho[1,2-*b*]quinolizinium chloride (9c)

Under inert-gas atmosphere a solution of 3-bromo-naphtho[1,2-*b*]quinolizinium bromide **8** (389 mg, 1.00 mmol), 4-fluorophenyl boronic acid (280 mg, 2.00 mmol), Pd(dppf)Cl_2-CH_2Cl_2 (24.5 mg, 0.03 mmol) and KF (232 mg, 4.00 mmol) in DME/MeOH/H_2O (12 mL; 2:1:1) was stirred under reflux for 18 h. After cooling to room temperature, the palladium-black was removed by filtration and the resulting solution was evaporated. EtOAc was added to the residue and the suspension was put in sonic bath for 30 minutes. The yellow solid was collected, washed with EtOAc and Et_2O. The desired compound was isolated by column chromatography (Al_2O_3, Activity I; $CHCl_3$-MeOH, 95:5). Recrystallization from MeOH, gave a pure product **9c** (42 mg; 10 %), as yellow needles.^{1}H-NMR (400 MHz, DMSO-d_6): δ = 7.44 (m, 2 H, H-3', H-5'), 8.01-8.06 (m, 3 H, H-2', H-6', H-10), 8.15 (d, J = 9.2 Hz, 1 H, H-5), 8.26 (m, 2 H, H-6, H-11), 8.31 (dd, J = 8.6, 1.9 Hz, 1 H, H-2), 8.52 (d, J = 1.9 Hz, 1 H, H-4), 8.63 (d, J = 8.6 Hz, 1 H, H-12), 9.17 (d, J = 8.6 Hz,1 H, H-1), 9.39 (d, J = 6.9 Hz, 1 H, H-9), 10.09 (s, 1 H, H-13), 10.28 (s, 1 H, H-7) . ^{13}C-NMR (100 MHz, DMSO-d_6): δ = 116.1 (2 CH_{Ar} J = 21 Hz), 120.5 (CH_{Ar}), 122.7 (CH_{Ar}), 123.9 (CH_{Ar}), 125.8 (2 C_q), 126.0 (CH_{Ar}), 126.9 (CH_{Ar}), 127.0 (CH_{Ar}), 127.4 (CH_{Ar}), 129.5 (2 CH_{Ar} J = 8 Hz), 132.8 (CH_{Ar}), 133.1 (CH_{Ar}), 134.1 (C_q), 134.8 (CH_{Ar}), 135.0 (C_q J = 3 Hz), 135.2 (C_q), 137.5 (CH_{Ar}), 139.0 (C_q), 142.0 (C_q), 162.3 (C_q J = 244 Hz). M.p.: 352 °C (dec.) Anal. Calcd for $C_{23}H_{15}ClFN$-$2H_2O$: C, 69.78; H, 4.84; N, 3.54. Found: C, 70.16; H, 4.30; N, 3.56.

3.2.1.9 Synthesis of 3-(*p*-Methylthiophenyl)naphtho[1,2-*b*] quinolizinium bromide (9d)

Under inert-gas atmosphere a solution of 3-bromo-naphtho[1,2-*b*]quinolizinium bromide **8** (389 mg, 1.00 mmol), 4-methylthiophenyl boronic acid (202 mg, 1.20 mmol), Pd(dppf)Cl_2-CH_2Cl_2 (24.5 mg, 0.03 mmol) and KF (232 mg, 4.00 mmol) in DME/MeOH/H_2O (12 mL; 2:1:1) was stirred under reflux for 18 h. After cooling to room temperature, MeOH (20 mL) was added to the reaction mixture and the yellow precipitate was collected and washed with EtOAc and Et_2O. The solid was suspended in acetone (in water-sonic bath for 15 minutes) and the product **9d**, as dark-yellow solid, was collected (52 mg, 12 %), pure, as ^{1}H-NMR analysis shows. M.p.: °C. ^{1}H-NMR (400 MHz, DMSO-d_6): δ = 2.58 (s, 3H, -SCH_3), 7.46 (d, J = 8.4 Hz, 2 H, H-3', H-5'), 7.94

(d, *J* = 8.4 Hz, 2 H, H-2', H-6'), 8.05 (m, 1 H, H-10), 8.15 (d, *J* = 8.9, 1 H, H-5), 8.24 – 8.28 (m, 2 H, H-6, H-11), 8.33 (dd, *J* = 7.0, 1.3 Hz, 1 H, H-2), 8.54 (d, *J* = 1.3 Hz, 1 H, H-4), 8.64 (d, *J* = 8.9 Hz, 1 H, H-12), 9.15 (d, *J* = 8.6 Hz, 1 H, H-1), 9.37 (d, *J* = 7.0, 1 H, H-9), 10.07 (s, 1 H, H-13), 10.26 (s, 1 H, H-7) . ^{13}C-NMR (100 MHz, DMSO-d_6): δ = 14.4 (-SCH_3), 120.4 (CH_{Ar}), 122.6 (CH_{Ar}), 123.8 (CH_{Ar}), 125.7 (2 C_q), 126.1 (CH_{Ar}), 126.3 (CH_{Ar}), 126.5 (CH_{Ar}), 126.9 (CH_{Ar}), 127.1 (CH_{Ar}), 127.6 (CH_{Ar}), 132.8 (CH_{Ar}), 133.0 (CH_{Ar}), 134.2 (CH_{Ar}), 134.6 (C_q), 134.8 (C_q), 135.2 (C_q), 137.4 (CH_{Ar}), 139.0 (C_q), 139.4 (C_q), 142.4 (C_q). M.p.: 355-358 °C (dec.). Anal. Calcd for $C_{24}H_{18}BrNS$-0.33H_2O: C, 65.75; H, 4.29; N, 3.20; S, 7.31. Found: C, 66.03; H, 4.05; N, 3.42; S, 7.59.

3.2.1.10 Synthesis of 3-(3-Thienyl)naphtho[1,2-*b*]quinolizinium bromide (9e)

Under inert-gas atmosphere a solution of 3-bromo-naphtho[1,2-*b*]quinolizinium bromide **8** (389 mg, 1.00 mmol), 3-thiophene boronic acid (141 mg, 1.10 mmol), Pd(dppf)Cl_2-CH_2Cl_2 (24.5 mg, 0.03 mmol) and KF (232 mg, 4.00 mmol) in DME/MeOH/H_2O (12 mL; 2:1:1) was stirred under reflux for 18 h. After cooling to room temperature, MeOH (20 mL) was added to the reaction mixture and the yellow precipitate was collected and washed with EtOAc and Et_2O. Recrystallization from MeOH gave a pure product **9e**, as yellow solid (89 mg, 23 %), as ^{1}H-NMR analysis shows. M.p.: °C. ^{1}H-NMR (400 MHz, DMSO-d_6): δ= 7.77 (m, 1 H, H-4'), 7.84 (m, 1 H, H-5'), 8.01 (m, 1 H, H-10), 8.09 (m, 1 H, H-5), 8.18 – 8.24 (m, 2 H, H-6, H-11), 8.27 (s, 1 H, H-2'), 8.33 (m, 1 H, H-2), 8.53 (m, 1 H, H-4), 8.60 (d, *J* = 8.7 Hz, 1 H, H-12), 9.07-9.11 (m, 1 H, H-1), 9.33 (d, *J* = 6.8, H-9), 10.02 (d, *J* = 2.3, 1 H, H-13), 10.23 (s, 1 H, H-7) . ^{13}C-NMR (100 MHz, DMSO-d_6): δ = 120.3 (CH_{Ar}), 122.6 (CH_{Ar}), 123.8 (2 CH_{Ar}), 125.5 (C_q), 125.7 (C_q), 125.9 (CH_{Ar}), 126.1 (CH_{Ar}), 126.3 (CH_{Ar}), 126.9 (CH_{Ar}), 127.0 (CH_{Ar}), 127.9 (CH_{Ar}), 132.7 (CH_{Ar}), 133.0 (CH_{Ar}), 134.3 (C_q), 134.7 (C_{Ar}), 135.2 (C_q), 137.4 (CH_{Ar}), 138.0 (C_q), 139.0 (C_q), 140.0 (C_q). M.p.: 352 °C (dec.). .). Anal. Calcd for $C_{21}H_{14}BrNS$: C, 64.29; H, 3.60; N, 3.57; S, 8.17. Found: C, 64.06; H, 3.41; N, 3.78; S, 8.47.

3.2.1.11 Synthesis of 3-(4-Pyridyl)naphtho[1,2-*b*]quinolizinium chloride (9f)

Under inert-gas atmosphere a solution of 3-bromo-naphtho[1,2-*b*]quinolizinium bromide **8** (389 mg, 1.00 mmol), 4-pyridine boronic acid (135 mg, 1.10 mmol), Pd(dppf)Cl_2-CH_2Cl_2 (24.5 mg, 0.03 mmol) and KF (232 mg, 4.00 mmol) in DME/MeOH/H_2O (12 mL; 2:1:1) was stirred under reflux for 18 h. After cooling to room temperature, the palladium-black was removed by filtration and the resulting solution was evaporated. EtOAc was added to the residue and the suspension was put in sonic bath for 30 minutes. The brown solid was collected, washed with EtOAc and Et_2O. The desired compound was isolated by column chromatography (Al_2O_3, Activity I; $CHCl_3$-MeOH, 95:5). Recrystallization from MeOH-EtOAc, gave a pure product **9f** (126 mg; 33 %), as brown-orange needles. ^{1}H-NMR (400 MHz, DMSO-d_6): δ = 8.08 (m, 2 H, H-3', H-5'), 8.09 (m, 1 H, H-10), 8.18 (d, J = 9.2 Hz, 1 H, H-5), 8.28 (m, 2 H, H-6, H-11), 8.44 (dd, J = 8.6, 1.9 Hz, 1 H, H-2), 8.67 (d, J = 8.6, 1 H, H-12), 8.70 (d, J = 1.8, 1 H, H-4), 8.77 (m, 2 H, H-2', H-6'), 9.24 (d, J = 8.6 Hz, 1 H, H-1), 9.41 (d, J = 6.8, 1 H, H-9), 10.16 (s, 1 H, H-13), 10.32 (s, 1 H, H-7) . ^{13}C-NMR (100 MHz, DMSO-d_6): δ = 121.0 (CH_{Ar}), 121.7 (2 CH_{Ar}), 123.0 (CH_{Ar}), 124.1 (CH_{Ar}), 125.9 (C_q), 126.1 (CH_{Ar}), 127.0 (CH_{Ar}), 127.2 (C_q), 127.4 (CH_{Ar}), 127.7 (CH_{Ar}), 132.6 (CH_{Ar}), 133.3 (CH_{Ar}), 134.1 (C_q), 134.9 (CH_{Ar}), 135.0 (C_q), 137.6 (CH_{Ar}), 139.0 (C_q), 140.0 (C_q), 145.0 (C_q), 150.5 (2 CH_{Ar}). M.p.: 357-360 °C (dec.). Anal. Calcd for $C_{22}H_{15}ClN_2$-HCl-0.33H_2O: C, 68.58; H, 4.36; N, 7.29. Found: C, 68.36; H, 4.66; N, 7.19

3.2.1.12 Synthesis of 3-[4-(*N,N*-dimethylaminophenyl)]naphtho[1,2-*b*]quinolizinium chloride (9g)

Under inert-gas atmosphere a solution of 3-bromo-naphtho[1,2-*b*]quinolizinium bromide **8** (389 mg, 1.00 mmol), 4-(*N,N*-dimethylamino)phenylboronic acid (182 mg, 1.10 mmol), Pd(dppf)Cl_2-CH_2Cl_2 (24.5 mg, 0.03 mmol) and KF (232 mg, 4.00 mmol) in DME/MeOH/H_2O (12 mL; 2:1:1) was stirred under reflux for 18 h. After cooling to room temperature, MeOH (10 mL) was added to the reaction mixture, the palladium-black was removed by filtration and the yellow precipitate was collected and washed with EtOAc and Et_2O. The desired compound was isolated by column chromatography (Al_2O_3, Activity I; $CHCl_3$-MeOH, 95:5). Recrystallization from MeOH gave a pure product **9g** (132 mg; 31 %), as dark red powder. ^{1}H-NMR (400 MHz, DMSO-d_6): δ =

3.02 (s, 6 H, 2 -NCH_3), 6.87 (d, J = 8.8 Hz, 2 H, H-3', H-5'), 7.83 (d, J = 8.8 Hz, 2 H, H-2', H-6'), 8.00 (m, 1 H, H-10), 8.08 (d, J = 9.2 Hz, 1 H, H-5), 8.20 – 8.25 (m, 3 H, H-2, H-6, H-11), 8.40 (d, J = 1.5 Hz, 1 H, H-4), 8.60 (d, J = 8.5 Hz, 1 H, H-12), 9.04 (d, J = 9.0 Hz, 1 H, H-1), 9.33 (d, J = 7.0 Hz, 1 H, H-9), 9.97 (s, 1 H, H-13), 10.23 (s, 1 H, H-7); ^{13}C-NMR (100 MHz, DMSO-d_6): δ = 40.8 (2 -NCH_3), 112.9 (2 CH_{Ar}), 120.2 (CH_{Ar}), 122.8 (CH_{Ar}), 123.8 (CH_{Ar}), 124.8 (C_q), 125.2 (CH_{Ar}), 125.5 (C_q), 125.9 (C_q), 126.1 (CH_{Ar}), 126.6 (CH_{Ar}), 127.2 (CH_{Ar}), 128.2 (2 CH_{Ar}), 133.1 (CH_{Ar}), 133.4 (CH_{Ar}), 134.7 (C_q), 135.0 (CH_{Ar}), 135.7 (C_q), 137.7 (CH_{Ar}), 139.2 (C_q), 143.6 (C_q), 151.0 (C_q); m.p.: 320 °C (dec.). Anal. Calcd for $C_{25}H_{21}ClN_2$-H_2O: C, 74.52; H, 5.75; N, 6.90. Found: C, 74.09; H, 5.69; N, 7.02.

3.2.1.13 Synthesis of 3-(2-naphthalenyl)naphtho[1,2-*b*]quinolizinium bromide (9h)

Under inert-gas atmosphere a solution of 3-bromo-naphtho[1,2-*b*]quinolizinium bromide **8** (389 mg, 1.00 mmol), 2-naphthaleneboronic acid (230 mg, 1.10 mmol), Pd(dppf)Cl_2-CH_2Cl_2 (24.5 mg, 0.03 mmol) and KF (232 mg, 4.00 mmol) in DME/MeOH/H_2O (12 mL; 2:1:1) was stirred under reflux for 18 h. After cooling to room temperature, MeOH (10 mL) was added to the reaction mixture, the palladium-black was removed by filtration. The yellow precipitate was collected and washed with EtOAc and Et_2O. Recrystallization from MeOH gave a pure product **9h** (214 mg; 49%), as dark yellow powder. ^{1}H-NMR (400 MHz, DMSO-d_6): δ = 7.60 (m, 2 H, H-6', H-7'), 8.00-8.19 (m, 6 H, H-5, H-10, H-3', H-4', H-5', H-8'), 8.25 (m, 1 H, H-11), 8.31 (d, J = 8.8 Hz, 1 H, H-6), 8.47 (dd, J = 8.6 Hz, 1.8 Hz, 1 H, H-2), 8.54 (s, 1 H, H-1'), 8.65 (d, J = 8.5 Hz, 1 H, H-12), 8.68 (d, J = 1.8 Hz 1 H, H-4), 9.20 (d, J = 8.5 Hz, 1 H, H-1), 9.36 (d, J = 6.7 Hz, 1 H, H-9), 10.09 (s, 1 H, H-13), 10.26 (s, 1 H, H-7); ^{13}C-NMR (100 MHz, DMSO-d_6): δ = 120.9 (CH_{Ar}), 123.1 (CH_{Ar}), 124.2 (CH_{Ar}), 125.4 (CH_{Ar}), 126.1 (C_q), 126.2 (C_q), 126.3 (CH_{Ar}), 126.7 (CH_{Ar}), 127.1 (CH_{Ar}), 127.2(CH_{Ar}), 127.3 (CH_{Ar}), 127.6 (CH_{Ar}), 127.9 (CH_{Ar}), 128.0 (CH_{Ar}), 128.8 (CH_{Ar}), 129.2 (CH_{Ar}), 133.1 (C_q), 133.2 (C_q) 133.4 (CH_{Ar}), 133.6 (CH_{Ar}), 134.5 (C_q), 135.1 (C_q), 135.5 (CH_{Ar}), 136.1 (C_q), 137.8 (CH_{Ar}), 139.3 (C_q), 143.1 (C_q); m.p.: 365 °C (dec.). .). Anal. Calcd for $C_{27}H_{18}$BrN-0.5H_2O: C, 71.37; H, 4.4; N, 3.08. Found: C, 71.35; H, 4.32; N, 3.12.

3.2.1.14 Synthesis of 3-(3,4,5-trimethoxyphenyl)naphtho[1,2-*b*] quinolizinium bromide (9i)

Under inert-gas atmosphere a solution of 3-bromo-naphtho[1,2-*b*]quinolizinium bromide **8** (389 mg, 1.00 mmol), 3,4,5-trimethoxyphenylboronic acid (189 mg, 1.10 mmol), Pd(dppf)Cl_2-CH_2Cl_2 (24.5 mg, 0.03 mmol) and KF (232 mg, 4.00 mmol) in DME/MeOH/H_2O (12 mL; 2:1:1) was stirred under reflux for 18 h. After cooling to room temperature, MeOH (10 mL) was added to the reaction mixture, the palladium-black was removed by filtration; the solvent was evaporated and the yellow powder was collected and washed with EtOAc and Et_2O. The desired compound was isolated by column chromatography (Al_2O_3, Activity I; $CHCl_3$-MeOH, 95:5). Recrystallization from MeOH-Et_2O gave a pure product **9h** (21.6 mg; 4.5 %), as yellow powder. ^{1}H-NMR (400 MHz, DMSO-d_6): δ = 3.76 (s, 3 H, -OCH_3), 3.96 (s, 6 H, 2 -OCH_3), 7.23 (s, 2 H, H-2', H-6'), 8.06 (m, 1 H, H-10), 8.16 (d, J = 9.1 Hz, 1 H, H-2), 8.24 – 8.30 (m, 2 H, H-6, H-11), 8.36 (dd, J = 8.6 Hz, J = 1.9 Hz, 1 H, H-2), 8.56 (d, J = 1.9 Hz, 1 H, H-4), 8.67 (d, J = 8.8 Hz, 1 H, H-12), 9.16 (d, J = 8.8 Hz, 1 H, H-1), 9.40 (d, J = 6.7 Hz, 1 H, H-9), 10.10 (s, 1 H, H-13), 10.30 (s, 1 H, H-7); ^{13}C-NMR (100 MHz, DMSO-d_6): δ = 56.2 (-OCH_3), 60.0 (2 -OCH_3), 104.8 (2 CH_{Ar}), 120.3 (CH_{Ar}), 122.6 (CH_{Ar}), 123.6 (CH_{Ar}), 125.6 (CH_{Ar}), 125.7 (C_q), 126.8 (CH_{Ar}), 126.9 (CH_{Ar}), 127.6 (CH_{Ar}), 132.7 (CH_{Ar}), 132.9 (CH_{Ar}), 134.0, (C_q), 134.1 (C_q), 134.8 (C_q), 135.1 (CH_{Ar}), 137.4 (C_q), 138.1 (CH_{Ar}), 138.9 (C_q), 143.1 (C_q), 153.3 (3 C_q). m.p.: 295 °C (dec.). Anal. Calcd for $C_{26}H_{22}BrNO_3$-2.5H_2O: C, 59.89; H, 5.22; N, 2.69. Found: C, 59.82; H, 4.92; N, 2.78.

3.2.1.15 Synthesis of 3-(6-methoxy-2-naphthalenyl)naphtho[1,2-*b*] quinolizinium bromide (9j)

Under inert-gas atmosphere a solution of 3-bromo-naphtho[1,2-*b*]quinolizinium bromide **8** (389 mg, 1.00 mmol), 6-methoxy-2-naphthaleneboronic acid (230 mg, 1.10 mmol), Pd(dppf)Cl_2-CH_2Cl_2 (24.5 mg, 0.03 mmol) and KF (232 mg, 4.00 mmol) in DME/MeOH/H_2O (12 mL; 2:1:1) was stirred under reflux for 18 h. After cooling to room temperature, MeOH (10 mL) was added to the reaction mixture, the palladium-black was removed by filtration and the yellow precipitate was collected and washed with EtOAc and Et_2O. The desired compound was isolated by column chromatography (Al_2O_3, Activity I; $CHCl_3$-MeOH, 9:1). Recrystallization from MeOH-Et_2O gave a pure product **9h** (42 mg; 9 %), as orange-yellow powder. ^{1}H-NMR (400 MHz, DMSO-d_6):

δ = 3.93 (s, 3 H, -OCH_3), 7.25 (dd, *J* = 9.0 Hz, 1.8 Hz, 1 H, H-7'), 7.41 (s, 1 H, H-5'), 7.95-8.10 (m, 4 H, H-10, H-3', H-4', H-8'), 8.15 (d, *J* = 9.0 Hz, 1 H, H-6), 8.25 (m, 1 H, H-11), 8.30 (d, *J* = 9.0 Hz, 1 H, H-5), 8.45 (m, 2 H, H-2, H-1'), 8.64 (m, 2 H, H-4, H-12), 9.18 (d, *J* = 8.5 Hz, 1 H, H-1), 9.37 (d, *J* = 7.0 Hz, 1 H, H-9), 10.08 (s, 1 H, H-13), 10.28 (s, 1 H, H-7); ^{13}C-NMR (100 MHz, DMSO-d_6): δ = 55.7 (-OCH_3), 106.2 (CH_{Ar}), 119.7 (CH_{Ar}), 120.8 (CH_{Ar}), 123.0 (CH_{Ar}), 124.2 (CH_{Ar}), 125.8 (CH_{Ar}), 126.0 (C_q), 126.1 (C_q), 126.3 (CH_{Ar}), 126.6 (CH_{Ar}), 127.2 (CH_{Ar}), 127.3 (CH_{Ar}), 127.7 (CH_{Ar}), 128.1 (CH_{Ar}), 129.1 (C_q), 130.9 (CH_{Ar}), 133.2 (CH_{Ar}), 133.3 (CH_{Ar}), 133.7 (C_q), 134.6 (C_q), 134.7 (C_q) 135.1 (CH_{Ar}), 135.6 (C_q), 137.8 (C_q), 139.3 (C_q), 143.3 (C_q), 158.3 (C_q); m.p.: 323 °C (dec.). Anal. Calcd for $C_{28}H_{20}BrNO$-1.5H_2O: C, 68.16; H, 4.70; N, 2.84. Found: C, 68.36; H, 4.63; N, 3.03.

3.2.1.16 Synthesis of 3-(5-pyrimidyl)naphtho[1,2-*b*]quinolizinium chloride (9k)

Under inert-gas atmosphere a solution of 3-bromo-naphtho[1,2-*b*]quinolizinium bromide **8** (389 mg, 1.00 mmol), 5-pyrimidylboronic acid (136 mg, 1.10 mmol), Pd(dppf)Cl_2-CH_2Cl_2 (24.5 mg, 0.03 mmol) and KF (232 mg, 4.00 mmol) in DME/MeOH/H_2O (12 mL; 2:1:1) was stirred under reflux for 18 h. After cooling to room temperature, MeOH (10 mL) was added to the reaction mixture, the palladium-black was removed by filtration and the brown precipitate was collected and washed with EtOAc and Et_2O. The desired compound was isolated by column chromatography (Al_2O_3, Activity I; $CHCl_3$-MeOH, 95:5). Recrystallization from MeOH-Et_2O gave a pure product **9k** (37.7 mg; 9.7 %), as brown-yellow powder. ^{1}H-NMR (400 MHz, DMSO-d_6): δ = 8.10 (m, 1 H, H-10), 8.20 (d, *J* = 9.3 Hz, 1 H, H-5), 8.27-8.32 (m, 2 H, H-6, H-11), 8.50 (dd, *J* = 8.6 Hz, 1.9 Hz, 1 H, H-2), 8.67 (d, *J* = 8.6 Hz, 1 H, H-12), 8.72 (d, *J* = 1.8 Hz, 1 H, H-4), 9.26 (d, *J* = 8.6 Hz, H-1), 9.31 (s, 1 H, H-3'), 9.42 (d, *J* = 6.6 Hz, 1 H, H-9), 9.46 (s, 2H, H-4', H-6'), 10.15 (s, 1 H, H-13), 10.28 (s, 1 H, H-7); ^{13}C-NMR (100 MHz, DMSO-d_6): δ = 121.3 (CH_{Ar}), 123.3 (CH_{Ar}), 124.6 (CH_{Ar}), 126.2 (C_q), 126.6 (CH_{Ar}), 127.2 (C_q), 127.4 (CH_{Ar}), 127.8 (CH_{Ar}), 128.0 (CH_{Ar}), 132.3 (C_q), 132.8 (CH_{Ar}), 133.7 (CH_{Ar}), 134.4 (C_q), 135.3 (C_q), 135.4 (CH_{Ar}), 137.1 (C_q), 138.0 (CH_{Ar}), 139.4 (C_q), 155.7 (2 CH_{Ar}), 158.4 (CH_{Ar}); m.p.: 365 °C (dec.). Anal. Calcd for $C_{21}H_{14}ClN_3$-2H_2O: C, 67.46; H, 4.67; N, 11.24. Found: C, 67.25; H, 4.51; N, 11.24.

3.2.2 SPECTROPHOTOMETRICAND SPECTROFLUORIMETRIC TITRATIONS

3.2.2.1 Spectrophotometric titrations

Spectrophotometric titration of 3-aryl-substituted-naphtho[1,2-*b*]quinolizinium derivatives **9** with stDNA were performed in phosphate buffer 10 mM at pH = 7.0 for the determination of the interaction between them and DNA.

The ligand concentration was 10 or 20 μM and the titrant solutions contained stDNA (4.5 mM (bp)) as well as the ligand at the same concentration as in the titrated solution to avoid dilution of the analyte in cuvette. Aliquots (3 ml) of the analyte solutions in phosphate buffer were placed into quartz spectrophotometric cells and titrated with the titrant solutions in 0.5-2 equivalent intervals. UV-Vis spectra were recorded on a Uv-Vis Perkin-Elmer Lambda 12 double beam spectrophotometer (wavelength range of 300-500 nm). The titrations were finished after no changes were observed in absorption spectra upon addition of at least three two-equivalent portions of the titrant. All the spectrophotometric titrations were performed at least three times to ensure the reproducibility. Moreover, to avoid secondary effects (charge-charge interactions), the titrations were confirmed using a higher ionic strength buffer (ETN 100 mM).

3.2.2.2 Spectrofluorimetric titrations

Spectrofluorimetric titrations were performed with the same methods of spectrophotometric titrations and this technique was chosen for the determination of binding constants because its high sensitivity. In this case, a ligand concentration c_L = 0,5 or 1 μM was used. The spectra were recorded on a Perkin-Elmer LS50B Fluorimeter (wavelength range 400-600 nm). All the spectrofluorimetric titrations were performed at least three times to ensure the reproducibility.

3.2.2.3 Evaluation of binding costants (K) and binding site size (n)

The concentration of the drug bound (C_b) to the DNA was calculated by these equations:

$$C_f = C_T \times \frac{(\frac{I}{I_0} - P)}{(1-P)}$$

$$C_b = C_T - C_f$$

Here C_f is the amount of free drug, C_T is the known added amount of drug, I_0 is the ratio of fluorescence intensity of drug in absence of DNA, I is the ratio of fluorescence intensity in presence of DNA and P is the ratio of observed quantum yield of fluorescence of the totally bound drug to that of the free drug; the quantity P was determined by adding DNA to a known quantity of drug until no further change in fluorescence emission was observed. The ratio $P = I_\infty / I_0$ was the obtained from the initial value of I and the plateau value of I at high DNA concentration.[68]
After that, the ratio of bound ligand molecules per DNA base pair (r) is:

$$r = \frac{C_b}{C_{DNA}}$$

The data were presented as Scatchard plot, i.e., r/C_f *vs* r values, and numerically fitted to the neighbour exclusion model of McGhee and von Hippel,[69] to determine the values of the binding constant (K) and the binding site size (n). The numerical fitting was performed using non-linear curve fitting algorithm implemented into the Sigma-Plot® software.

$$\frac{r}{C_f} = K\,(1 - nr)\left(\frac{1-nr}{1-(n-1)\,r}\right)^{n-1}$$

3.2.3 LINEAR DICHROISM

Linear dichroism is defined as the differential absorption of orthogonal forms of linearly polarized light:

$$LD = A_{//} - A_{\perp}$$

$A_{//}$ corresponds to the absorbance of the sample when the light is polarized parallel to the orientation of flow, and $A_{\perp}$ is the perpendicular absorbance. The "reduced" linear dichroism, LD_r, reflects the dependance of the LD on the wavelength:

$$LD_r = \frac{LD}{A_{iso}}$$

A_{iso} is the absorbance of an isotropic sample, determined by the measurement of absorption spectra of ligand-DNA complexes. The "reduced" linear dichroism may be related to the orientation of DNA (S) and the angle between the respective light-absorbing transition moment and the DNA helix axis:[70]

$$LD_r = \frac{3}{2} \times S\,(3\cos^2\alpha - 1)$$

Assuming a value of $\alpha = 90°$ for the DNA bases for a ligand bound to it, α_L is can be given:

$$\alpha_L = \arccos \sqrt{\frac{\frac{1}{3} - (LD_r)_L}{3\,(LD_r)_{DNA}}}$$

$(LD_r)_L$ is the reduced LD for the ligand, $(LD_r)_{DNA}$ is the reduced LD for DNA and α_L defines the ligand-DNA relative orientation. In the case of intercalation, $\alpha_L \approx 90°$ and $(LD_r)_L \approx (LD_r)_{DNA}$. The measurements of absoption spectra of ligand-DNA complexes were recorded in phosphate buffer in a flow cell on a Jasco J500A spectropolarmeter equipped with an IBM PC and a Jasco J interface. Partial alignment of the DNA was provided by a linear-flow device at a shear gradient of 800 RPM. 173. Concentration of DNA was 0.75 mM (bp) and measurements were performed at [Ligand]/[DNA] = 0, 0.02, 0.04. 0.08, 0.2.

3.2.4 CIRCULAR DICHROISM SPECTROSCOPY

Circular dichroism is defined as the differential absorption of right- (A_R) and left-handed (A_L) circularly polarized light. At a given wavelength:

$$CD(\lambda) = A_R(\lambda) - A_L(\lambda)$$

Linearly polarized light is a electromagnetic radiation defined by an electric field vector, that oscillates in one plane, similar to a sine wave. In circularly light polarized the electric field rotates along the propagation direction, defining a helix in the space, moving a track: if this is a left-handed helix, the light is referred to as left circularly polarized, conversely for right-handed helix. The electric field of light beam causes a linear displacement of charge when interacting with a molecule, whereas the magnetic field of it causes a circulation of charge. These two motions combined result in a helical displacement when light is impinged on a molecole. So, in a achiral sample, the absorbition of light will be the same from right or left with generation of plane polarized light. In a chiral sample, there will be a CD signal, due to fact that one of the two types of circularly polarized light are absorbed in different extents. Due to the interaction with the molecule, the electric field vector of the light traces out an elliptical path while propating. The circular dichroism effect is small so the ellipticity values usually ar on the order of mdeg;[71,72] the ellipticity in radians is:

$$\theta_r = \frac{2.303}{4}(A_L - A_R)\ [rad]$$

And it could be converted into mdeg:

$$\theta_r = \frac{2.303}{4}(A_L - A_R)\frac{180}{\pi}\ [\text{deg}]$$

Circular dichroism spectra were recorded in 10 mM phosphate buffer solution, pH = 7.0 in a quartz sample cuvette, (pathlength ℓ = 1 cm) at 20 °C on a Chirascan (Applied Photophysics Limited, UK) apparatus. At first, measurements with DNA alone and ligand alone (10 μM) were performed; the other measurements were performed at

[Ligand]/[DNA] = 0, 0.08, 0.2 ratios on a Chirascan (Applied Photophysics Limited, UK) apparatus.

3.2.5 IRRADIATION PROCEDURE

HPW 125 Philips lamps, emetting at 365 nm, were used for irradiation experiments. The spectral irradiance of the source 4.0 mW cm^{-2} as measured, at the sample level, by aCole-Parmer Instrument Company radiometer (Niles, IL), equipped with a 365-CX sensor.

3.2.6 DNA PHOTOCLEAVAGE

In order to investigate the DNA photocleavage activity, all the compounds were irradiated, under aerobic conditions in phosphate buffer, in the presence of supercoiled double stranded pBR322 plasmid, which it is a very sensitive tool for damages detection. The irradiation of a photosensitizier could make a damage at single or both strands of the plasmid, inducing the formation of different hydrodynamic forms as OC (form II: open circular) and L (form III: linear). It is possible to separate the three different forms with horizontal electrophoresis because of their different hydrodynamic properties. So the reaction mixtures were resolved by agarose electrophoresis and the DNA bands were detected and quantified.

3.2.6.1 Determination of strand breaks

The plasmid solution (40 μl), containing pBR322 (0.20 μg) and the selected compound at increasing [Drug]/[DNA] ratios = 0.5, 1, 1.5, was irradiated with different UVA doses (En = 0, 3.75 and 7.5 J/cm^2). After the addition of 4 μl of loading buffer (0.25% bromophenol blue, 0.25% xylene cianol, 30% glycerol in water), the samples were loaded on 1% agarose gel and the run was carried out in TAE buffer (40 mM Tris-acetate, 1 mM EDTA) at 80 V for 2 hours. After staining with ethidium bromide solution (0.5 μg/ml), gel was washed with water and the DNA bands were detected with a UV transilluminator. Photographs were taken by a digital photocamera Kodak DC256 and the quanitification of the bands was achieved by image analyzer software Quantity one (BIO-RAD, Milano, Italy). The fractions of supercoiled DNA (Form I) were calculated by this equation:

$$\text{sc} - \text{DNA} = \frac{\text{Area}_{sc}}{\text{Area}_{sc} + \sum_{i=1}^{n} \text{Area}_{cl}/1.66}$$

$Area_{sc}$ is the area of supercoiled DNA (form I) and $Area_{cl}$ is the area of the open circular or linear DNA (form II and III, espectively) obtained by the densiometric analysis of gel. The presence of coefficent 1,66 in the formula is due to fact that ethiudium bromide bound to the supercoiled pBR322 is 1,66 times less than that bound to form II and III.[73] Each experiment was repeated at least three times.

3.2.7 CELLULAR CYTOTOXICITY AND PHOTOTOXICITY

3.2.7.1 Cell Cultures

Various human tumor cell lines were tested, both leukemic and solid tumor, as: Jurkat are human T-lymphoblastic cells; K562 are chronic myelogenous leukemia cells, CEM are human T lymphoblastic cells, RS 4;11 are human B-lymphoblastic acute leukemia cells, SEM are human B-lymphoblastic acute leukemia cells, MV 4;11 are monocytic acute leukemia cells. All leukemic cells were grown in RPMI-1640 medium supplemented with 115 units/ml of penicillin G, 115 μg/ml streptomycin and 10% heat-inactivated fetal bovine serum (complete RPMI-1640 medium). Cells were kept at 37° C in 5% CO_2 humidified atmosphere and re-seeded into fresh medium three times a week.

MCF-7 are human breast carcinoma cells; A549 are human lung carcinoma cells, A431 are human epidermic carcinoma, HeLa are human cervix carcinoma cells, HT29 are colon adenocarcinoma cells. All these cells were grown in DMEM medium supplemented with 115 units/ml of penicillin G, 115 μg/ml streptomycin and 10% heat-inactivated fetal bovine serum (complete DMEM medium). Cells were kept at 37° C in 5% CO_2 humidified atmosphere and re-seeded into fresh medium twice a week.

3.2.7.2 Evaluation by MTT test

Individual wells of 96-well tissue culture microtiter plate were inoculated with 100 μl of complete medium containing 5000 cells. The plates were incubated at 37°C in a humidified 5% CO_2 incubator for 24 hours prior the cell viability experiments. The compounds were dissolved in DMSO, then diluted with appropriate complete medium

for cytotoxicity assay. After medium removal, 100 µl of the drug solution in different concentrations were added to each well and incubated at 37°C for 72 hours.

In the case of photocytotoxicity, the compounds were diluted in Hank's Balance Salt Solution (HBSS pH = 7,2), and cells were incubated with them for 30 minutes at 37°C and then irradiated with UVA (En = 2.5 and 3.75 J/cm^2). Finally, the drug solution was replaced with the appropriate complete medium and the plates were incubated for 72 hours.

After the period of incubation, in both cases, the cell viability was evaluated by MTT [(3-(4,5-dimethylthiazol2yl)2,5 diphenyl tetrazolium bromide)] test.[74] In each well, 10 µl of MTT, 5 mg/ml in PBS, were added and plates were put into the incubator for 3 hours. MTT is a yellow dye that can be absorbed by cells and reduced by mitochondrial dehydrogenases, producing blue insoluble crystals. After incubation, crystals were solubilized adding 100 µl of 0.08 N HCl in isopropanol and plates were detected through microplate BIO-RAD reader at λ = 570 nm. The absorbance of ach sample was corrected by instrument which subtracted the mean value of blanks, i.e., well in which there is medium except cells. The absorbance is proportional with cellular viability, so the cellular survival was calculated by this equation:

$$\% \text{ cell survival} = \frac{A_{100\%} - A_{sample}}{A_{100\%}}$$

$A_{100\%}$ = means of control, i.e., cells without drug or irradiation exposure, which represent 100% of survival.

A_{sample} = absorbance of various samples in which cells were in contact with drug or irradiated in presence of drug.

For every cellular line, GI_{50}, i.e., the drug concentration that induce 50% of inhibition of growth of treated cells, was calculated by SigmaPlot® software. Each experiment was repeated at least three times.

3.2.7.3 Evaluation by trypan blue test

Individual wells of 24-well tissue culture microtiter plate were inoculated with 1 ml of complete medium containing 300000 cells. The experiment is based on the counting cells at t = 0 h (cells non treated with drugs), at t = 24 h, 48 h and 72 h (cells treated

with drug respectively at 24 h, 48 h, 72 h from exposure). After the counting of cells (t = 0 h), drug was added in each well to have 2.5 μM, 5 μM, 10 μM concentrations. The counting of cells was carried out by microscope after adding 5 μl of trypan blue ((3*Z*,3'*Z*)-3,3'-[(3,3'-dimethylbiphenyl-4,4'-diyl)di(1*Z*)hydrazin-2-yl-1-ylidene] bis(5-amino-4-oxo-3,4-dihydronaphthalene-2,7-disulfonic acid)) to 25 μl of cell suspension.

3.2.8 CONFOCAL MICROSCOPY

The confocal microscope is a technique that provides true three dimensional imaging and resolution.
In a 35 mm Petri dishes, 150.000 HeLa cells were incubated at 37°C in the presence of the selected compounds for 1-2 h. Cellular fluorescence images were acquired with an video-confocal microscope (NIKON), using a Nir Apo 60X/1.0W water immersion objective (NIKON). Emission filter settings were used to separate the emission of the probes from that of the test compounds.

3.2.9 FLOW CYTOMETER

Flow cytometry is an useful and important technique to obtain cellular characteristics (presence of membrane antigens with immunofluorescence methods, cellular volume, granularitym or cellular membrane permeability); also, it makes statistical analysis in samples of microscopic dispersed particles in liquid suspension, throught light diffusion and fluorescence phenomena. Flow cytometry presents numerous advantages: the possibility of multiparametric analysis, reproducibility, high speed of analysis, high number of analysed cells and semplicity of preparation of samples.
The instrument (Figure 3.1) is composed by:

- A fluidic system composed by a flow cell (a special capillary, usually in quartz) where an hydrodinamic apparatus allowed to obtain the so-called “hydrodinamic focalization”. In this system, single particles are forced to flow at the centre of this capillary, where ideally they can perform laminar flow. Inside this flow cell, particles are in single line, so the instrument has the possibility to take single measures sequentially;

- An optical system: the light source can be a laser or a mercury vapour lamp. The optical system lets the beam arrives in the capillary core where it is focalized to each single cell flowing. Signals from cells are sent to respective photomultipliers. There is also an optical system parallel and orthogonal to light beam to check side scattering (SS) and forward scattering (FS). The first one givs information about cellular morphology (shape, cytoplasmatic granularity), while the second one about the size of objects. In the SS there are also fluorescent phenomena if fluorochromes are used for analysis (FITC, PE);
- an electronic system and a mechanic system;
- a data SW-analysis-system: the emitted light is checked for spectral analysis (separation of wavelength by dichroic spectra) and it is sent to a photomultiplier to amplify signals that are trasformed to electric impulses and digitised. A computer analyses data and lets their visualization.

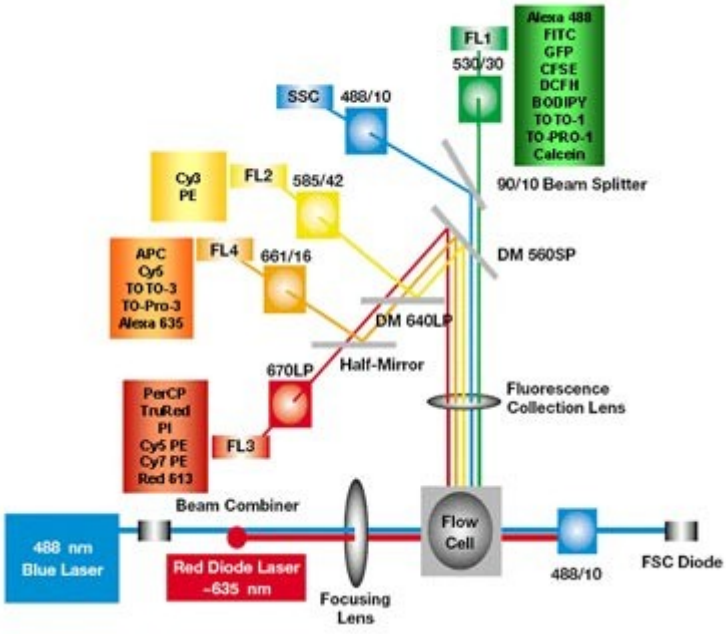

Figure 3.1 Schematic representation of a flow cytofluorimeter.

3.2.9.1 Analysis of cell cicle

The analysis of cell cycle was conducted through flow cytometry; this test is based in the fact that each phase presents a different content of DNA.
Diagrams of growing cultures display the characteristic x-axis distribution according to the DNA content, the first peak corresponding to the diploid peak, i.e., to cells in the G1 phase, and the second peak to cells with doubled DNA content, i.e., to cells in G2/M phase.
Cells with an intermediate DNA content are in the S phase. When DNA is fragmented, as in apoptotic cells, the affinity with the intercalating PI dye is decreased and a so-called hypodiploid peak is present to the left of the G1 peak (Figure 3.2).

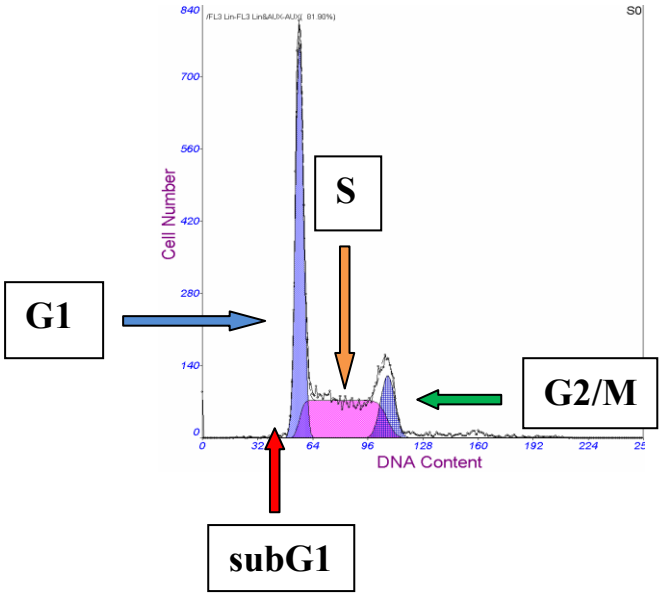

Figure 3.2 Schematic representation of cell cycle distribution.

For flow cytometric analysis of DNA content, $5x10^5$ A549 cells were treated with the selected compounds for 24 hours at 2.5, 5, 10 µM concentrations. After the incubation period, cells were centrifuged and fixed with ice-cold ethanol (70%), then treated overnight with PBS buffer containing RNAse (10 KU/ml) and propidium iodide (PI, 10 µg/ml) (Figure 3.3). When intercalated in DNA, PI fluoresces in the red (620 nm, FL3), if it is excited at 488 nm.

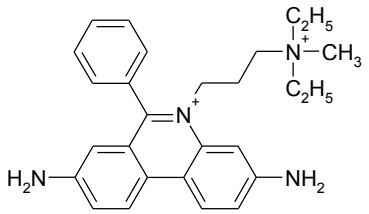

Figure 3.3 Structure of Propidium Iodide (PI)

Each experiment was repeated three times. Samples were analyzed on a Becton Coulter Epics XL-MCL flow cytometer. For cell cycle analysis, results were examined using MultiCycle for Windows (Phoenix Flow Systems, San Diego, CA).[75] Data were expressed as fractions of cells in the different cycle phases.

3.2.10 TOPOISOMERASE I AND II ASSAY

3.2.10.1 Topoisomerase I relaxation and cleavable complex assay

This assay was adapted from Bridewell *et al.*179. Incubation mixtures (20 μl) conteined 50 mM Tris-HCl (pH=7.5), 50 mM KCl, 10 mM $MgCl_2$, 0.5 mM dithiothreitol (DTT), 0.1 mM EDTA, 30 μg/ml of BSA, 0.25 μg pBR322 supercoiled plasmid DNA and 10 units of Topoisomerase I. Reactions were assembled on ice with drug (0-100 μM) and topoisomerase being added last, incubated at 37°C for 30 min and terminated by the addition of pre-warmed SDS (final concentration 1%) followed by proteinase K (final concentration 50 μg/ml) for an additional digestion at 37°C for 15 min. The reaction was terminated by addition of 2 μl of loading buffer (0.25% bromophenol blue, 50% glycerol).[76] The samples contained the compounds were successively extracted with chloroform and isoamyl alchool (CIA 24:1) prior to load. The reaction mixtures were analyzed by electrophoresis on 1% agarose gel in TAE buffer (40 mM Tris-acetate, pH=8.0, 1 mM EDTA) at 20 V overnight and then stained with a solution containing 0.5 μg/ml of ethidium bromide. DNA bands were visualized by UV light and photographed through a digital photocamera Kodak DC256.

For the clavable complex assay, the final reaction mixtures were loaded in a 1% agarose gel contained 0.5 μg/ml of ethidium bromide, run overnight, as previously described, and then washed with distilled water.

3.2.10.2 Topoisomerase II relaxation assay

Assay mixtures (20 μl) contained 100 ng of pBR322 supercoiled plasmid DNA and 2 units of Topoisomerase IIα and 0-100 μM of selected compounds in aqueos solution (50 mM Tris-HCl (pH=8.0), 50 mM KCl, 120 mM $MgCl_2$, 0.5 mM dithiothreitol (DTT), 30 μg/ml of BSA). The reactions for relaxation assay were carried out as described in section 3.2.10.1.

3.2.10.3 Topoisomerase II cleavable complex assay

Incubation mixtures (20 μl) conteined 50 mM Tris-HCl (pH=8.0), 50 mM KCl, 120 mM $MgCl_2$, 0.5 mM dithiothreitol (DTT), 0.1 mM EDTA, 30 μg/ml of BSA, 0.10 μg pBR322 supercoiled plasmid DNA and 6 units of Topoisomerase IIα. Reactions were assembled on ice with drug (0-100 μM) and topoisomerase being added last, incubated at 37°C for 30 min and terminated by the addition of pre-warmed SDS (final concentration 0.5%) followed by proteinase K (final concentration 50 μg/ml) for an additional digestion at 45°C for 1 h. The reaction was terminated by addition of 2 μl of loading buffer. The samples contained the compounds were successively extracted with chloroform and isoamyl alchool (CIA 24:1) prior to load. The reaction mixtures were analyzed by electrophoresis on 1% agarose gel in TAE buffer (40 mM Tris-acetate, pH=8.0, 1 mM EDTA) at 20 V overnight and then stained with a solution containing 0.5 μg/ml of ethidium bromide. DNA bands were visualized by UV light and photographed through a digital photocamera Kodak DC256.

4. RESULTS AND DISCUSSION

4.1 COMPOUNDS

The strategy for the synthesis of 3-aryl-substituted-naphtho[1,2-*b*]quinolizinium derivatives **9**, starting from 3-bromo-naphtho[1,2-*b*]quinolizinium bromide **8**, was represented by the Suzuki-Miyaura cross-coupling reaction. The desired 3-bromo-naphtho[1,2-*b*]quinolizinium bromide **8**, lead compound from which to obtain the aryl-derivatives, was planned to be synthetized from the methyl 6-bromo 2-naphthoate **5** (Scheme 4.1). At first, the reduction of the methyl ester **5** to alcohol **6a** was tried with $LiAlH_4$, but the reaction (monitoring by TLC) did not work. In contrast, it was found that DIBAL-H is the most effective and selective reagent for this reduction.[66] The bromination was performed with PBr_3 and the products of the following reactions were used without further purification. By ^{1}H-NMR spectroscopy and {1H-1H} COSY experiments, it was shown that the angular cyclization of **7b** gave the 3-bromo-naphtho[1,2-*b*]quinolizinium bromide **8**.

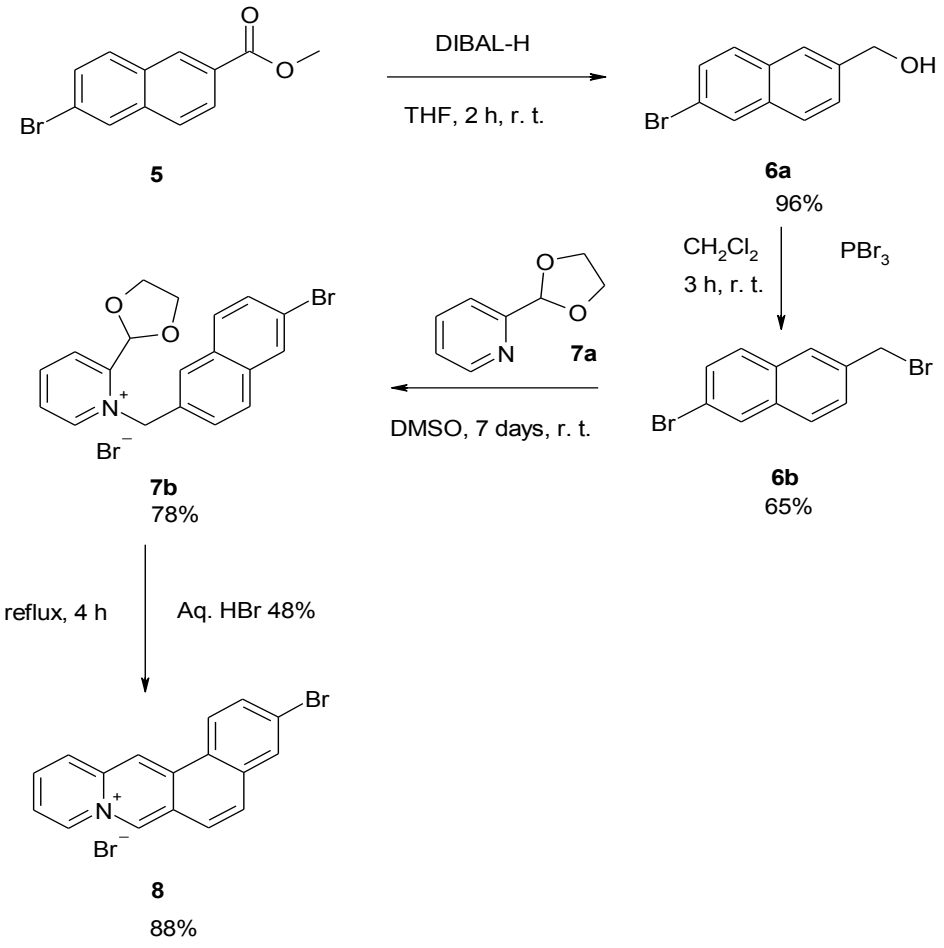

Scheme 4.1 Synthesis of 3-bromo-naphtho[1,2-*b*]quinolizinium bromide **8.**

As mentioned before, the synthesis of 3-aryl-substituted-naphtho[1,2-*b*]quinolizinium derivatives **9** was carried out by the Suzuki-Miyaura cross-coupling reaction.[65] This reaction couples an aryl- or vinyl-boronic acid with an aryl- or vinyl-halide and is catalyzed by a palladium(0) complex. It is widely used to synthesize poly-olefins, styrenes, and substituted biphenyls, and has been extended to incorporate alkyl bromides (Scheme 4.2).

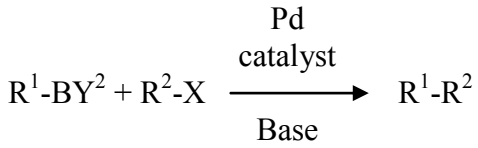

Scheme 4.2 Suzuki Cross Coupling.

The mechanism of the Suzuki reaction is best viewed from the perspective of the palladium catalyst. The first step is the oxidative addition of palladium to the halogen-carbon of **2** to form the organo-palladium species **3**. Ligand exchange with fluoride gives intermediate **4**, which *via* transmetalation with the boronate complex **6** forms the organopalladium species **8**. Reductive elimination of the desired product **9** restores the original palladium catalyst **1** (Scheme 4.3).[77,78]

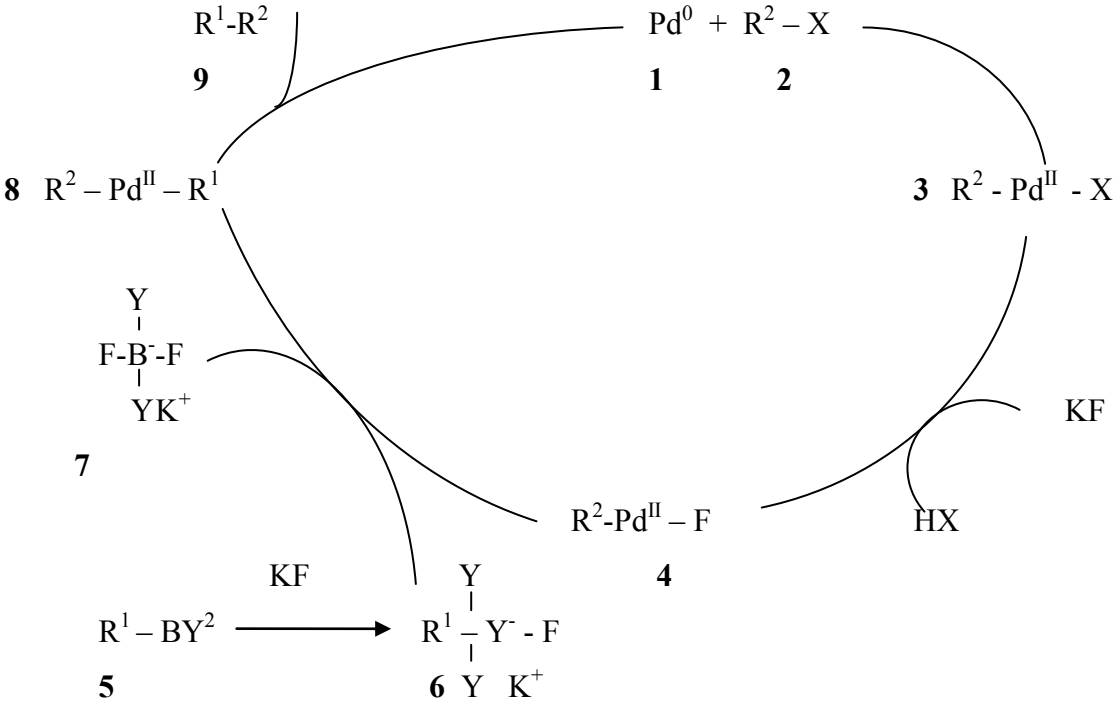

Scheme 4.3 Mechanism of Suzuki-Coupling reaction.

These are the derivatives synthesized by Suzuki-Miyaura cross-coupling (Figure 4.1)

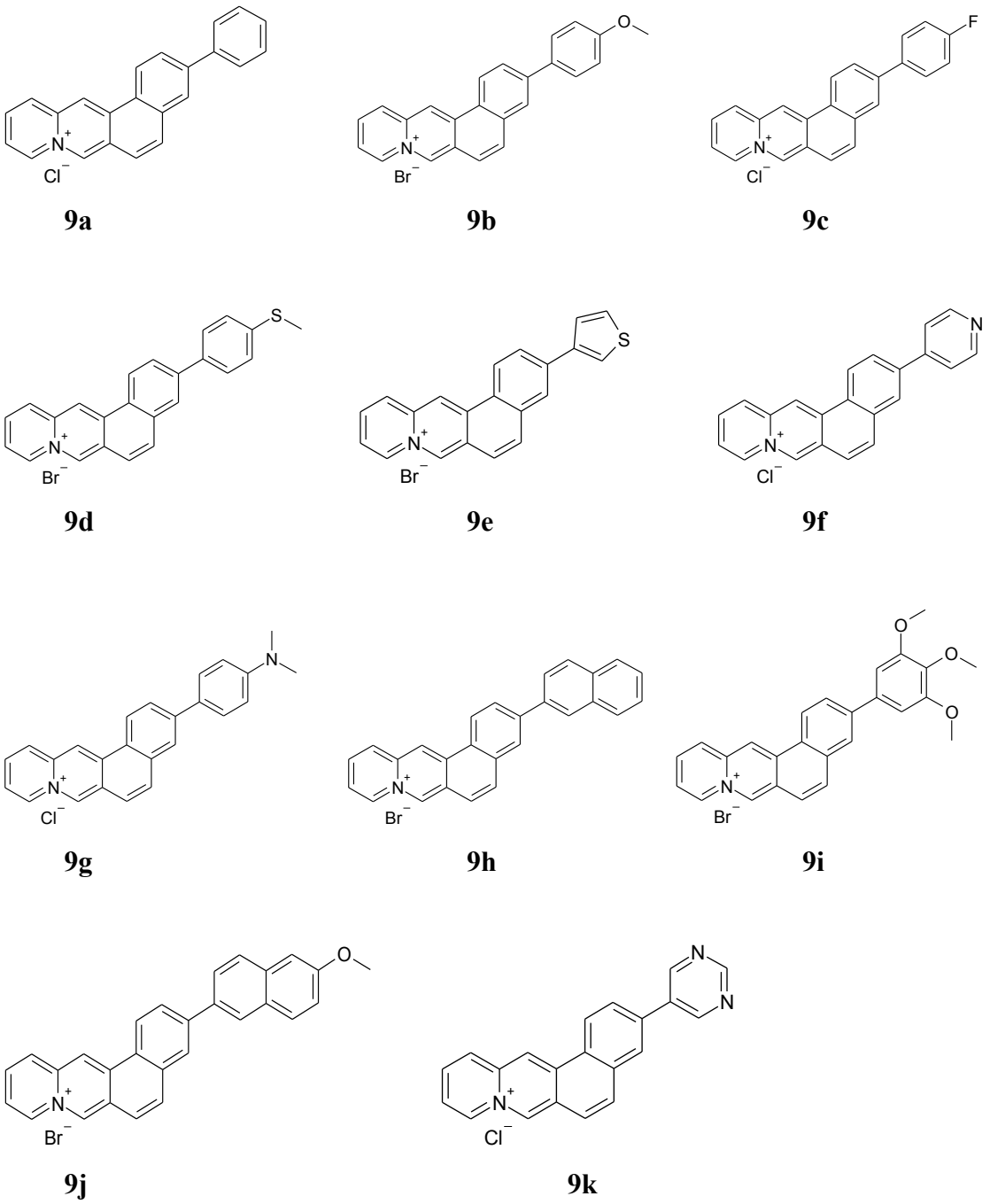

Figure 4.1 Chemical structures of 3-aryl-substituted-naphtho[1,2-*b*]quinolizinium derivatives **9.**

The counter ion should be the bromine but by the elemental analysis it has been possible to evaluate that the purified compounds after column chromatography (Al_2O_3, Activity I) could have chlorine as counter ion. It was shown that quinolizinium salts can exchange the counter ion converting it as chlorine after this kind of separation and

purification.[79] So it is reasonable to suppose that also some of 3-aryl-substituted-naphtho[1,2-*b*]quinolizinium derivatives could be involved in a similar procedure.

4.2 DNA BINDING PROPERTIES

The association of these compounds with DNA should induce modifications on their spectroscopic properties. To investigate the interaction between DNA and compounds, it is useful to gain qualitatively and quantitatively information by spectrophotometric and spectrofluorimetric titrations; about the orientation of the dye molecule relative to the DNA and binding mode, circular (CD) and linear dichroism (LD) spectroscopic techniques are useful. Moreover, these spectroscopic methods are advantageous because organic dyes absorb and emit at wavelengths that do not interfere with the absorption of DNA bases ($\lambda_{max} \approx 260$ nm).

4.2.1 SPECTROPHOTOMETRIC TITRATIONS

In a complex with DNA, the guest molecule is positioned in an environment which is different from that of the uncomplexed compound in solution: thus the two forms can have different absorption properties. So, the addition of DNA to a solution of an intercalator or groove binder induces a change in the spectrum like a shift of the absorption maximum to longer wavelengths (bathochromic shift or red shift) and a decrease of the absorbance (hypocromicity).[25] By these changes, it is possible to study the association process of complex compound-DNA adding aliquots of stDNA solution to a solution of guest compound and the absorption spectra at each compound-DNA ratio were determinated. The experiment was monitored in phosphate buffer 10 mM with stDNA and moreover, to avoid secondary effects (charge-charge interactions), the titrations were confirmed using a higher ionic strength buffer (ETN 100 mM). Compounds **9a**, **9b**, **9c**, **9d**, **9e**, **9f**, **9k** have shown a bathochromic shift (Table 4.1) and a hypochromic effect and this could indicate an interaction between the dyes and the macromolecule.

Table 4.1 Bathochromic shift of compounds **9a, 9b, 9c, 9d, 9e, 9f, 9k**.

Compounds	$\Delta\lambda_{max}$ (bathocromic shift)
9a	**11 nm**
9b	**6 nm**
9c	**12 nm**
9d	**8 nm**
9e	**9 nm**
9f	**8 nm**
9k	**8 nm**

It was not possible to evaluate the compounds **9g**, **9h** and **9j** because of their low solubility in phosphate buffer 10 mM, ETN 10 mM and 100 mM at same concentrations of the other compounds; moreover, compounds **9g**, **9h**, **9i, 9j** have shown a non-specific effect due to their absorption to the cuvette walls so that a possible decrease of absorbance could be due to this and not to interaction with DNA. In order to investigate the interaction of these compounds with DNA, circular and linear dichroism can give other informations.

9a **9b**

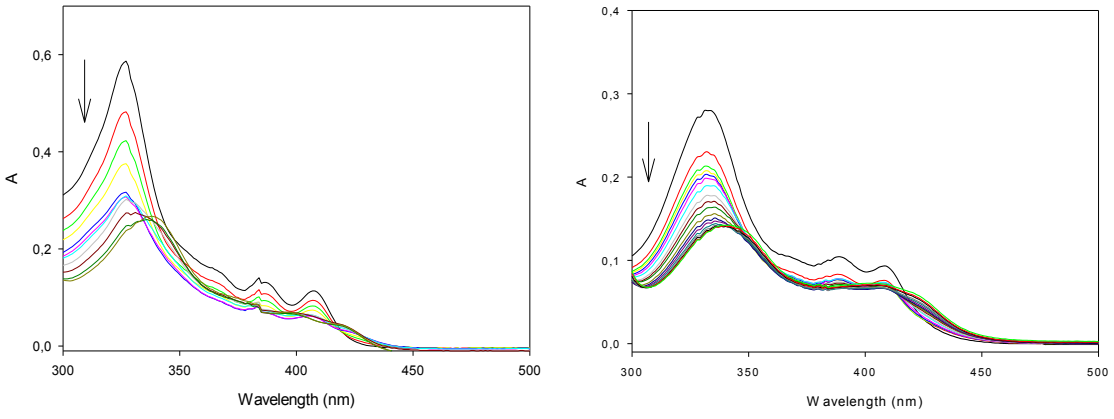

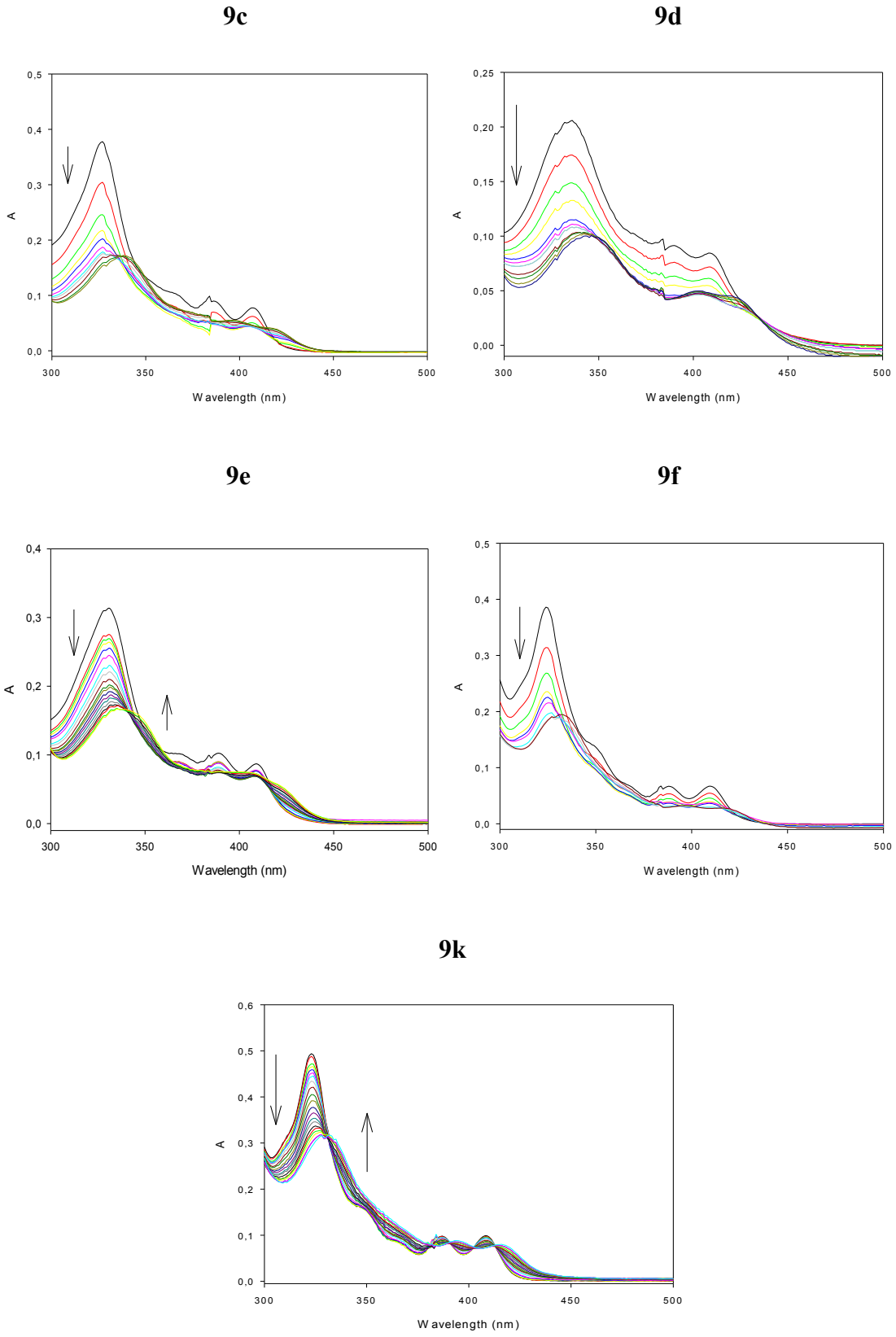

Figure 4.2 Spectrophotometric titrations of stDNA (0-0.1 mM) to compounds **9a**, **9b**, **9c**, **9d**, **9e**, **9f**, **9k** at a ligand concentration of 10 μM in phosphate buffer at 25°C. Arrows indicate the changes of the intensity of the absorption upon addition of stDNA.

For compounds **9a**, **9b**, **9c**, **9d**, **9e**, **9f**, **9k,** the bathochromic and hypochromic effects (Figure 4.2) demonstrate that an interaction with DNA takes place. Isosbestic points are generally present for almost all compounds and reveal that each absorption spectrum arises from almost exclusively species (complexed and uncomplexed dye). Because it is likely that each binding mode results different absorption properties, an isosbestic point indicates that mainly one particular binding mode between the DNA and the guest molecule occurs.

4.2.2 SPECTROFLUORIMETRIC TITRATIONS

If an uncomplexed molecule has fluorescence emission properties in a solution, the addition of DNA can determinate changes in the spectrum, as in the spectrophotometric titration.[25] If there is interaction with DNA, an increasing or decreasing of intensity of maximum of fluorescence, or a shift of this, could take place. It must be consider that the absorption at a particular wavelength also changes on the DNA addition, which also leads to a modification of the emission intensity on excitation at this wavelength; so, to avoid this secondary effect, the fluorophore should be excited at the isosbestic point obtained by spectrophotometric titrations, and to carry out the experiment in this condition. In addition to the information about the interaction between macromolecule and dye, by spectrofluorimetric titrations it was possible to obtain quantitative data about the formation of the complex dye-DNA, because the fluorimetric technique is much more sensitive. By this experiment (always in phosphate buffer 10 mM), the variation of the spectrum was determined after the addition of increasing aliquots of DNA. It was not possible to have precise and reproducible values for compounds **9g**, **9h**, **9i, 9j:** they have shown non-specific effect because of their absorption to the cuvette walls faking the quantitative calculation. Moreover, compounds **9g** and **9i** have shown a low intensity of fluorescence at the same concentrations of the other compounds.

9a

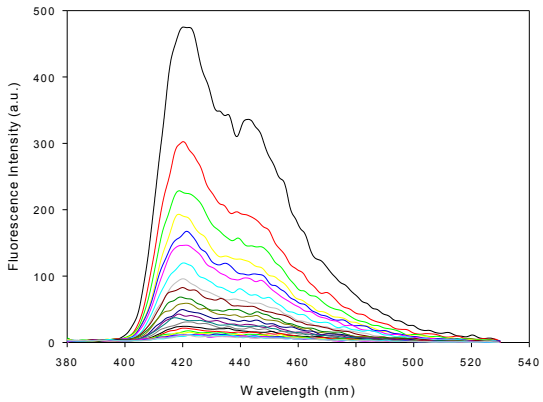

9b

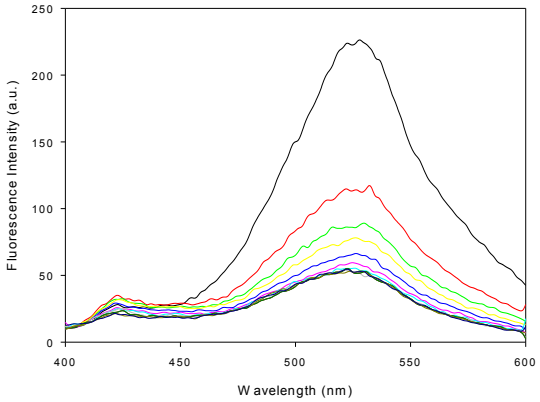

9c

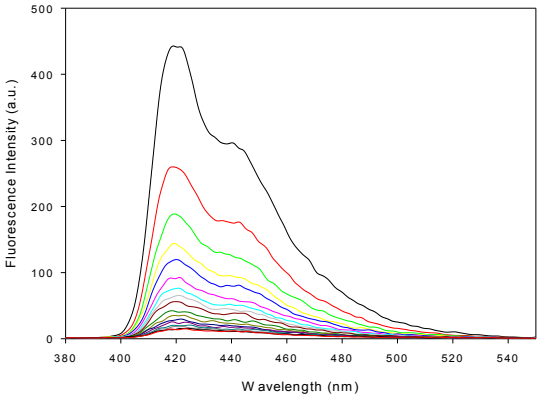

9d

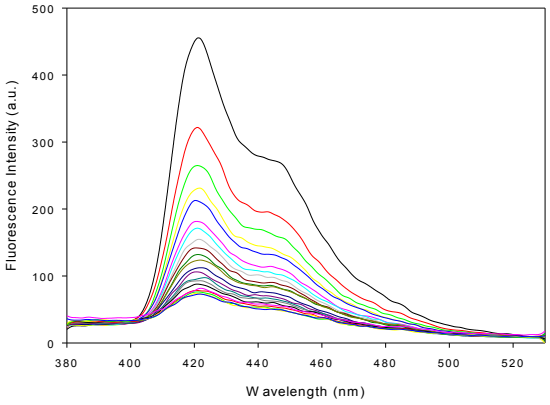

9e

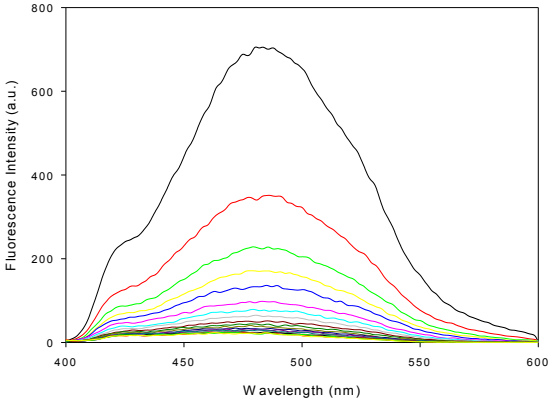

9f

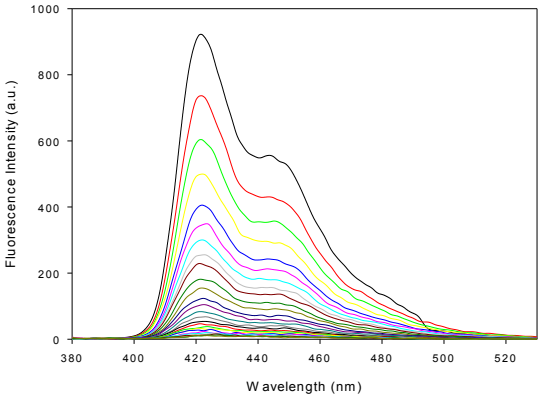

9k

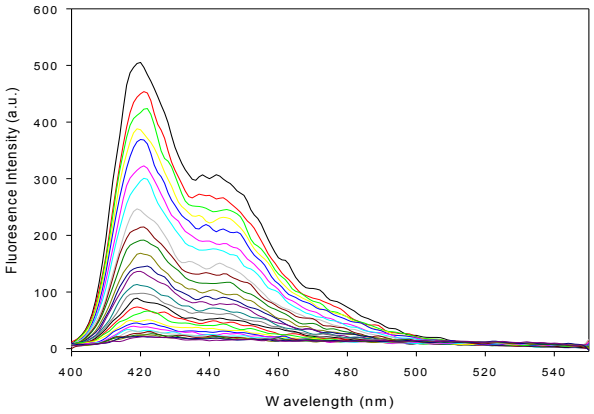

Figure 4.3 Spectrofluorimetric titrations of stDNA (0-0.5 mM) to compounds **9a**, **9b**, **9c**, **9d**, **9e**, **9f**, **9k** at a ligand concentration of 0.5 or 1 μM in phosphate buffer at 25°C.

The fluorescence of studied derivatives (**9a**, **9b**, **9c**, **9d**, **9e**, **9f**, **9k**), after DNA addition, is significantly quenched (Figure 4.3). A shift of red maximum was not observed. So, this technique has shown that there is an interaction between dye and macromolecule. All these data can be utilized to determine quantitative parameters (for detailed description see Experimental procedures, section 3.2.2.3) and they are exploited to obtained the Scatchard plot;[80] by binding analysis of the experimental data is performed according to the McGhee and Von Hippel model,[69] it was possible to determinate the association constant (K) and the binding site-size (*n*). All compound, compared to the naphthoquinolizinum bromide **2**[31], have shown high binding constants (Table 4.2), also producing in most of cases an improvement, confirming a higher affinity to DNA.

The binding-site size (*n*) is a measure of the binding sites (base pairs) occupied by one guest molecule and gives additional information about the binding mode, according to the neighbour-exclusion principle, an intercalator occupies two binding sites, so that at full saturation, an alternating sequence of occupied and free binding sites is observed. So, an intercalator shows a value $n = 2$; when n is significantly larger than 2, the test compound could be a groove binder. The derivatives analyzed show a possible intercalation binding mode (the value of (*n*) for the compounds is from 1.6 to 2.3). Only compound **9f** has (*n*) value > 2, but for similar structure the hypothesis of intercalation system is preferred. So, according to this data, the substituent in pos.3 could have chemical influence on the tetracyclic structure, increasing the ability of the compound to interact with DNA.

Table 4.2. DNA binding constants (*K*), binding-site size (*n*) of the studied derivatives by fluorimetric titrations. DNA binding constants (*K*), binding site size (*n*) of compound **2** is known by literature.[31]

Compounds	K (10^5 M^{-1})[a]	n / bp[b]
9a	**4.87 ± 1.5**	**1.6 ± 0.2**
9b	**6.80 ± 2.0**	**2.1 ± 0.1**
9c	**7.08 ± 0.6**	**1.8 ± 0.1**
9d	**2.68 ± 0.2**	**2.3 ± 0.1**
9e	**10.04 ± 0.1**	**2.2 ± 0.4**
9f	**5.74 ± 0.4**	**4.8 ± 0.6**
9k	**1.45 ± 0.4**	**2.3 ± 0.1**
2[c]	**1.90 ± 0.1**	**2.6 ± 0.1**

[a] Apparent binding contstans. [b] Binding-site size (in base pairs) calculated from fitting according to the McGhee and von Hippel model. [c] From ref.31 and from spectrophotometric titration with ctDNA.

4.2.3 LINEAR DICHROISM SPECTROSCOPY

Linear dichroism is defined as the differential absorption of linearly polarized light and is useful for determination of the binding mode of a dye-DNA complex. DNA is composed of aromatic molecules (bases) stacked vertically and twisted about a helix axis. The accessible DNA transitions are π-π* transitions of these bases, whose absorption starts from about 300 nm and runs down into the far UV. When ligands bind to DNA, they may:

- Intercalate between the DNA bases, in which case their π-π* transitions are parallel to those of the DNA bases and their LD signals are the same as those of the local DNA bases.
- Bind along the minor groove, in which case their long axis transition are 45° from the helix axis, with positive LD signals, and their short axis transitions line parallel to the DNA bases, with negative LD signals.
- Bind in the major groove, where geometry constraints are less rigid (Figure 4.4).
- Associate non-specifically with the DNA backbone, in which case the LD signal will be very small or zero.

Figure 4.4 Binding modes of small molecules with DNA

In a hydrodynamic field most of the DNA molecules are partially arranged along the flow lines (with the transition moment of DNA bases that has a 90° angle (α) with respect to the reference axis, the direction of hydrodynamic field), so that the DNA bases afford a clear negative LD signal (λ ≈ 260 nm). Because of their coplanarity, intercalators should usually give a negative LD signal; in contrast a groove binder should give a positive signal (Figure 4.5), which is relatively weaker compared with that of a intercalator.[70,71]

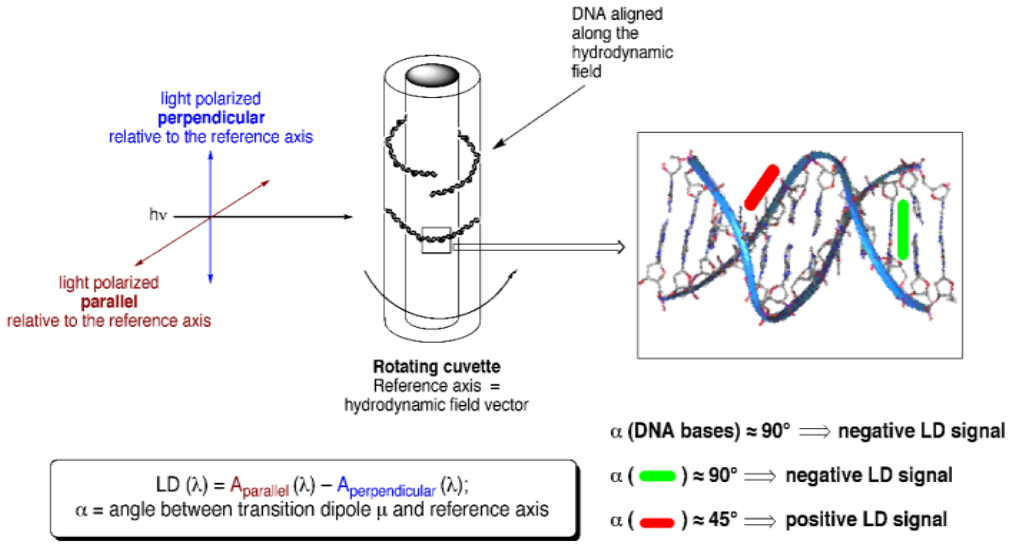

Figure 4.5 Generation of LD signals for an intercalator and a groove binder.

Analyzing these compounds, LD signals of complex dye-DNA are negative at different ligand-to-DNA ratios, in the DNA absorption region (molecule stiffening, better orientation of the double helix along the flow lines and increasing of negative signal) and in the region where only molecules absorb (300-500 nm) (Figure 4.5); the negative LD signals in this long-wavelength region indicate that the ligands are coplanar with the nucleic bases upon binding with DNA. In the LD spectra, the signal of the intensity of DNA increases on addition of compounds, becoming most intensive increasing the

compound/DNA ratio; this effect could reflect a stiffening of the DNA helix due to intercalation, which results in a better orientation of the macromolecule in the hydrodynamic field. Furthermore, all analyzed compounds show a negative signal in the region of ligand absorption, typical of intercalation, which becomes more intensive when the compound/DNA ratio increases and that demonstrates the intercalation. For the compounds **9a,** this signal is more intensive, but also for **9c, 9e, 9f** and **9i** the perturbation of the band is significant, so it is possible to hypothesize a strong interaction of these molecules with DNA (Figure 4.6).

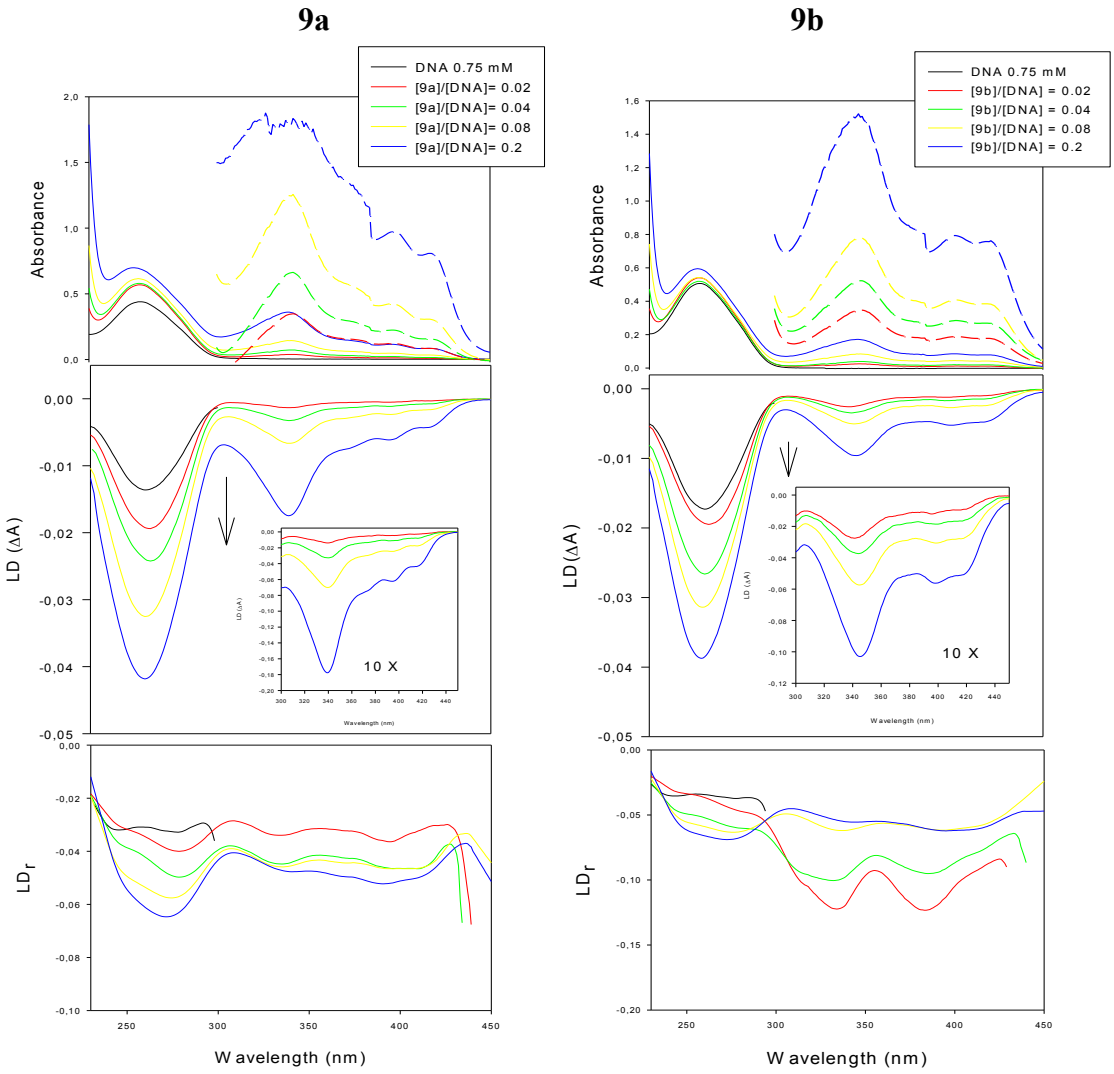

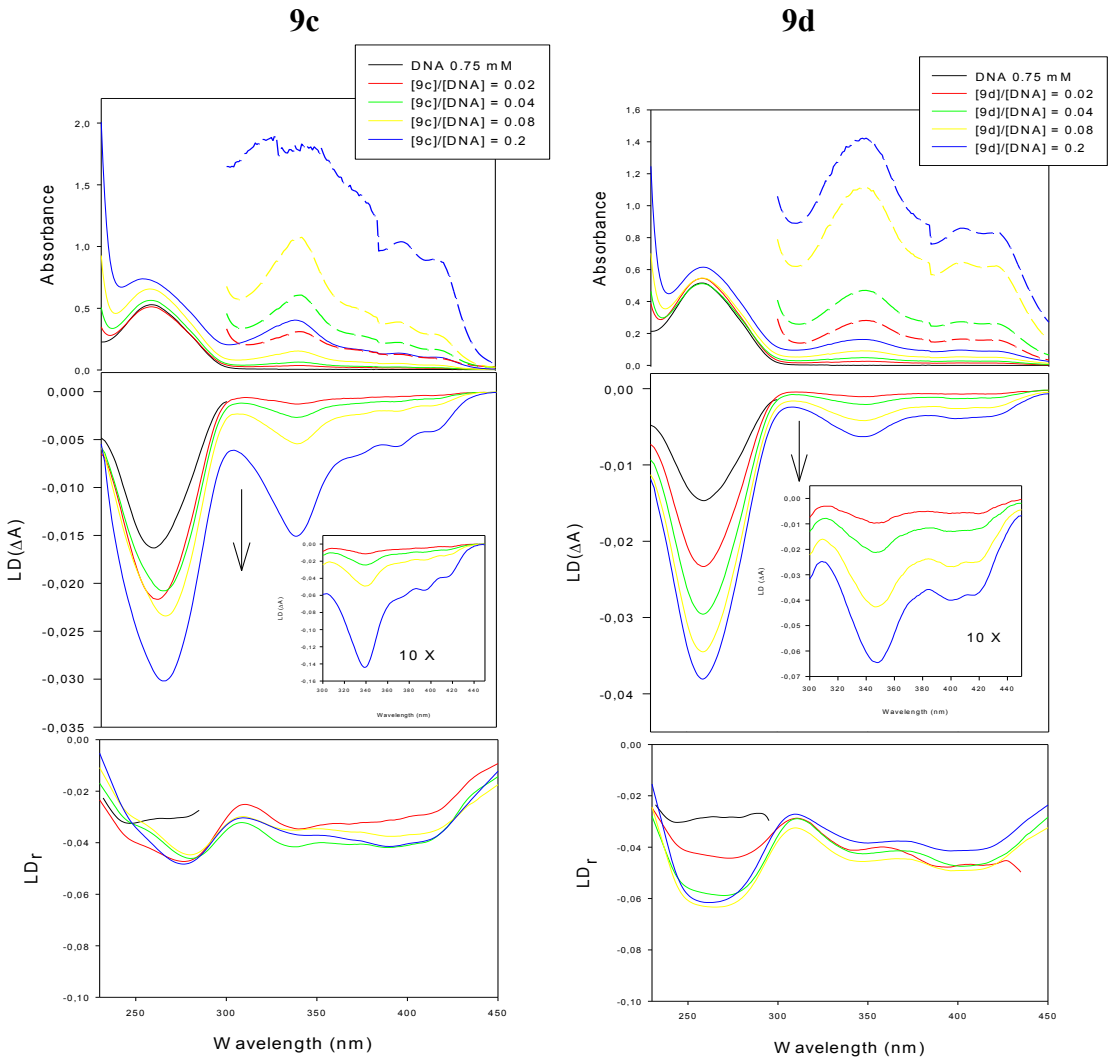
9c
9d
DNA 0.75 mM
[9c]/[DNA] = 0.02
[9c]/[DNA] = 0.04
[9c]/[DNA] = 0.08
[9c]/[DNA] = 0.2
[9d]/[DNA] = 0.02
[9d]/[DNA] = 0.04
[9d]/[DNA] = 0.08
[9d]/[DNA] = 0.2
Absorbance
LD(ΔA)
LDr
10 X
W avelength (nm)

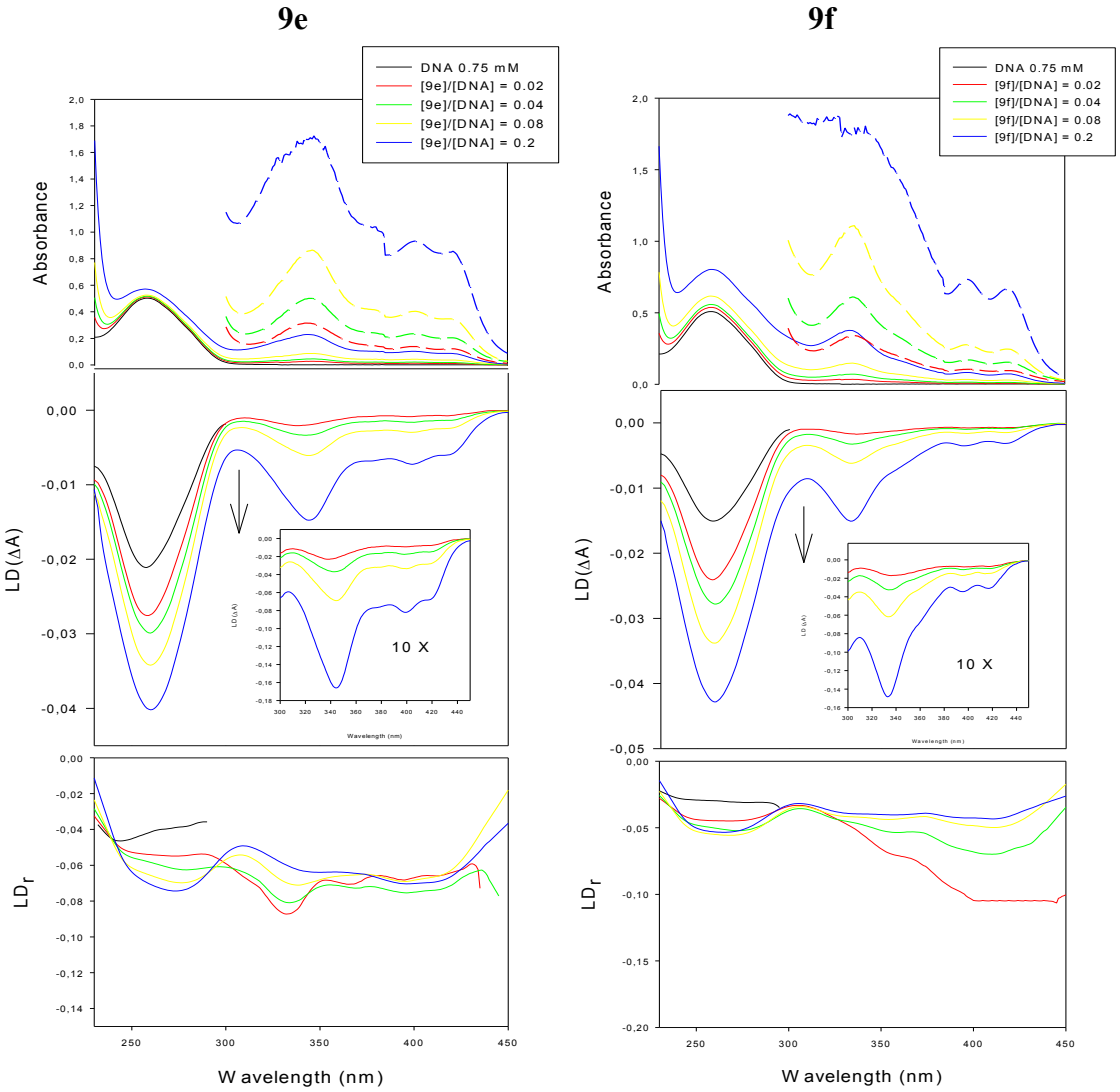
9e
9f
DNA 0.75 mM
[9e]/[DNA] = 0.02
[9e]/[DNA] = 0.04
[9e]/[DNA] = 0.08
[9e]/[DNA] = 0.2
[9f]/[DNA] = 0.02
[9f]/[DNA] = 0.04
[9f]/[DNA] = 0.08
[9f]/[DNA] = 0.2
Absorbance
LD(ΔA)
LDr
10 X
W avelength (nm)

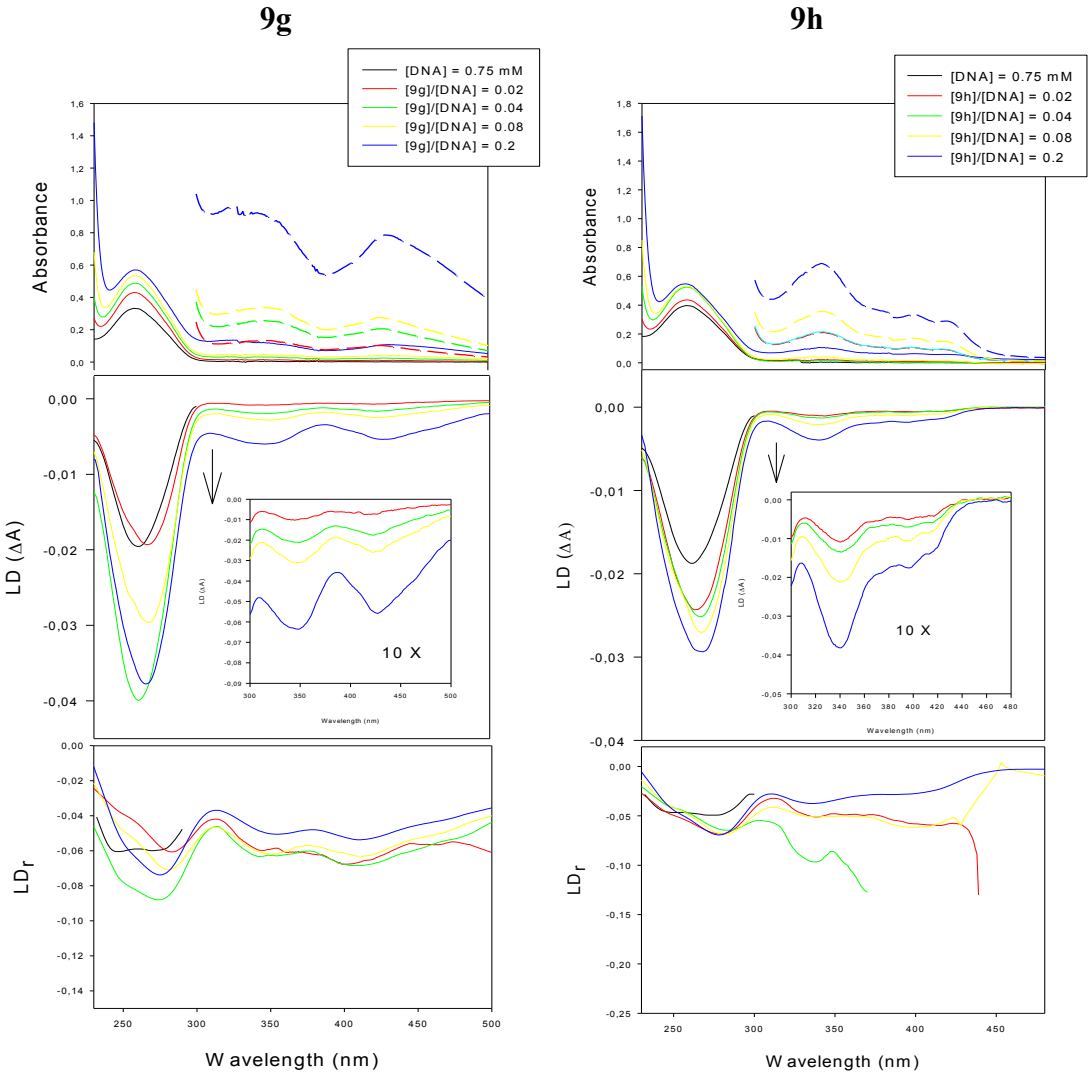
9g
9h
[DNA] = 0.75 mM
[9g]/[DNA] = 0.02
[9g]/[DNA] = 0.04
[9g]/[DNA] = 0.08
[9g]/[DNA] = 0.2
[9h]/[DNA] = 0.02
[9h]/[DNA] = 0.04
[9h]/[DNA] = 0.08
[9h]/[DNA] = 0.2
Absorbance
LD (ΔA)
LDr
10 X
Wavelength (nm)
W avelength (nm)

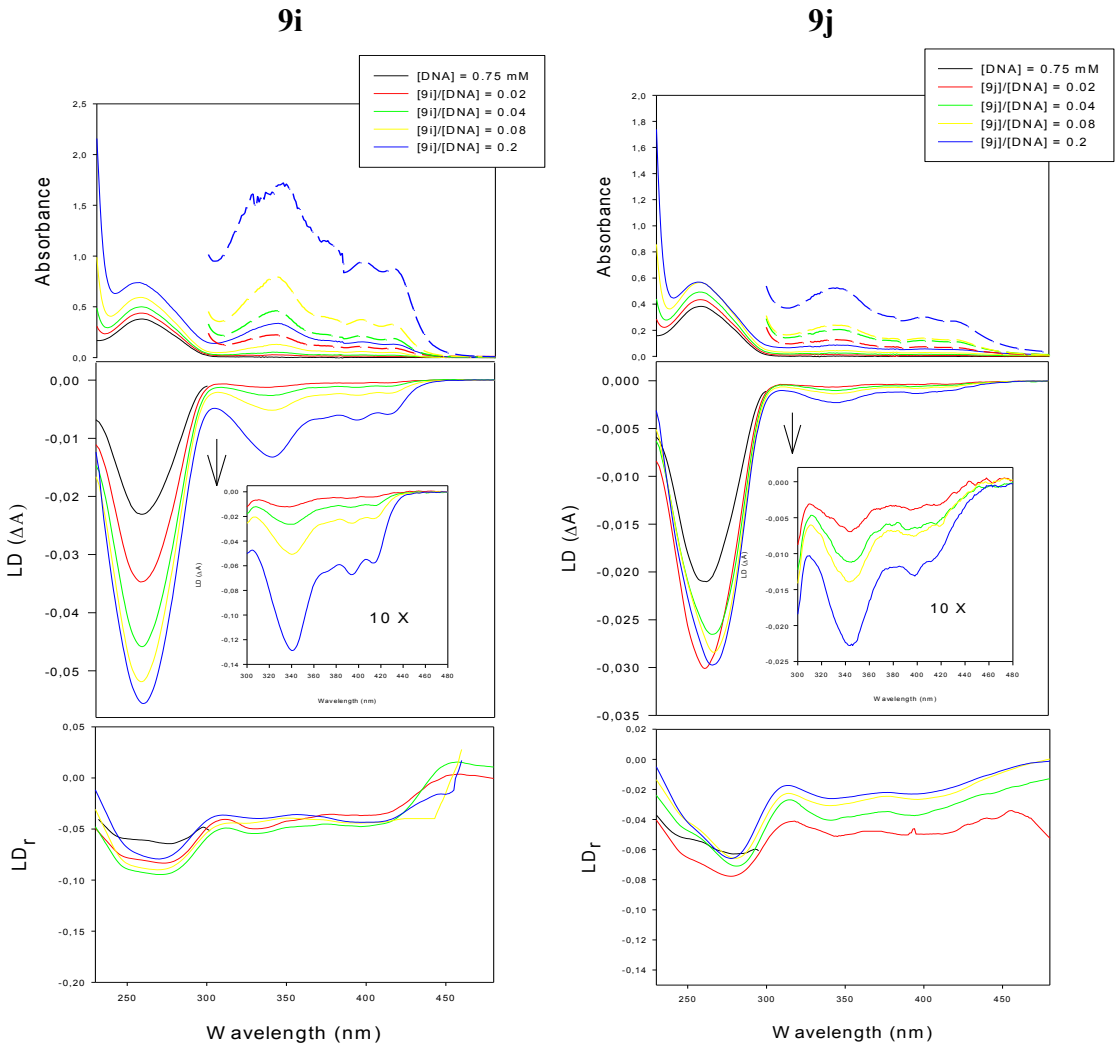
9i
9j
[DNA] = 0.75 mM
[9i]/[DNA] = 0.02
[9i]/[DNA] = 0.04
[9i]/[DNA] = 0.08
[9i]/[DNA] = 0.2
[9j]/[DNA] = 0.02
[9j]/[DNA] = 0.04
[9j]/[DNA] = 0.08
[9j]/[DNA] = 0.2
Absorbance
LD (ΔA)
LDr
10 X
W avelength (nm)

9k

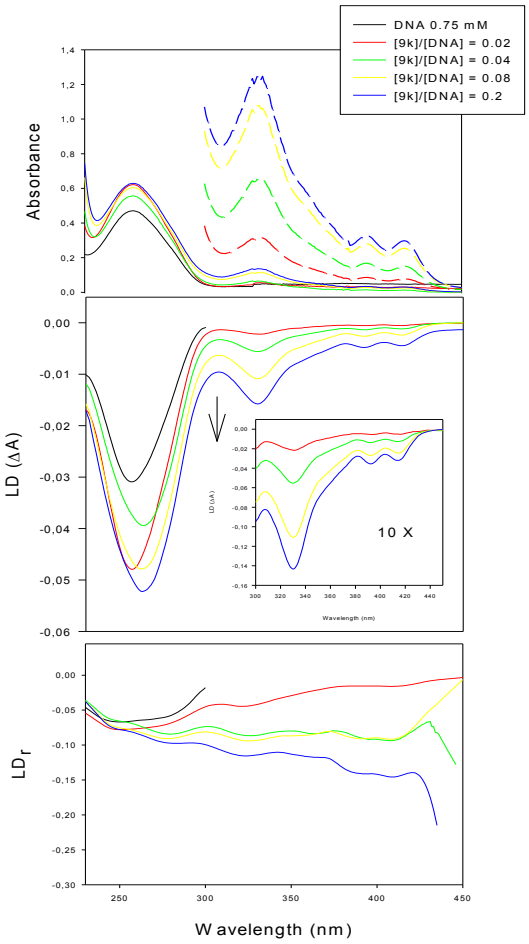

Figure 4.6 Absorption, linear dichroism (LD) and reduced LD (LD_r) spectra of all compounds in the presence of stDNA (0.75 mM) in phosphate buffer at different ligand-to-DNA ratios (r = 0, 0.02, 0.04, 0.08, 0.2). Arrows indicate the changes of LD signals at different ligand-to-DNA ratios.

The "reduced" linear dichroism (LD_r) is obtained by dividing the LD value by the absorbance of the unoriented sample. The LD_r spectra of dye-DNA complexes can give informations about the orientation of the molecular plane of the aromatic dye relative to the DNA bases and allow to distinguish between homogeneous and heterogeneous binding. The negative LD_r signal of compounds **9a**, **9c**, **9d**, **9g**, **9i**, **9j**, is almost independent from the wavelength in the dye-absorption region (300-450 nm, 500 nm) which confirms an intercalative binding mode (Figure 4.6).[31] For compounds **9b**, **9e**, **9f**, **9h**, **9k**, the LD_r spectra show that the values are not totally constant in that region, exhibiting a deviation from perfect intercalation into the double helix: it is conceivable an inhomogeneous binding; anyway for all compounds, there is an additional binding mode (presumably the outside stacking) with a different orientation of the compound as

well as the principal intercalative binging. This different behavior could be due to the different influence that the substituent in pos. 3 makes in the naphtho[1,2-*b*]quinolizinium **2** structure.

4.2.4 CIRCULAR DICHROISM

Circular dichroism (CD) is defined to be the differential absorption of the right and left-handed circularly polarized light. It is not observed for achiral molecules, but when they form complexes with DNA, they are placed within a chiral environment and give an induced CD signal (ICD). The induced CD can derive from a non-covalent interaction between the bound compound and the double helix of DNA, so, its presence, confirms the compound-DNA interaction and might provide further information about the position of the molecule in its complex with the double helix. Although an intercalator shows a negative ICD signal and a groove binder a strong positive ICD signal, there are many experimental data that prove the opposite theory. Generally an intercalator usually has a weak and negative ICD signal, when its transitions are polarized along the long axis of the intecalation pocket, or positive ICD, for transitions in the intercalator plane that are perpendicular to the intercalator-pocket long axis.[25] So, to gain the correct results, it is necessary before to give a proper interpretation of the spectra ad then compare them to other type of investigation.[71,72]

Aqueous solution of achiral acridizinium salts does not show CD activity, while B-DNA shows a spectrum characterized by a negative band at $\lambda \approx 240$ nm and a positive one at $\lambda \approx 270$. These bands of the DNA region can exhibit a perturbation in the presence of increasing concentrations of dyes; but, in order to evaluate an interaction compound-DNA, the presence of signal (ICD signal) in the region of absorption of ligand (300-500 nm) is important.

9a

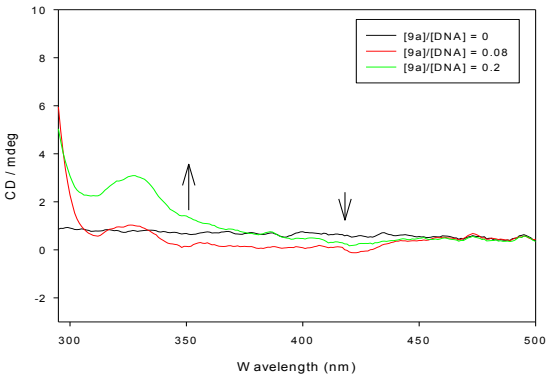

9b

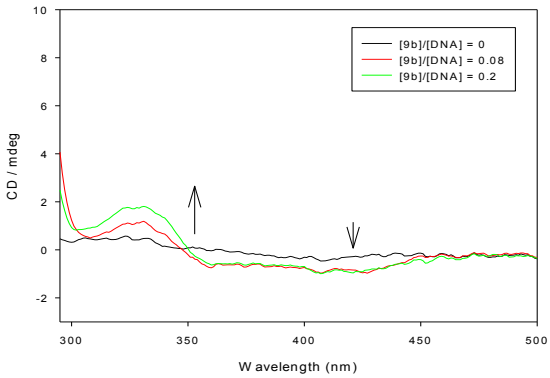

9c

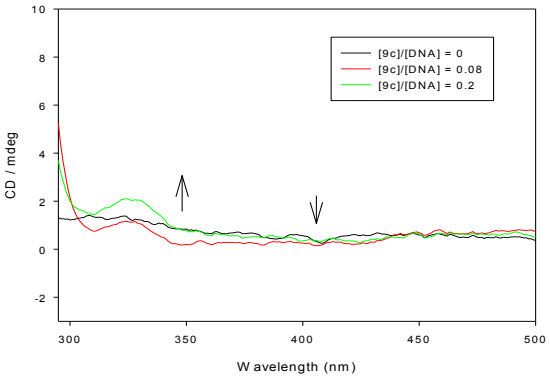

9d

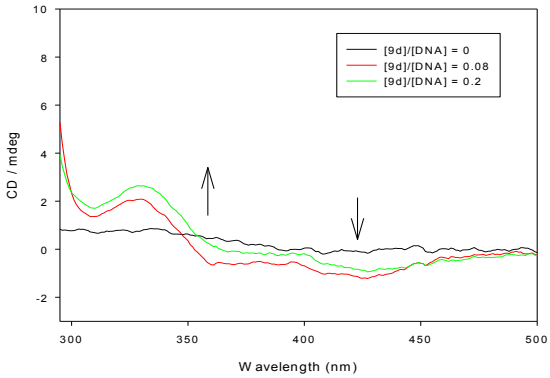

9e

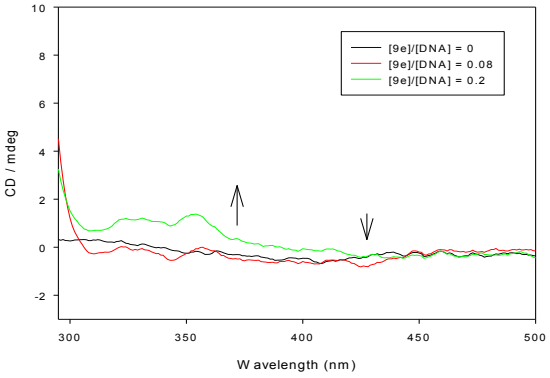

9f

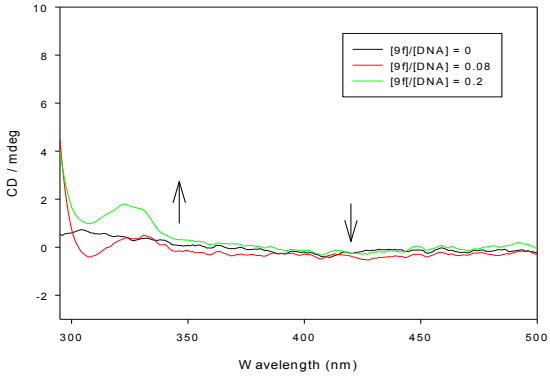

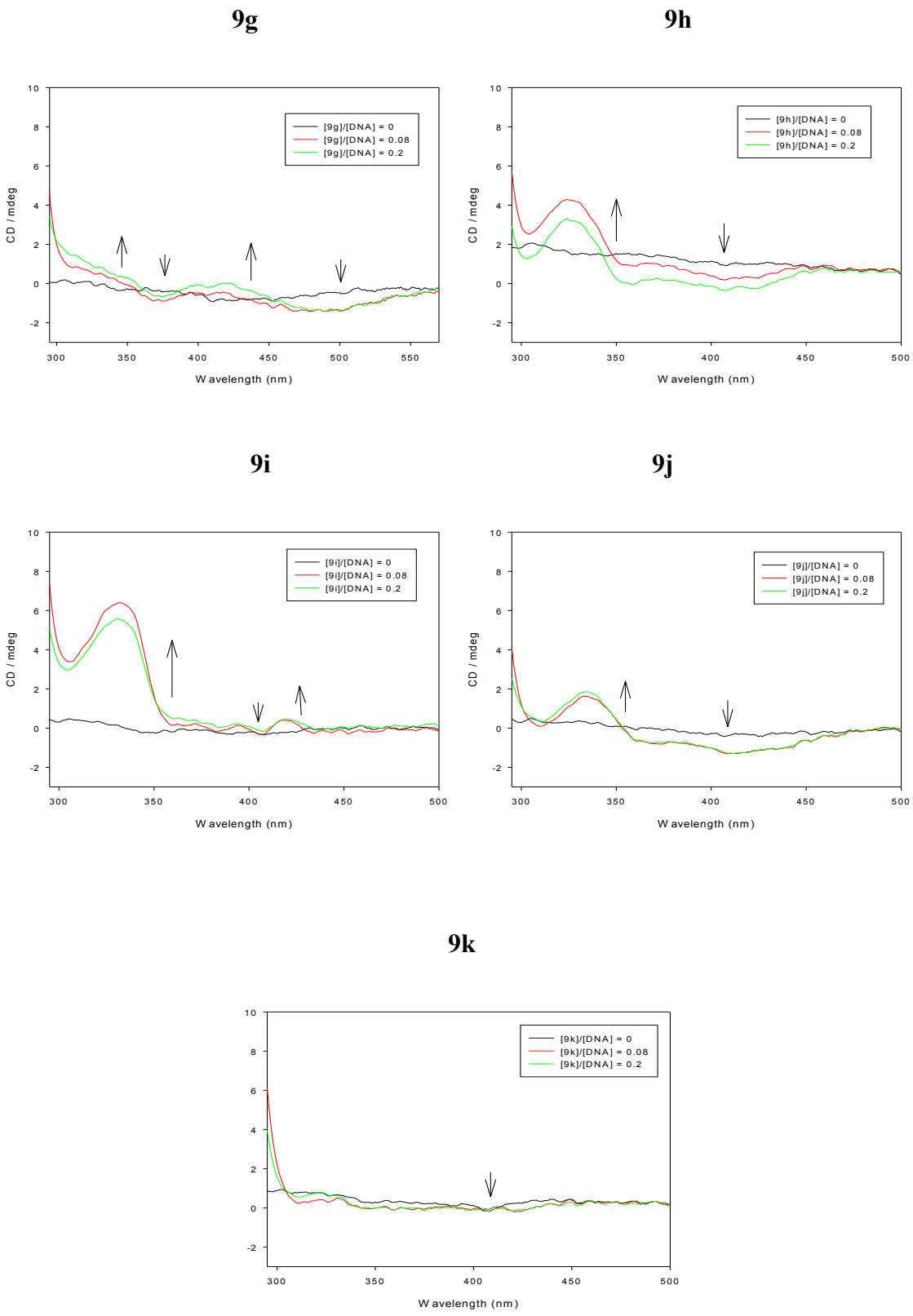

Figure 4.7 CD spectra (ICD part) of the compounds in presence of ctDNA (0.89 mM) in phosphate buffer at different ligand-to-DNA ratios (0, 0.08, 0.2). Concentrations of ligand alone 10 μM. Arrows indicate the changes of LD signals at different ligand-to-DNA ratios.

The ICD spectra of all derivatives (Figure 4.7) show a weak negative ICD signal (usually from 380-450 nm) and a more important positive ICD signal in correspondence of the maximum of absorption of the compound (about from 320-350 nm). This signal can be more intensive for compounds **9a**, **9h**,and **9i**. Only for compound **9k,** the ICD bands are very weak. In comparison to the spectrum of naphtho[1,2-*b*]quinolizinium **2**,[31] in which the positive ICD signal has been shown a consequence of an intercalation system and in relationship to the structure of molecule, the positive ICD signal of studied compounds confirms an interaction of intercalative type with the double helix. So, this positive ICD signal shows that the transition moments of the intercalated salt (and thus approximately the long axis of the chromophore) are aligned almost perpendicular to the long axis of the pair-bases pocket. Also considering the negative ICD, an additional binding mode could take place, probably due to the presence of the substituent in pos.3, although the intercalation is the most important binding mode that occurs between the compounds and the nucleic acids.

4.2.5 DNA-PHOTOCLEAVAGE

It is known that the intercalation of planar polycyclic aromatic molecules into double stranded DNA leads to a hindered or suppressed function of the nucleic acid in physiological processes; furthermore, some of these intercalators agents have shown to be also photosensitizers against nucleic acids, because the light can be used then as a trigger for the nuclease activity, representing another kind of damage to DNA. While the association of heterocycles compounds to DNA, and thus the DNA modification, is reversible process, the DNA damage, which occurs on irradiation of drug-DNA complexes, is often irreversible. So, this kind of DNA damage often leads to cell death or mutations, and must be avoided in healthy system. However, it may be applied in photochemotherapy to remove unwanted cells.[31]

The DNA photocleavage activity of synthesized derivatives was investigated by electrophoresis on agarose gel (1%); the compounds were irradiated, in aqueous phosphate buffer 10 mM in presence of pBR322 plasmid at different [compound]/[DNA] ratios and at increasing UV-A doses (3,75 e 7,5 J cm^{-2}).

9a

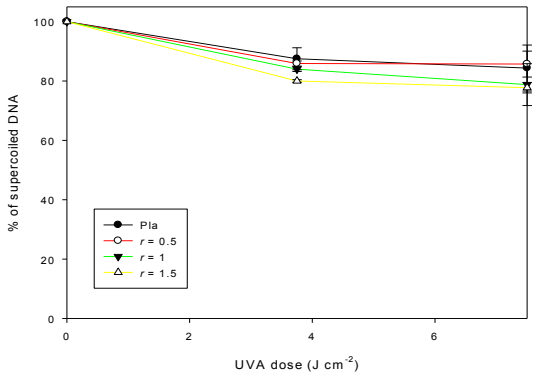

9b

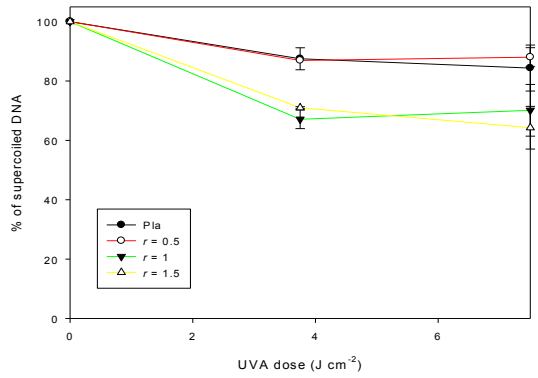

9c

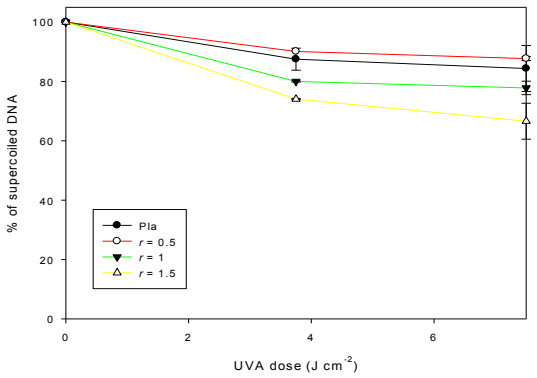

9d

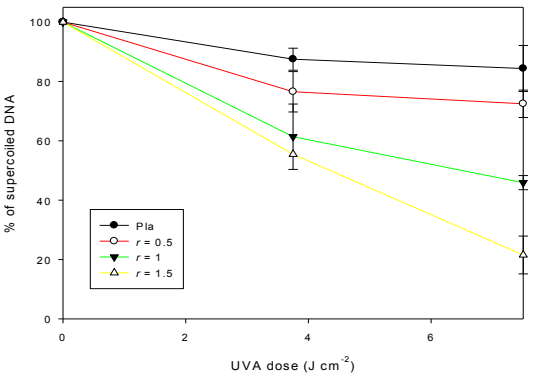

9e

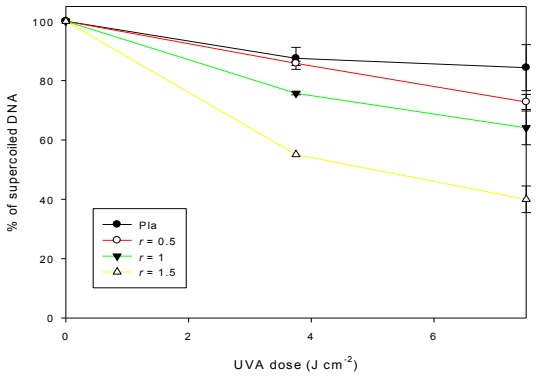

9f

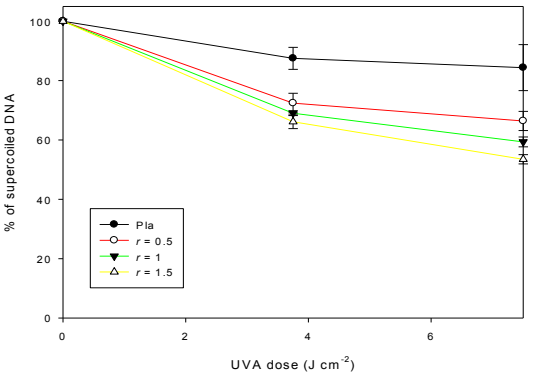

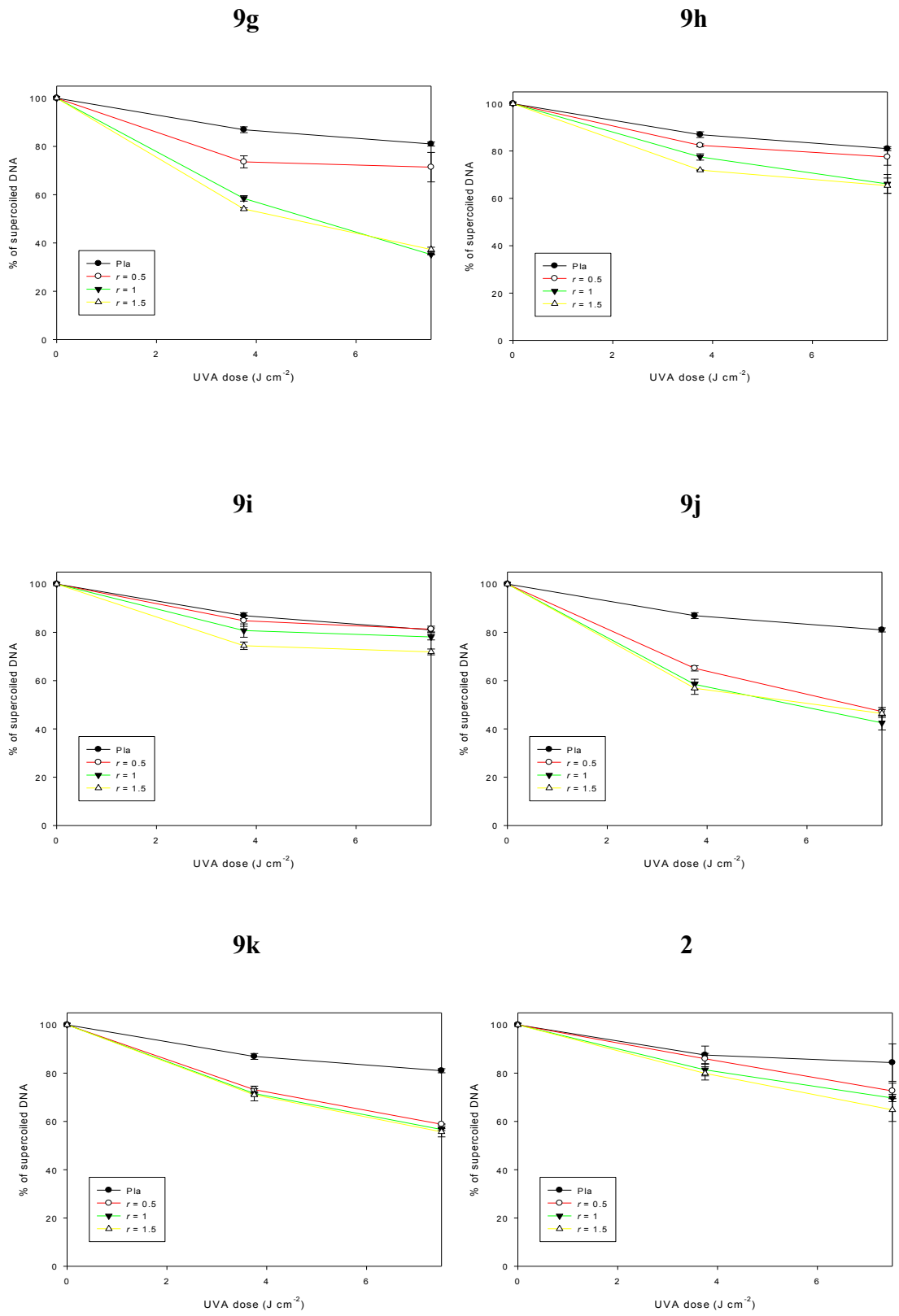

Figure 4.8 Strand breaks of plasmid DNA pBR322 expressed as percentage of form I after UV-A irradiation in the presence of the different compounds at increasing [Dye]/[DNA] ratios (r = 0.5, 1, 1.5).

The results show no DNA cleavage for all compounds (Figure 4.8) in the experiments in "dark condition". Increasing of concentrations of analyzed derivatives and UV-A irradiation dose induce breakage in the nucleic acids structure: there is a decrease of the percentage of supercoiled DNA, identifying an hypothetic photodamage. The pBR322 aliquots irradiated in the presence of compounds at ratio r = 0.5 usually show a weak photodamage; but if the ratio increases (r = 1.5), photodamage is very evident. This happens quantitatively for compounds **9b, 9c, 9d, 9e, 9f, 9g, 9h, 9j;** but for compounds **9a, 9c, 9k** and the reference (**2**) this behaviour is not so evident. For compounds that act provoking a better photodamage, their substituents probably induce a better ability of binding to macromolecule or a better photo-activation.

4.2.6 CONCLUSIONS ON DNA BINDING PROPERTIES

In summary, the 3-substituted-naphtho[1,2-*b*]quinolizinium derivatives **9** have shown a strong interaction with DNA-double helix. The introduction of fourth aromatic ring, in comparison to the tricyclic benzo[*b*]quinolizinium **1**[31] and the introduction of the substituent in pos. 3 in comparison to the naphtho[1,2-*b*]quinolizinium **2** have improved the interactions between the dye and the DNA bases producing higher binding constants. This effect is due to the additional benzene moiety which extends the surface of the planar chromophore and increases the π stacking between the dye and the DNA, while the substituent in pos. 3 could has chemical influence on the tetracyclic structure, increasing its ability to interact with DNA or producing an external binding. However, it is difficult to establish which chemical change in the substituent (presence of heteroatoms in the ring, introduction of different chemical groups, etc..) leads to improved DNA affinity. The results of the LD and CD experiments are generally in agreement and reveal a principal intercalative binding mode, not excluding the hypothesis of an additional binding mode (presumably the outside stacking). All experiments of DNA-binding are in agreement about the interaction of these derivatives with DNA: it could happen that the tetracycle is involved in the intercalation with the DNA base pairs, whereas the remaining substituent points outside the intercalation pocket. Finally, the experiments about the DNA-photocleavage have shown that after UV-A irradiation, there is an evident breakage in the nucleic acids structure.

4.3 BIOLOGICAL ACTIVITY

4.3.1 CELLULAR CYTOTOXICITY

About the cellular toxicity, two kinds of experiments were considered: before, MTT test was useful to evaluate the cytotoxocity by an metabolic inhibition; then Trypan blue test was useful to discriminate the growth inhibition from the dead cells.

4.3.1.1 Evaluation by MTT test

Various human tumor cell lines were tested, both leukemic and solid tumor, as: Jurkat are human lymphoblastic cells; K562 are chronic myelogenous leukemia, CEM are human T lymphoblastic cells, RS 4;11 are human lymphoblastic leukemia cells, SEM are human lymphoblastic leukemia cells, MV 4;11 are monocytic acute leukemia cells, MCF-7 are human breast carcinoma cells; A549 are human lung carcinoma cells, A431 are human epidermic carcinoma, HeLa are human cervix carcinoma cells, HT29 are colon adenocarcinoma cells. The cells were treated with increasing concentrations of the derivatives (20, 10, 5, 2.5, 1.25, 0.625 μM) and cytotoxicity was evaluated after 72 h of incubation by MTT test.[74] MTT is a yellow dye that can be absorbed by cells and reduced by mitochondrial dehydrogenases, producing insoluble blue crystals, which after incubation (3 h) are solubilized and the absorbance detected at λ = 570 nm All compounds synthesized were tested and naphtho[1,2-*b*]quinolizinium bromide **2**, without substituent in pos. 3 was used as reference compound; cytotoxicity was calculated as GI_{50} micromolar values (Table 4.3)

Table 4.3 Cytotoxicity of the tested compounds against different human tumor cell lines.

IC_{50} (μM)[a]						
Compounds	**JURKAT**	**RS 4;11**	**K562**	**CEM**	**SEM**	**MV 4;11**
9a	**0.86 ± 0.18**	**0.31 ± 0.06**	**1.59 ± 0.11**	**1.41 ± 0.27**	**0.54 ± 0.12**	**0.68 ± 0.19**
9b	**0.87 ± 0.13**	**0.26 ± 0.03**	**1.34 ± 0.19**	**1.30 ± 0.34**	**1.00 ± 0.16**	**0.40 ± 0.12**
9c	**4.10 ± 1.10**	**0.91 ± 0.18**	**2.53 ± 0.31**	**1.52 ± 0.48**	**1.80 ± 0.52**	**1.24 ± 0.20**
9d	**0.78 ±0.12**	**0.79 ± 0.09**	**1.57 ± 0.20**	**1.57 ± 0.22**	**1.90 ± 0.37**	**1.50 ± 0.19**
9e	**2.3 ± 0.55**	**0.20 ± 0.04**	**2.25 ± 0.24**	**2.72 ± 0.44**	**0.84 ± 0.13**	**0.51 ± 0.16**
9f	**> 20**	**> 20**	**> 20**	**> 20**	**> 20**	**19.2 ± 3.2**
9g	**0.84 ± 0.10**	**0.21 ± 0.07**	**3.33 ± 0.52**	**1.34 ± 0.15**	**0.31 ± 0.05**	**0.35 ± 0.05**
9h	**3.29 ± 0.39**	**0.71 ± 0.16**	**5.26 ± 0.31**	**2.55 ± 0.23**	**0.82 ± 0.44**	**1.00 ± 0.30**
9i	**9.95 ± 0.32**	**0.37 ± 0.05**	**> 20**	**7.33 ± 0.26**	**4.80 ± 1.40**	**3.90 ± 0.80**
9j	**0.97 ± 0.10**	**0.90 ± 0.15**	**5.67 ± 0.44**	**2.67 ± 0.13**	**0.67 ± 0.11**	**2.90 ± 0.50**
9k	**> 20**	**> 20**	**> 20**	**> 20**	**> 20**	**19.8 ± 2.5**
2[b]	**4.98 ± 0.20**	**14.4 ± 2.2**	**13.47 ± 1.5**	**4.80 ± 0.50**	**> 20**	**18.6 ± 2.3**

Compounds	**A549**	**MCF-7**	**HeLa**	**HT29**	**A431**
9a	**0.20 ± 0.11**	**5.53 ± 0.44**	**0.72 ± 0.34**	**0.83 ± 0.32**	**4.99 ± 1.00**
9b	**1.10 ± 0.24**	**4.70 ± 0.47**	**1.30 ± 0.55**	**1.40 ± 0.22**	**4.60 ± 0.63**
9c	**3.70 ± 1.70**	**6.44 ± 0.32**	**3.90 ± 1.00**	**1.90 ± 0.28**	**6.78 ± 0.65**
9d	**5.50 ± 1.20**	**4.05 ± 0.59**	**1.10 ± 0.29**	**1.10 ± 0.30**	**6.21 ± 0.69**
9e	**2.80 ± 0.80**	**5.71 ± 0.70**	**0.74 ± 0.53**	**3.10 ± 0.81**	**6.60 ± 0.72**
9f	**3.40 ± 1.30**	**> 20**	**10.1 ± 3.20**	**> 20**	**> 20**
9g	**0.96 ± 0.13**	**1.42 ± 0.11**	**0.61 ± 0.02**	**0.70 ± 0.20**	**5.76 ± 0.40**
9h	**2.40 ± 0.24**	**2.72 ± 0.49**	**4.50 ± 0.40**	**3.10 ± 0.60**	**> 20**
9i	**13.5 ± 0.67**	**10.17 ± 0.62**	**> 20**	**10.2 ± 3.10**	**> 20**
9j	**1.20 ± 0.25**	**1.91 ± 0.10**	**0.98 ± 0.26**	**1.10 ± 0.20**	**9.92 ± 0.51**
9k	**2.40 ± 0.70**	**> 20**	**> 20**	**12.6 ± 1.1**	**> 20**
2[b]	**1.71 ± 0.20**	**4.40 ± 0.60**	**> 20**	**> 20**	**> 20**

[a] Concentration of compound required to inhibit the cell growth by 50% after 72 h of exposure as determined by MTT assay.[74] [b] For compound **2**, the cytotoxicity on Jurkat, K-562, CEM, A549, MCF-7 is known by literature.[81]

Almost all derivatives show a micromolar GI_{50} concentration. On some leukemic cell lines, for the compounds **9a**, **9b**, **9d**, **9g** and **9j**, the GI_{50} is below the micromolar. The compounds **9f** and **9k** are both only active on A549; moreover **9f** is active only on HeLa and **9k** only on HT29. This could be explained by the characteristics of compounds or of the cell line, probably for different molecular target or different cellular uptake. Moreover, these two compounds have a similar substituent in pos.3: so the introduction of a heterocyclic substituent containing nitrogen decreases the cytotoxic activity because of a reduced ability of the molecule to interact with molecular target or of a reduced ability to get it. Anyway, for almost all 3-aryl derivatives, the cytotoxicity is stronger than the reference compound **2**: these data could show that the introduction of phenyl group (**9a**), a phenyl group with a electron donor group in *para* position in the ring, like a dimethyl-amino group (**9g**) or a methoxyl group (**9b**), a thiophene group (**9e**) in pos. 3, increases cytotoxic activity; furthermore, about the methoxyl group, the same previous hypothesis can be formulated comparing compounds **9h** and **9j**; the second one, which has a $-OCH_3$ group in pos 6' on the naphthalene structure, shows a higher cytotoxicity than the first one, which has not a substituent in the naphthalenyl group. Finally, the presence of three electron donor groups (**9i**) in the phenyl ring seems to decrease the cytotoxicity. For the successive experiments on biological activity, **9a**, **9b**, **9d, 9g** and **9j** were chosen because of their low concentration of GI_{50}.

4.3.1.2 Evaluation by Trypan blue test

The trypan blue test allows to distinguish quantitatively inhibition growth and the dead cells: it is a dye that is able to pass the cellular membrane of dead cells, giving the typical blue coloration, but not of viable cells that will remain white: in the counting by microscope, both types of cells will be considered.[82] The experiment was carried out on Jurkat cell line testing compounds **9a**, **9b**, **9d** because their low concentration of GI_{50}; the cells were treated with increasing concentrations of the derivatives (10 μM, 5 μM, 2.5 μM): the cytotoxicity, counting viable cells (white) and dead cells (blue), was evaluated after 0 h, 24 h, 48 h and 72 h.

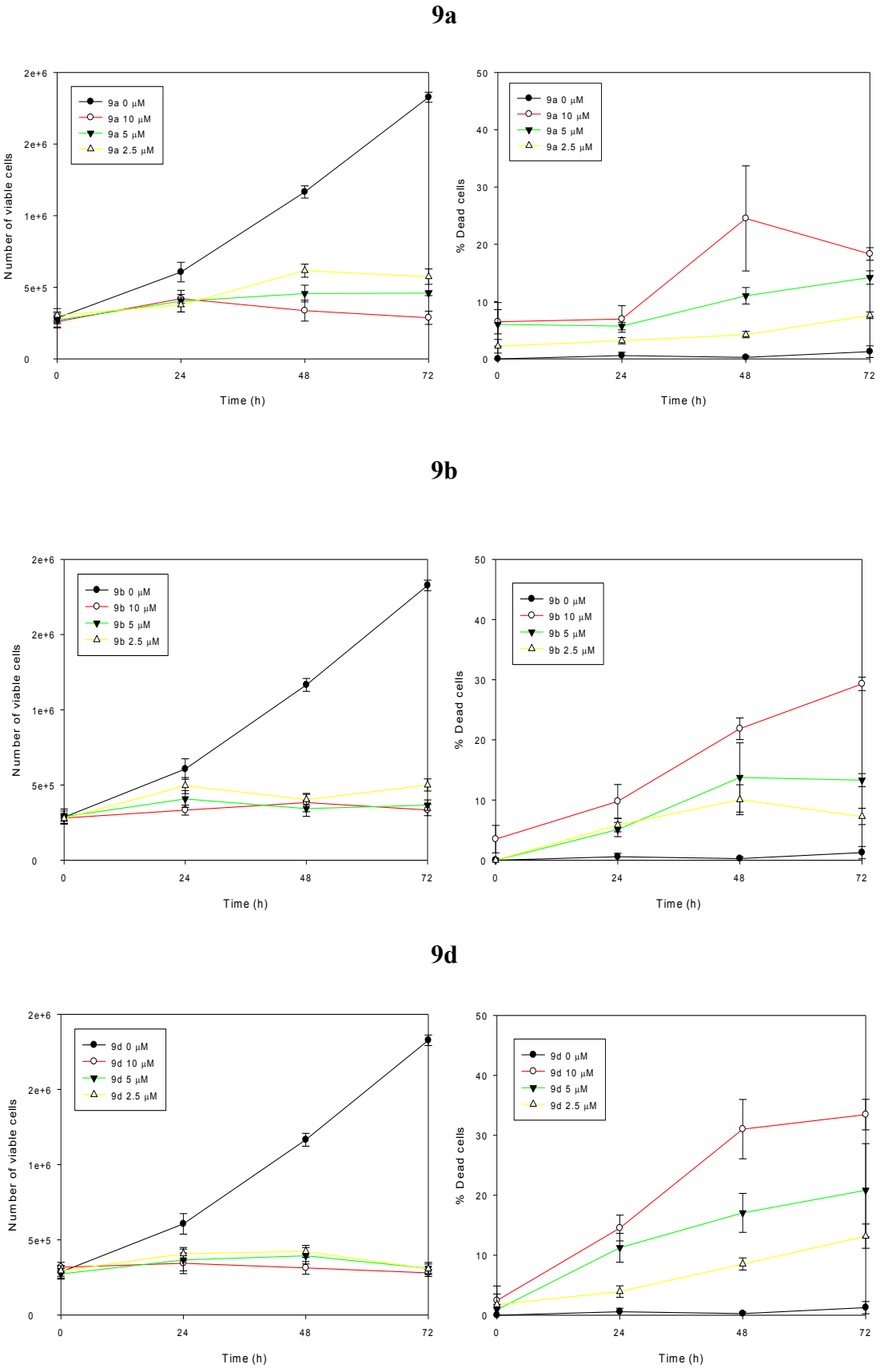

Figure 4.9 Number of viable cells and % of dead cells from 0 to 72 h of compounds **9a**, **9b** and **9d**.

From these results (Figure 4.9), for the analyzed compounds, the proliferation of viable cells is strongly slowed; about the dead cells, the percentage is higher at 72 hours, also reaching 30% (compound **9d**); although this percentage is significant, is reasonable to suppose that compounds mainly act by inducing a cytostatic effect.

4.3.2 CELLULAR PHOTOCYTOTOXYCITY

In order to evaluate if it is possible to improve the biological activity after UV-A irradiation, experiments of cellular phototoxicity on leukaemic Jurkat cell line were carried out; the cells were treated with increasing concentration of compounds (10, 5, 2.5, 1.25 μM) solubilized in HBSS aqueous buffer and then irradiated with two UV-A doses (En = 2.5 J/cm^2 and 3.75 J/cm^2) (Table 4.4).

Table 4.4 Photocytotoxicity of the tested compounds against Jurkat cell line.

IC_{50} (μM)[a] Jurkat		
Compounds	**2,5 J/cm^2[b]**	**3,75 J/cm^2**
9a	**1.97 ± 0.22**	**0.95 ± 0.30**
9b	**1.33 ± 0.30**	**0.95 ± 0.13**
9c	**2.60 ± 0.21**	**1.79 ± 0.02**
9d	**1.57 ± 0.22**	**1.24 ± 0.14**
9e	**2.48 ± 0.14**	**1.81 ± 0.19**
9f	**3.25 ± 0.24**	**1.51 ± 0.16**
9g	**3.30 ± 0.22**	**2.46 ± 0.27**
9h	**1.90 ± 0.38**	**1.78 ± 0.17**
9i	**> 10**	**> 10**
9j	**2.57 ± 0.57**	**2.48 ± 0.09**
9k	**> 10**	**> 10**
2	**> 10**	**> 10**

[a] Concentration of compound required to inhibit the cell growth by 50% after 30 minutes of exposure as determined by MTT assay after 72 h.[74] [b] UVA dose expressed in J/cm^2 as measured at 365 nm with a Cole-Parmer radiometer.

The photocytotoxicity was evaluated, after 72 h from irradiation, by MTT test[74] and calculated as GI_{50} micromolar values. As reference compound was used naphtho[1,2-*b*]quinolizinium bromide **2**, without substituent in pos. 3. Compounds **9c**, **9e**, **9f**, **9h** have shown an improvement of cytotoxic activity: this could be due to the effect of UV-A irradiation. For the remaining compounds, the UV-A irradiation does not increase antiproliferative activity: this behavior could depend on the different nature of substituents and their role in the photoactivation process or simply on the fact that they did not enter the cells for the brief period of incubation before irradiation (30 min).

4.3.3 INTRACELLULAR LOCALIZATION

The cellular localization of the compounds is evaluated to check the distribution of molecules inside cells to clarify the eventual cellular structure involved in the cytotoxic action. In order to investigate the intracellular localization (due to physicochemical properties such as hydrophobicity, charge interactions, etc.) of quinolizinium derivatives through confocal microscopy, HeLa cells were incubated at 37°C in the presence of compounds **9g** and **9j** (10 μM). After 1-2 h (Figure 1.10), a general diffusion in the cytoplasmatic compartment is evident and this fact confirms that the compounds enter inside the cell causing the cytotoxic effect.

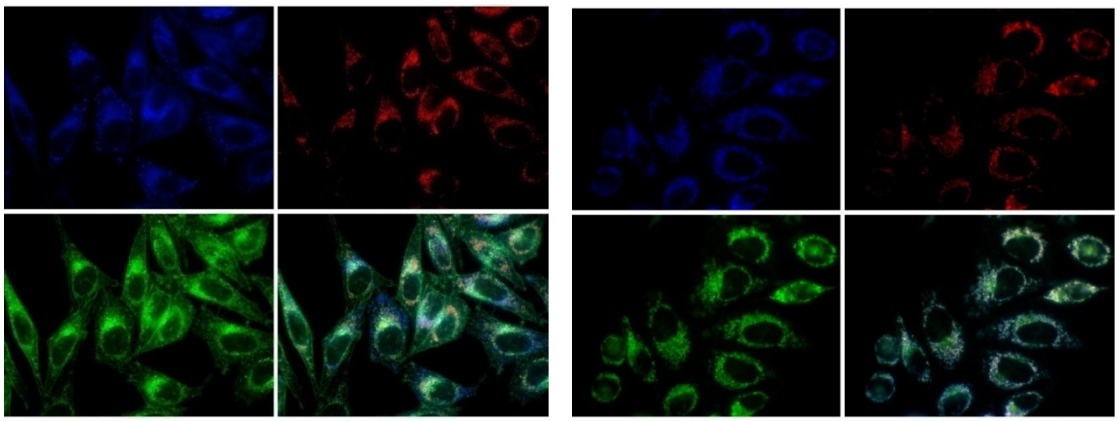

A **B**

Figure 4.10 Fluorescence images showing the intracellular localization of **9g** (panel A) and **9j** (panel B) in HeLa cells.

4.3.4 ANALYSIS OF CELL CICLE

Many antiproliferative drugs are able to block one particular phase of cell cycle (G1, S or G2/M phase). Then, the cells can repair the damage induced by a exogenous molecule and they return into the cycle (from G0 to G1), or if there is permanent damage, they can undergo apoptosis or necrosis. This analysis was conducted by flow cytometry and the different content of cellular DNA in each phase is evaluated. A typical diagram of growing cultures displays a first peak corresponding to G1 phase, a second peak characteristic of G2/M phase with an intermediate area corresponding to the S phase. When DNA is fragmented, as in apoptotic cells, a phase sub-G1 (hypodiploid peak) becomes apparent on the left of G1 peak. (For details see also section 3.2.9.1)

A549 cells were treated with compounds **9a**, **9b** and **9d** at concentrations 10, 5, 2.5 μM; Jurkat cells were treated with compounds **9a**, **9b**, **9d** and **9h**; HeLa cells were treated with compounds **9a**, **9b**, **9d**, **9g** and **9h**. After 24 h of incubation, the cells were marked with PI, which intercalates into DNA giving a fluorescence in the red (620 nm) if it is excited at 488 nm.

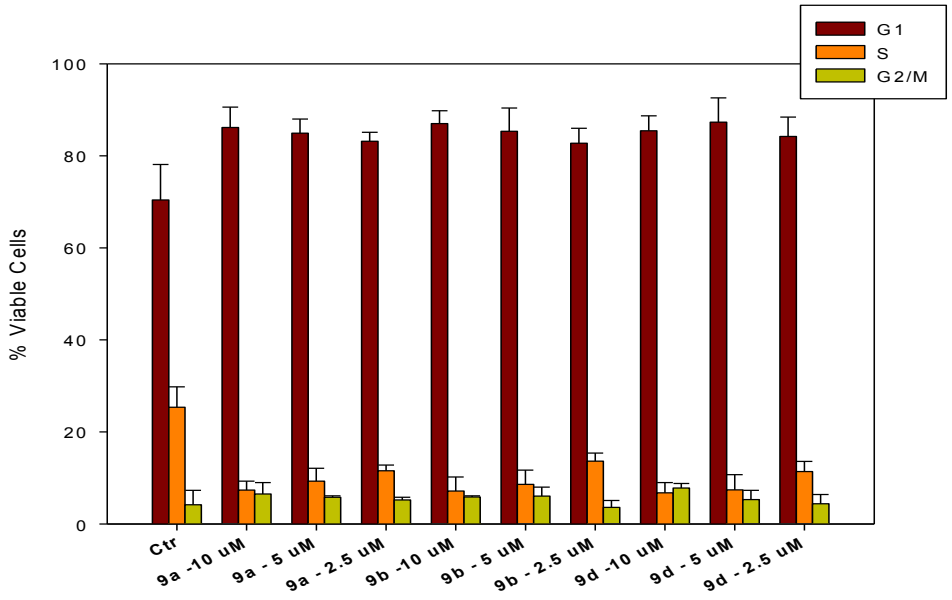

Figure 4.11 Percentage of A549 cells in the different phases of cell cycle after 24 h of incubation with compounds **9a**, **9b**, **9d**. Ctr = control cells not treated.

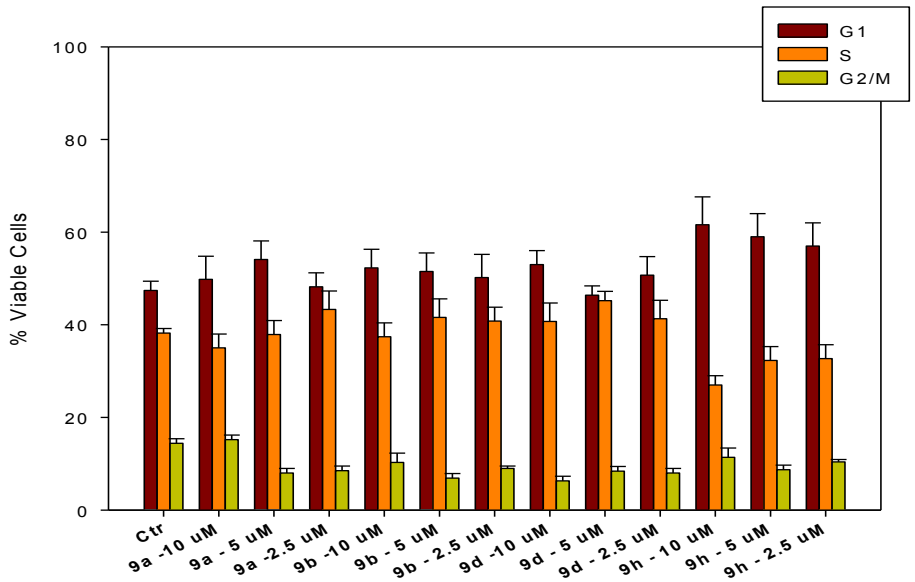

Figure 4.12 Percentage of Jurkat cells in the different phases of cell cycle after 24 h of incubation with compounds **9a**, **9b**, **9d**, **9h**. Ctr = control cells not treated.

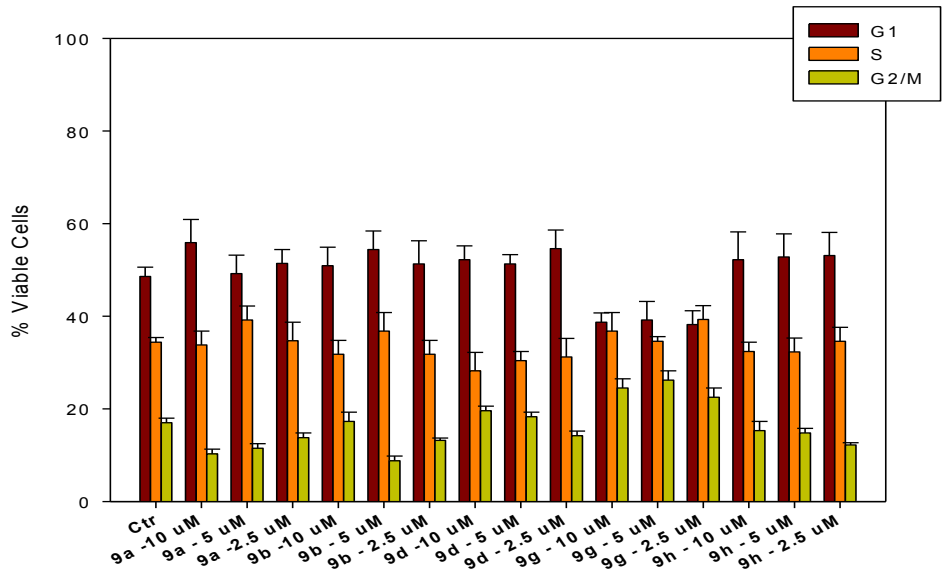

Figure 4.13 Percentage of HeLa cells in the different phases of cell cycle after 24 h of incubation with compounds **9a**, **9b**, **9d**, **9g** and **9h**. Ctr = control cells not treated.

A weak increase of percentage of cells in G1 phase is evident for all compounds and all concentrations in comparison to the control cells (not treated cells) in A549 cell line (Figure 4.11). In Jurkat cells, this effect can be observed only for compound **9h** (Figure 4.12); for the other ones, no changes in the cell cycle are present and the same thing happens in HeLa cells (Figure 4.13).

4.3.5 TOPOISOMERASE I AND II ASSAY

Topoisomerase are important enzymes about the resolution of topological problems in DNA, such as overwinding, underwinding, catenation, which arise during replication, transcription and other biochemicals DNA processes. In eukaryotic cells, two type of topoisomerase have been identified (I and II): their action is the formation of enzyme-bridged strand-breaks (topoisomerase I breaks one strand duplex DNA, topoisomerase II breaks both strands of the double helix) that act as transient gates for the passage of other DNA strands. After that, the religation takes place and the final result is the introduction of negative or positive supercoils into the DNA. Topoisomerase-targeting drugs appear to interfere with the breakage-reunion of DNA, by the production of a ternary aborted reaction intermediate, the "cleavable complex", that inhibits the religation. As result of this action, drugs "poison" of topoisomerase could be converted in cellular toxins that generate breaks and degradation of the genetic materials of treated cells. This action and its cellular effects could be useful in the identification and in the development of new anticancer molecules.

4.3.5.1 Inhibition of topoisomerase I

The ability of the antitumor agent coralyne to stabilize the "cleavable complex" between topoisomerase I and DNA was demonstrated,[44] so coralyne was chosen as reference compound because its structural analogy with quinolizinium derivatives and naphtho[1,2-*b*]quinolizinium bromide **2** was chosen to clarify the role the substituent in pos. 3. Firstly, the ability of compounds **9a**, **9b**, **9d**, and **9g** to act as catalytic inhibitors was analyzed by horizontal electrophoresis with a agarose 1% gel in absence of ethidium bromide. In a second time, their capability of stabilizing the cleavable complex was checked by agarose 1% gel containing 0.5 μg/ml of ethidium bromide. In order to clarify and to find the molecular target, the possible action on topoisomerase I of compound **9f**, which is not cytotoxic on the most of the treated cell lines, was evaluated. The compounds were incubated at increasing concentrations (0.1 - 100 μM) with supercoiled pBR322 and human Topoisomerase I.

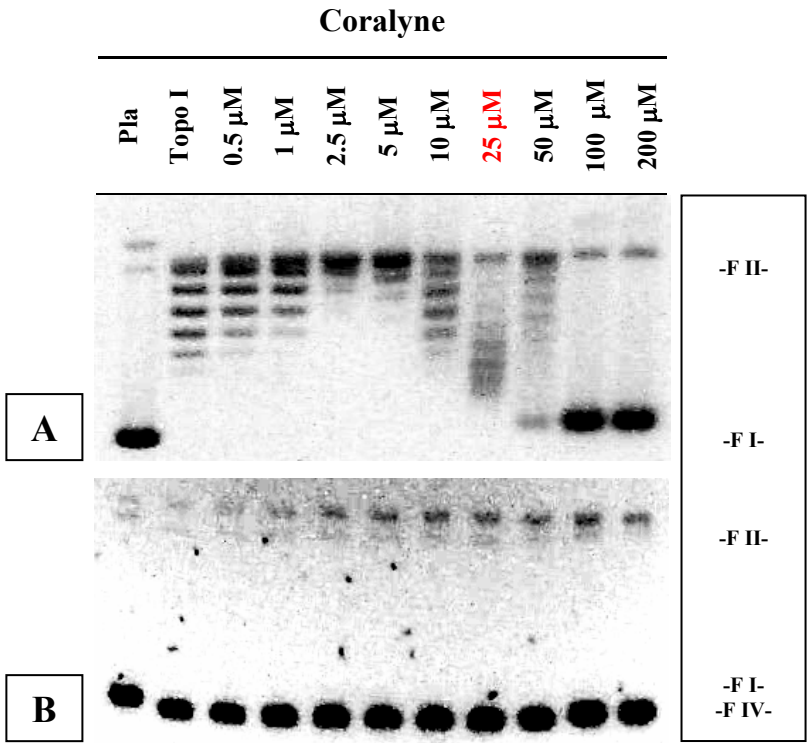
Coralyne
Pla
Topo I
0.5 µM
1 µM
2.5 µM
5 µM
10 µM
25 µM
50 µM
100 µM
200 µM
A
B
-F II-
-F I-
-F II-
-F I-
-F IV-

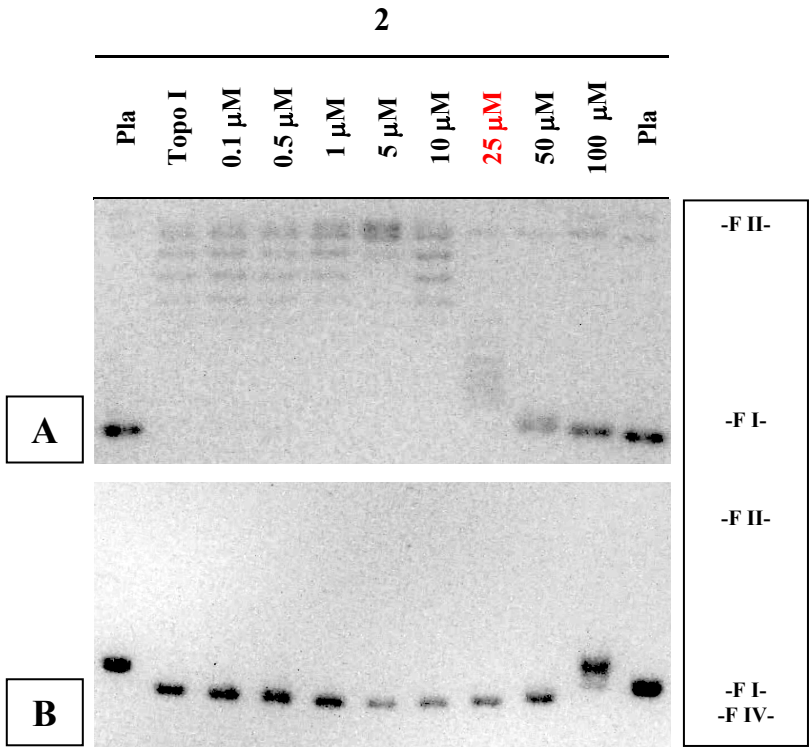
2
Pla
Topo I
0.1 µM
0.5 µM
1 µM
5 µM
10 µM
25 µM
50 µM
100 µM
Pla
A
B
-F II-
-F I-
-F II-
-F I-
-F IV-

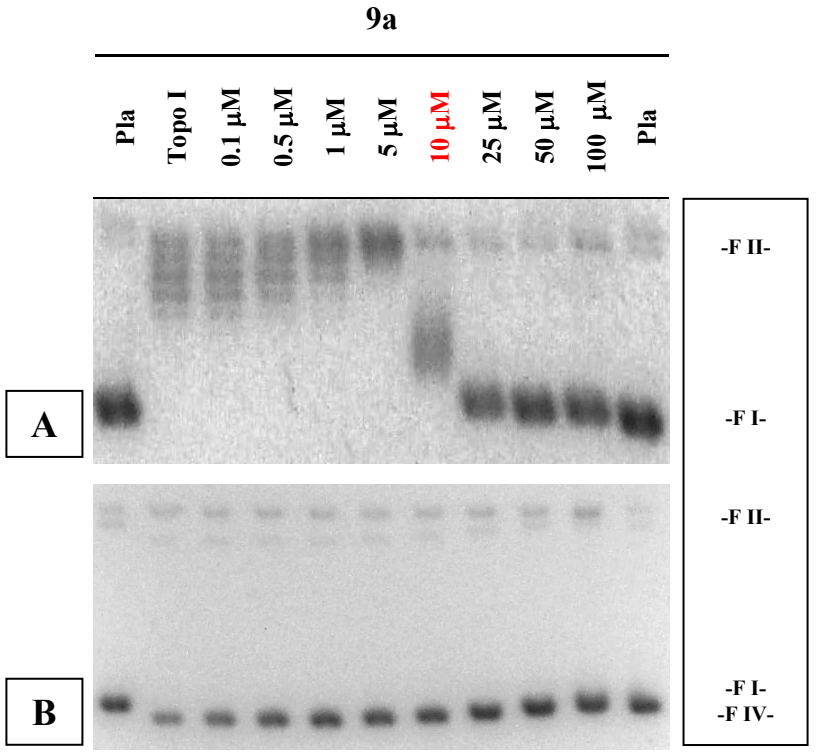
9a
Pla
Topo I
0.1 µM
0.5 µM
1 µM
5 µM
10 µM
25 µM
50 µM
100 µM
Pla
A
B
-F II-
-F I-
-F II-
-F I-
-F IV-

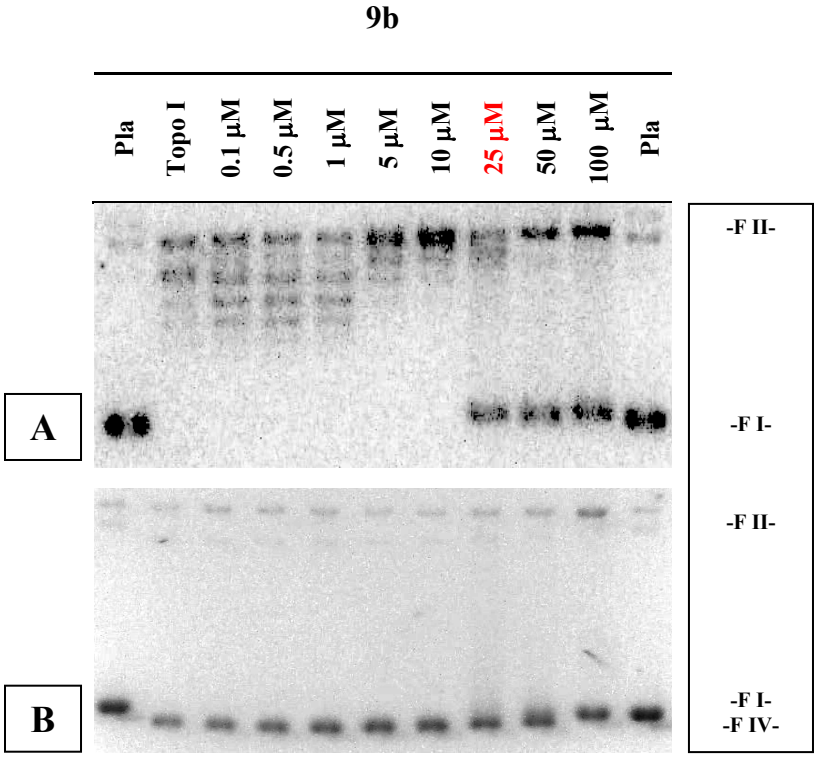
9b
Pla
Topo I
0.1 µM
0.5 µM
1 µM
5 µM
10 µM
25 µM
50 µM
100 µM
Pla
A
B
-F II-
-F I-
-F II-
-F I-
-F IV-

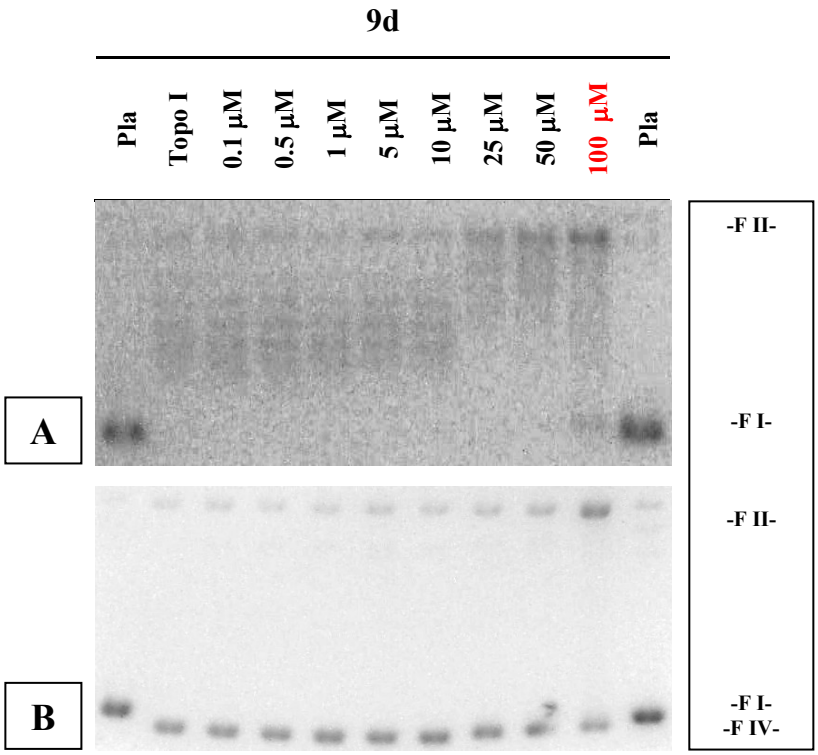
9d
Pla
Topo I
0.1 µM
0.5 µM
1 µM
5 µM
10 µM
25 µM
50 µM
100 µM
Pla
A
B
-F II-
-F I-
-F II-
-F I-
-F IV-

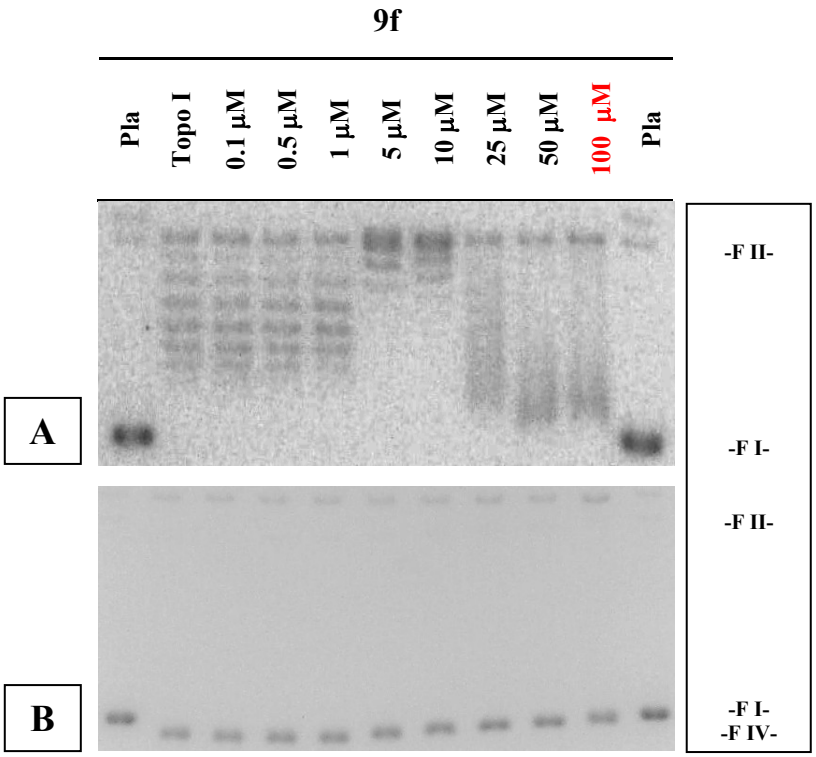
9f
Pla
Topo I
0.1 µM
0.5 µM
1 µM
5 µM
10 µM
25 µM
50 µM
100 µM
Pla
A
B
-F II-
-F I-
-F II-
-F I-
-F IV-

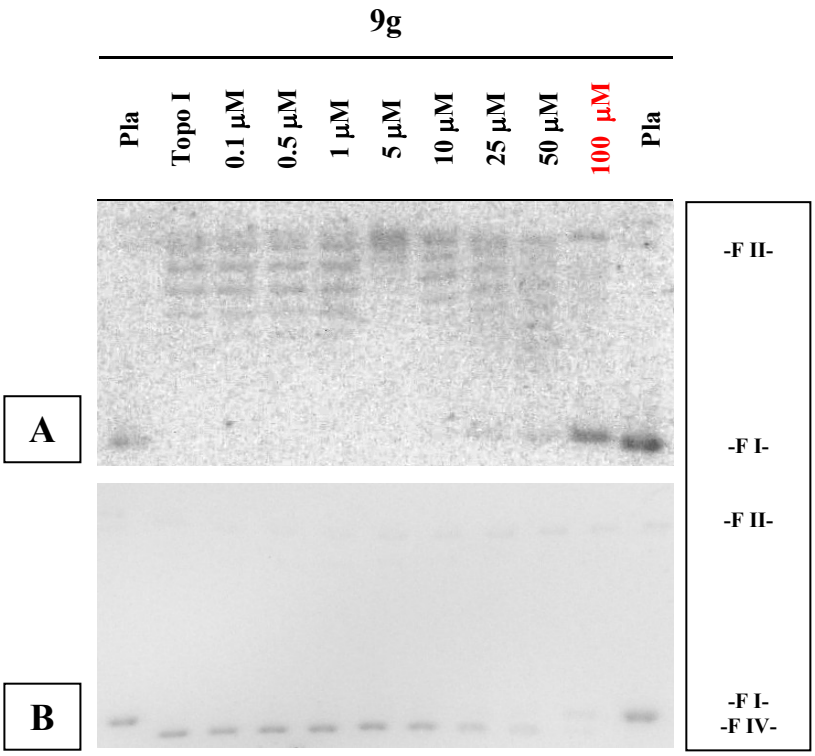

Figure 4.14 Effects of increasing concentrations of selected compound on topoisomerase I. Panel A: relaxation assay. The supercoiled plasmid pBR322 (lane pla) was incubated with topoisomerase I in the absence (lane Topo I) and in presence of compounds at indicated concentrations. Reactions were stopped with SDS and treatment with proteinase K. DNA samples were separated by electrophoresis on agarose gel and the stained with a solution containing ethidium bromide. F I = form I, supercoiled; F II = form II, nicked-open circular. Panel B: cleavable complex assay. The supercoiled plasmid pBR322 (lane pla) was incubated with topoisomerase I in the absence (lane Topo I) and in presence of drugs at indicated concentrations. Reactions were stopped with SDS and treatment with proteinase K. DNA samples were separated by electrophoresis on agarose gel containing ethidium bromide. F I = form I, supercoiled; F II = form II, nicked-open circular; Form IV = form IV, relaxed.

From the analysis of agarose gels without ethidium bromide (Figure 4.14, Panel A), all compounds act, in different concentrations, as catalytic inhibitor towards topoisomerase I, making a block in the cut of DNA by enzyme: there is the presence of form F II (nicked-open circular) and of the topoisomers in respect with the form FI (supercoiled) until determined concentrations; in respect with the references, that are coralyne and naphtho[1,2-*b*]quinolizinium bromide **2** (for both inhibition at 25 µM), the compound **9a** shows the most important catalytic inhibition, about at 10 µM; **9b** shows a relaxation inhibition at 25 µM. The compounds **9d** and **9g** show a relaxation block at 100 µM. Moreover, it is interesting to evaluate that the compound **9f**, weakly cytotoxic on almost all cell lines, shows, as previously compounds, a catalytic block at 100 µM. From the analysis of agarose gels in presence of ethidium bromide (Fig 4.14 Panel B), the

compounds do not act as poisons toward the enzyme: there is not a clear presence of the form "nicked" (Form II), because the compounds do not block the DNA religation activity of the enzyme, except of compound **9a** and **9d** but this happens just at high concentration (100 μM) in respect with the form FIV (relaxed).

Catalytic inhibition, although in concentrations higher than GI_{50} calculated by MTT test, could be explained by a hypothetic mechanism about which the 4-rings-structure intercalates in DNA with consequent block of binding of the enzyme to the nucleic acid. Only compounds **9a** shows a stronger relaxation inhibition: so, is reasonable to suppose that the presence of a determined substituent in pos. 3 could increase the ability of molecule to inhibit the enzyme.

4.3.5.2 Inhibition of topoisomerase II

Some experiments are carried out in order to verify an eventual interaction with topoisomerase II, because it is known from literature that there are molecules that interact with DNA that can inhibit both enzymes. As reference compound was chosen etoposide,[48] because its ability to inhibit topoisomerase II is known by literature. Naphtho[1,2-*b*]quinolizinium bromide **2** was also chosen as reference compound to evaluate the role of the substituent in pos. 3.

Compounds **9a**, which showed better cytotoxicity and better ability to produce a catalytic inhibition of topoisomerase I, was tested for the relaxation assay and cleavable complex assay. Compounds **9g** and **9j** were tested only for the relaxation assay.

For the relaxation assay, supercoiled plasmid pBR322 was incubated with human topoisomerase IIα and concentration of **9a, 9g** and **9j** ranging from 1 to 100 μM. The reference compounds, etoposide and naphtho[1,2-*b*]quinolizinium bromide **2** were analyzed at 100 μM in two different lanes.

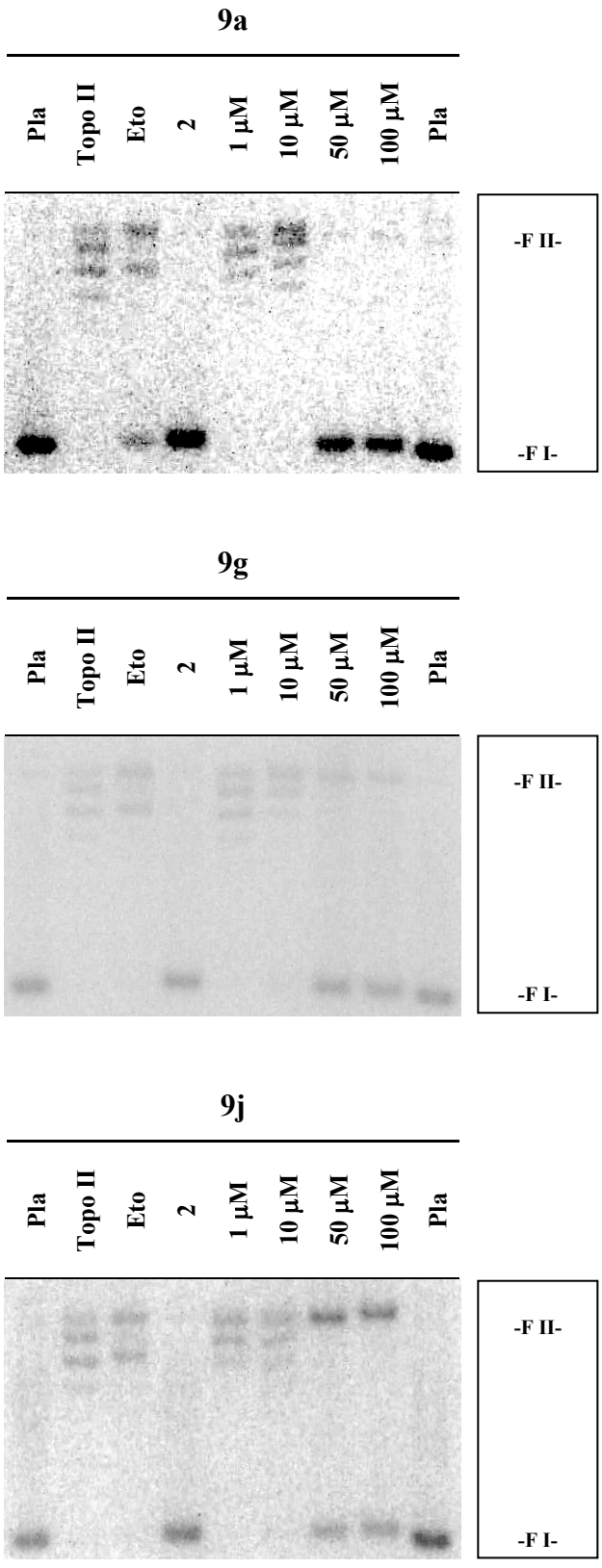

Figure 4.15 Effect of increasing concentrations of **9a, 9g** and **9j** on toposiomerase IIα: relaxation assay. Native supercoiled plasmid pBR322 (lane pla) was incubated with 2 units of topoisomerase II in the absence (lane topo II) and in the presence of drugs at the indicated concentrations. Etoposide (lane ETO) and **2** (lane 2) were used at 100 μM. Reactions were stopped with SDS and treatment with proteinase K. DNA samples were separated by electrophoresis on agarose gel and then stained with a solution containing ethidium bromide. F I= form I, supercoiled; F II=form II, nicked-open circular.

The gels shown in figure 4.15 indicate that for compounds **9a**, **9g** and **9j** between the concentrations of 10 and 50 μM the relaxation of DNA was inhibited, most likely as a result of the intercalation of the tetracycle into DNA (as previously observed for topoisomerase I). In comparison to the lanes of etoposide and the reference compound **2**, that does not show the presence of topoisomers at 100 μM, is reasonable to hypothesize that the structure with 4 rings intercalates into DNA and the substituent in pos.3 increases weakly the ability of the derivatives analyzed to block the protein, decreasing the concentration of inhibition.

For the cleavable complex assay, supercoiled plasmid pBR322 was incubated with human topoisomerase IIα and concentration of **9a** ranging from 1 to 100 μM.

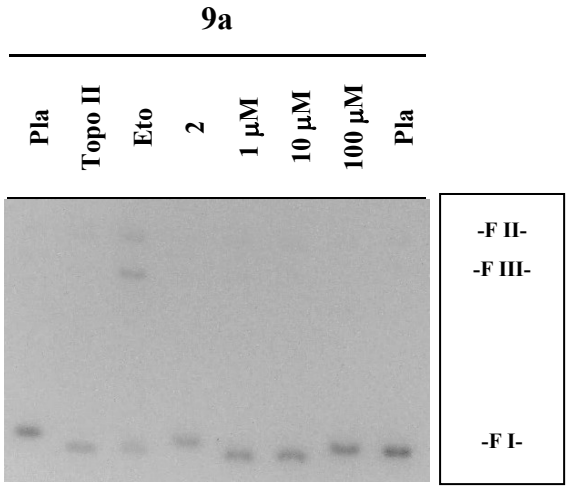

Figure 5.12 Effect of increasing concentrations of **9a** on topoisomerase IIα: cleavable complex assay. Native supercoiled plasmid pBR322 (lane pla) was incubated with 6 units of topoisomerase II in the absence (lane topo II) and in the presence of drugs at the indicated concentrations. Etoposide (lane ETO) and **2** (lane 2) were used at 100 μM. Reactions were stopped with SDS and treatment with proteinase K. DNA samples were separated by electrophoresis on agarose gel containing ethidium bromide. F I=form I, supercoiled; F II=form II, nicked-open circular; F III=form III, linear.

The gel of the cleavable complex assay (fig. 5.12) reveals that **9a** (but also the reference compound **2**) does not induce permanently breakage, as it can been observed for etoposide (form FIII), which makes a stabilization of "clavable ternary complex". Finally, the relaxation inhibition can due to the ability to intercalate into DNA.

4.3.6 CONCLUSION ON BIOLOGICAL ACTIVITY

Cytotoxicity experiments have clearly revealed that the introduction of the fourth aromatic ring and subsequently of an aryl substituent in pos. 3 on the naphtho[1,2-*b*]quinolizinium structure produces a high antiproliferative activity, with micromolar or submicromolar GI_{50} values by MTT test. However, the results of trypan blue test together with the absence of subG1 peak in cell cycle profile let me hypothesise a cytostatic mechanism. Almost all substituents have shown this improvement with optimal results (compounds **9a**, **9b**, **9g**), except heterocycles containing nitrogen (compounds **9f, 9k**). This low cytotoxicity could be justified by the difficult of these two compounds to get the hypothetical molecular target, because in the test without involving the cells (DNA binding properties, topoisomerase I inhibition), they have not shown a different behaviour compared to the other compounds.

About the activity against the topoisomerase I, the analyzed compounds have shown a relaxation inhibition, but there is not a clear block of religation (except for compounds **9a** and **9d**, although this is weak); about the topoisomerase II, the behaviour is the same: the relaxation is inhibited, but there is not a stabilization of "cleavable ternary complex". The high antiproliferative activity, confirmed by intracellular localization, cannot be justified by the partial inhibition of the topoisomerase I and II; these enzymes cannot be the molecular targets, which could instead be represented by the nucleic acids. Anyway more detailed studies on the mechanism of action are needed to reveal other possible molecular targets.

About the photobiological activity, only the compounds **9c**, **9e**, **9f**, **9h** have shown an improvement of cytotoxic activity after UV-A irradiation.

5. REFERENCES

5. REFERENCES

1. Foye W.O., Lemke T.L. and Williams D.A., Principi di chimica farmaceutica. *ed. Piccin,* **2011**.

2. S.L. Wolfe, Biologia molecolare e cellulare. *Ed. EdiSES*, **1994.**

3. Balmer C.M., Valley A.W. and Iannucci A. Cancer Treatment and chemotherapy. In: Dipiro J.T., Talbert R.L., Yee G., Matzek G.R., Wells B.G., Posey L.M., Pharmacotherapy A Pathophysiologic Approach. 6th ed. USA: McGraw-Hill Companies, Inc., **2005**, 2279-2328.

4. Zaman G.J.R.,. Flens M.J., Van Leusden M.R.,. De Haas M,. Mulder H.S., J. Lankelma, Pinedo H.M., Scheper R.J., Baas F., Broxterman H.J., Borst P., The human multidrug resistance-associated protein MRP is a plasma membrane drug-efflux pump. *Medical Science*s, **1994**, 91, 8822-8826.

5. Breier A., Barancík M., Sulová Z., Uhrík B., P-glycoprotein--implications of metabolism of neoplastic cells and cancer therapy. *Curr. Cancer Drug Targets*. **2005**, 5(6), 457-468.

6. Sen'kova A.V., Mironova N. L., Patutina O. A., . Ageeva T. A, . Zenkova M. A ., The Toxic Effects of Polychemotherapy onto the Liver Are Accelerated by the Upregulated MDR of Lymphosarcoma. *ISRN Oncology* **2012,** Article ID 721612.

7. Lerman L. S., Structural considerations in the interactions of deoxyribonucleic acid and acridines, *Journal of Molecular Biolology*, **1961**, 3, 18-30.

8. Zimmer C. and Wahnert U., Non-intercalating DNA-binding ligands: specificity of the interaction and their use as tools in biophysical, biochemical and biological investigations of the genetic material. *Prog. Biophys. Mol. Biol.,* **1986**, 47, 31-112.

9. Campbell N. H., Neidle S., G-Quadruplexes and Metal Ions, *Metal Ions in Life Sciences*, **2012**, 10, 119-134.

10. Sun D. et al., Inhibition of human telomerase by a G-quadruplex-interactive compound, *J. Med. Chem.,* **1997**, 40, 2113-2116.

11. Wang J.C., DNA topoisomerases. *Annu. Rev. Biochem.,* **1996**, 65, 635-692.

12. Deweese J.E. and Osheroff N., The DNA cleavage reaction of topoisomerase II: wolf in sheep's clothing, *Nucleic Acids Research*, **2009**, 37 (3), 738–748.

13. Russell P.J., Igenetics, *Benjamin-Cummings*, **2001**.

14. Joyce C., Steitz T., Polymerase structures and function: variations on a theme?. *J. Bacteriol.,* **1995,** 177 , 22, 6321–6329.

15. Bickle T., Krüger D., Biology of DNA restriction. *Microbio. Rev.*, **1993**, 57, 434–450.

16. Doherty A., Suh S., Structural and mechanistic conservation in DNA ligases. *Nucleic Acids Res.*. **2000**, 28, 21, 4051–4058.

17. Tuteja N., Tuteja R., Unraveling DNA helicases. Motif, structure, mechanism and function. *Eur. J. Biochem.*, **2004**, 271 ,10, 1849–1863.

18. Stryer L., Biochimica. *Ed. Zanichelli,* **1996**.

19. Saenger W., Principles of nucleic acids structure. *New York: Springer-Verlag*, **1984**.

20. Foloppe N. and MacKerell A.D.J., Intrinsic conformational properties of deoxyribonucleosides: implicated role for cytosine in the equilibrium among the A, B, and Z forms of DNA. *Biophys. J.,* **1999**, 76, 3206-3218.

21. Chen G., Chen S.J., Quantitative analysis of the ion-dependent folding stability of DNA triplexes. *Phys Biol.,* **2011**, 8, 6

22. Basham B, Schroth G.P., Ho P.S., An A-DNA triplet code: thermodynamic rules for predicting A- and B-DNA, *Proc. Natl. Acad. Sci, USA,* **1995***,* 92 (14): 6464–6468

23. Rich A., Nordheim A. and Wang A.H., The chemistry and biology of left-handed Z-DNA. *Annu. Rev. Biochem.,* **1984**, 53, 791–846.

24. Zhang H., Yu H., Ren J., Qu X., Reversible B/Z-DNA transition under the low salt condition and non-B-form polydApolydT selectivity by a cubane-like europium-L-aspartic acid complex, *Biophysical Journal,* **2006,** 90 (9), 3203–3207.

25. Ihmels H., Faulhaber K. and Viola G., Evaluation of the DNA-binding properties of cationic dyes by absorption and emission spectroscopy. *Highlights in Bioorg. Chem. Meth. and Appl.,* Ed. by Carsten Schmuck and Helma Wennemers, **2004.**

26. Hayashi M., Harada Y., Direct observation of the reversible unwinding of a single DNA molecule caused by the intercalation of ethidium bromide. *Nucleic Acids Res.*, **2007**, 35, 19

27. Kelly J.M., Tossi A.B., McConnell D.J., Oh Uigin C,. A study of the interactions of some polypyridylruthenium (II) complexes with DNA using fluorescence spectroscopy, topoisomerisation and thermal denaturation. *Nucl.Acids Res.***, 1985,** 13, 6017.

28. Görner H., Direct and sensitized photoprocesses of bis-benzimidazole dyes and the effects of surfactants and DNA. *Photochem.Photobiol.* **2001,** 73, 339.

29. Haq I., Thermodynamics of drug-DNA interactions. *Arch.Bioch. and Bioph.,* **2002**, 403, 1.

30. Ihmels H., Faulhaber K., Sturm C., Bringmann G., Messer K., Gabellini N., Vedaldi D. and Viola G., Acridizinium salts as novel class of DNA-binding and site-selective DNA-photodamaging chromophores. *Photochem. Photobiol.,* **2001**, 74, 505-512.

31. Viola G., Bressanini M., Gabellini N., Vedaldi D., Dall'Acqua F. and Ihmels H., Naphtoquinolizinium derivatives as a novel platform for DNA-binding and DNA photodamaging chromophores. *Photochem. Photobiol. Sci.,* **2002**, 1, 882-889

32. Pilch D.S., Yu C., Makhey D., LaVoie E.J., Srinivasan A.R., Olson W.K., Sauers R.S., Breslauer K.J., Geacintov N.E. and Liu L.F., Minor groove-directed and intercalative ligand-DNA Interactions in the poisoning of human DNA topoisomerase I by protoberberine analogs. *Biochemistry,* **1997**, 36, 12542-12553.

33. Rubenstein, Irwin, and Susan M. Wick., Cell. *World Book Online Reference Center*, **2008**.

34. Alberts B., Johnson A., Lewis J., Raff M., Roberts K. and Walter P., Molecular Biology of the Cell. *Garland Science: New York,* **2008**.

35. Roque T., Kalkan Z., Zylka W., Biological effectiveness in hypofractionation: Modeling tumor survival probability for large doses with a stochastic cell-cycle model. *Biomed. Tech.,* **2012**, 57

36. Nigg E.A., Cyclin-dependent protein kinases: key regulators of the eukaryotic cell cycle. *BioEssays*, **1995**, 17, 6, 471–480.

37. Israels E.D., Israels L.G., The cell cycle. *The Oncologist* **2000**; 5, 510-513.

38. Shapiro G.I. and J. Wade Harper J., Anticancer drug targets: cell cycle and checkpoint control, *J. Clin. Invest.,* **1999**, 104 (12), 1645–1653.

39. McCledon A.K. and Osheroff N., DNA topoisomerase II, genotoxicity, and cancer. *Mut. Res.,* **2007**, 623, 83-97.

40. Palumbo M., Gatto B., Moro S., Sissi C. and Zagotto G., Sequenze-specific interactions of drugs interfering with the topoisomerase-DNA cleavage complex. *Biochim. Biophys. Acta,* **2002**, 1587, 145-154.

41. Bakshi R.P., Galande S., Muniyappa K,. Functional and regulatory characteristics of eukaryotic type II DNA topoisomerase. *Crit. Rev. Biochem. Mol. Biol*., **2001**, 36, 1-37.

42. Pommier Y., Pourquier P., Fan Y. and Strumberg D., Mechanism of action of eukaryotic DNA topoisomerase I and drugs targeted to the enzyme. *Biochim. Biophys. Acta,* **1998**, 1400, 83-106.

43. Pourquier P. and Pommier Y., Topoisomerase I-mediated DNA damage. *Adv. Cancer Res.* **2001**, 80, 189, 216.

44. Wang L.K., Rogers B.D. and Hecht S.M., Inhibition of topoisomerase I function by coralyne and 5,6-dyhyrocoralyne. *Chem. Res. Toxicol.,* **1996**, 9, 75-83.

45. Fortune J.M. and Osheroff N., Topoisomerase II as a target for anticancer drugs: when enzymes stop being nice. *Prog. Nucleic Acid Res. Mol. Biol.*, **2000**, 64, 221-253.

46. Schoeffler A.J. and Berger J.M. Recent advances in understanding structure-function relationships in the type II topoisomerase mechanism. *Biochem. Soc. Trans.*, **2005** ,33, 1465-1470.

47. Berger J.M., Gamblin S.J., Harrison S.C. and Wang J.C., Structure and mechanism of DNA topoisomerase II. *Nature*, **1996**, 379, 225-232.

48. Baldwin E.L. and Osheroff N., Etoposide, topoisomerase II and cancer. *Curr. Med. Chem.,* **2005**, 5, 363-372.

49. Viola G., Dall'Acqua F., Photosensitization of Biomolecules by Phenothiazines Derivatives. *Current Drug Targets,* **2006,** 7, 1135-54

50. Coohill T.P., Action spectroscopy: ultraviolet radiation. In *Handbook of organic photochemistry and photobiology, CRC Press, Inc.,* **1995**.

51. Weichenthal M., Schwarz T., Phototherapy: how does UV work?, *Photodermatol. photoimmunol. photomed.,* **2005**, 21, 260-266.

52. Simon J.C., Pfieger D., Schöpf E., Recent advances in phototherapy, Eur. *J. Dermatol.* **2000,** 10, 642-645.

53. Peak M.J., Peak J.G. and Carnes B.A., Induction of direct and indirect single-strand breaks in human cell DNA by far- and near-ultraviolet radiations: action spectrum and mechanism. *Photochem. Photobiol.,***1987**, 45, 381-390.

54. Foote C.S., Definition of type I and type II photosensitized oxidation. *Photochem. Photobiol*., **1991**, 54, 659.

55. Misiaszek R., Crean C., Joffe A., Geacintov N.E. and Shafirovich V., Oxidative DNA damage associated with combination of guanine and superoxide radicals and repair mechanism *via* radical trapping. *J. Biol. Chem.,* **2004**, 279, 32106-32115.

56. Dall'Acqua F.*,* Viola G.*,* Vedaldi D.*,* Cellular and molecular target of psoralen, in "*CRC Handbook of Organic Photochemistry and Photobiology*", W. M. Hoorspool*,* F Lenci*, ed*. *CRC* Press*,* **2004,** 1–17.

57. Gasparro F.P., The role of PUVA in the treatment of psoriasis. Photobiology issues related to skin cancer incidence. *Am J Clin Dermatol*., **2000,** 1, 6, 337-348.

58. Bethea D., Fullmer B., Syed S., Seltzer G., Tiano J., Rischko C., Gillespie L., Brown D., Gasparro F.P., Psoralen photobiology and photochemoterapy: 50 years of science and medicine. *J.Dermatol. Sci.,* **1999**, 19, 78-88.

59. Oliven A., Shechter Y., Extracorporeal photopheresis: a review. *Blood Rev.,* **2001**, 15, 103-108.

60. Jori G., Molecular and cellular mechanisms in photodmedicine: porphyrins in cancer treatment. In *Primary photo-processes in biology and medicine, Ed Plenum Press,* **1985**.

61. Basili S., Bergen A., Dall'Acqua F., Faccio A., Granzhan A., Ihmels H., Moro S., Viola G., Relationship beetween the Structure and the DNA Binding Properties of Diazoniapolyclic Duplex- and Triple-DNA Binders: Efficiency, Selectivity and Binding Mode. *Biochemistry,* **2007**, *46*, 12721-12736.

62. Ihmels H., Faulhaber K., Vedaldi D., Dall'Acqua F. and Viola G., Intercalation of organic dye molecules in to double-stranded DNA. Part 2: the annelated quinolizinium ion as a structural motif in DNA intercalators. *Photochem. Photobiol.,* **2005**, 81, 1107-1115.

63. Basili S., Basso G., Faccio A., Granzhan A., Ihmels H., Moro S., Viola G., Diazoniapolycylic Ions Inhibit the Activity of Topoisomerase I and the Growth of Certain Tumor Cell Lines, *ChemMedChem*, **2008**, 3, 1671-1676.

64. Tian M., Ihmels H., Synthesis of Fluorescent 9-Aryl-Substituted Benzo[*b*]quinolizinium Derivatives. *Synthesis,* **2009**, 24, 4226-4234.

65. Miyaura N., Suzuki A., Palladium-Catalyzed Cross-Coupling Reactions of Organoboron Compounds, *Chem. Rev.,* **1995**, 95, 2457-2483.

66. Yu-Ming P., Yi.Yin K., Grieme T., Lawrence A. Black, Ashok V. Bhatia, Cowart M., An expedient and Multikilogram Synthesis of Naphthalenoid H_3 Antagonist, *Organic Process Research and Development,* **2007**, 11, 1004-1009.

67. Jones R.G., Soper Q.F., Behrens O.K., Corse J.W., Biosynthesis of Penicellins, VI. N-2-Hydroxyethylamides of Some Polycyclic and Heterocyclic Acetic Acids as Precursor *J. Am. Chem. Soc.*, **1948**, 70, 9, 2843-2848.

68. Chaires, J.B., Dattagupta N., Crothers D.M., Studies on Interaction of Anthracycline and Deoxyribonucleic Acid: Equilibrium Binding Studies on Interaction of Daunomycin with Deoxyribonucleic Acid, *Biochemistry***, 1982,** 21, 3933-40.

69. McGhee D. and Von Hippel P.H., Theoretical aspects of DNA-protein interactions: co-operative and non-co-operative binding of large ligands to a one-dimentional homogeneous lattice. *J. Mol. Biol.,* **1974**, 86, 469-489.

70. Norden B., Kubista M. and Kurucsev T., Linear dichroism spectroscopy of nucleic acids. *Q. Rev. Biophys.,* **1992**, 25, 51-170.

71. Norden B. and Kurucsev T., Analysing DNA complexes by circular and linear dichroism. *J. Mol. Recognit.,* **1994**, 7, 141-156.

72. Lyng R., Hard T. and Norden B., Induced circular dichroism of DNA intercalators: electric dipole allowed transitions. *Biopolymers,* **1987**, 26, 1327-1345.

73. Ciulla T.A., Van Camp J.R., Rosenfeld E., Kochevar I.E., Photosensitization of single-strand breaks in pBR322 DNA by rose Bengal. *Photochem. and Photobiol.*, **1989**, 49, 293-298.

74. Mosmann T., Rapid colorimetric assay for cellular growth and survival: application to proliferation and cytotoxic assay. *J. Immunol. Meth.,* **1983**, 65, 55-63.

75. Darzynkiewicz Z., Juan G., Li X., Gorczyca W., Murakami T., Traganos F., Cytometry in cell necrobiology: analysis of apoptosis and accidental cell death (necrosis). *Cytometry,* **1997**, 21, 1-20.

76. Bridwell D.J.A., Finlay G.J. and Baguley B.C., Mechanism of cytotoxicity of N-[2-(dimethylamino)ethyl] acridine-4-carboxamide and of its 7-chloro derivative: the roles of topoisomerases I and II. *Cancer Chemother. Pharmacol.,* **1999**, 43, 302-308.

77. Miyaura N., Diederich F., De Meijere A (Eds), Metal Catalyzed Cross-coupling Reactions, Wiley-VCH: New York, **2004**.

78. Timothy E. Barder, Shawn D. Walker, Joseph R. Martinelli, and Stephen L. Buchwald, Catalysts for Suzuki-Miyaura Coupling Processes: Scope and Studies of the Effect of Ligand Structure. *J. Am. Chem. Soc.*, **2005**, 127, 4685-4696.

79. Dai W. X., Petersen J. L., Wang K.K., Synthesis of indeno-fused derivatives of quinolizinium salts, imidazo[1,2-a]pyridine, pyrido[1,2-a]indole, and 4h quinolizin-4-one via benzannulated enyne-allenes. *J. Org. Chem.* **2005**, 70, 6647-6652.

80. Scatchard G., The attraction of proteins for small molecules and ions. *Ann. N. Y. Acad. Sci.,* **1949**, 51, 660-672.

81. Faccio A., New penta- and hexacyclic derivatives of quinolizinium ion: DNA-binding and DNA-photocleavaging properties. *[Tesi di dottorato],* **2008.**

82. Strober W., Trypan blue exclusion test of cell viability, *Curr Protoc Immunol.* Appendix 3B **2001.**

6. ACKNOWLEDGEMENTS

- Dipartimento di Scienze del Farmaco, University of Padova, Italy:

  Prof. Francesco Dall'Acqua
  Prof.ssa Daniela Vedaldi
  Dott.ssa Alessia Salvador

- Department of Pediatrics, University of Padova, Italy

  Dott. Giampietro Viola

- Department of Organic Chemistry II, University of Siegen, Germany:

  Prof. Heiko Ihmels